2013

Biological effects of trogocytosis on CD4+ T lymphocytes

Douglas Grant Osborne
The University of Montana

BIOLOGICAL EFFECTS OF TROGOCYTOSIS ON $CD4^+$ T LYMPHOCYTES

By

DOUGLAS GRANT OSBORNE

BS, University of Washington, Seattle, Washington, 2005

Dissertation/Thesis

presented in partial fulfillment of the requirements
for the degree of

Doctor of Philosophy
Microbiology, Integrated Microbiology and Biochemistry

The University of Montana
Missoula, MT

January 2013

Approved by:

Sandy Ross, Associate Dean of The Graduate School
Graduate School

Dr. Bill Granath, Chair
Integrated Microbiology and Biochemistry

Dr. Scott Wetzel, Thesis advisor
Integrated Microbiology and Biochemistry

Dr. Jesse Hay
Integrated Microbiology and Biochemistry

Dr. Kevin Roberts
Center for Environmental Health and Safety

Dr. Dave Shepherd
Center for Environmental Health and Safety

Dr. Mike Minnick
Integrated Microbiology and Biochemistry

Osborne, Douglas, Ph.D., Fall 2012 Microbiology

BIOLOGICAL EFFECTS OF TROGOCYTOSIS ON $CD4^+$ T LYMPHOCYTES

Chairperson: Dr. Bill Granath

Abstract

Antigen recognition by $CD4^+$ T cells leads to large-scale spatial and temporal molecular redistributions, forming the immunological synapse. We have previously shown that upon dissociation, T cells capture large membrane fragments from antigen-presenting cells directly from the immunological synapse. The mechanism and biological significance of this process, termed trogocytosis, is still unclear. In this thesis I examined the impact that trogocytosis has on the individual T cell after capturing molecules from the antigen presenting cell. I employed murine fibroblast cell lines expressing an I-E^k molecule loaded with a covalently attached antigenic peptide (moth cytochrome C 88-103) and with or without a GFP-tagged cytoplasmic tail as antigen presenting cells for T cells from a peptide-specific TCR transgenic mouse. Using a combination of high-resolution microscopy and flow cytometry, I showed that the trogocytosed material is retained on the surface of the T cell and is associated with sustained signaling after removal of the antigen presenting cells. The intercellular trogocytosis correlates with alterations in and is associated with sustained survival of the trogocytosis-positive ($trog^+$) cells *in vitro*. I also showed that sustained signaling in $trog^+$ T cells occurs at the trogocytosed spot and is initiated by the trogocytosed material. I conclude, that after trogocytosis, $trog^+$ T cells present antigen and induce activation of antigen-specific naïve T cells. The findings from this thesis will help to elucidate the role of trogocytosis on $CD4^+$ T cells.

Table of Contents

Figures:

Tables:

Acknowledgements:

Scott A. Wetzel – For giving me the opportunity to pursue openly my research and introducing me the greatest immune cell: T lymphocytes. I owe a large part of my laboratory skills to him.

Lindsay Thuesen – For helping me maintain mice and cell lines, and being a great friend.

Thesis Committee Members (Kevin Roberts, Bill Granath, Mike Minnick, Dave Shepherd, and Jesse Hay) for mentoring me and their encouragement through my graduate work.

Pam Shaw – For training and assisting me with flow cytometry, and specifically helping me with clogs and compensation.

Current and Former Members of the Wetzel lab: for taking care of my responsibilities when I was MIA, for trusting me to assist them in their research, and maintaining an open environment to discuss idea and troubles.

My wife Jessa: For her incredible patience through the process and her kind nature.

Chapter 1:

Introduction

T cell activation

During an adaptive immune response, T lymphocytes play a central role in the recognition and clearance of pathogens. The two general types of αβ T cells are $CD8^+$ and $CD4^+$, named for the coreceptor that the cells express. $CD8^+$ T cells, or cytotoxic T lymphocytes (CTL), are essential in cellular immune responses. $CD8^+$ T cells lyse target cells by releasing cytolytic granules containing perforin, a protein that forms pores in the cell membrane, and granzymes; proteases that induce apoptosis. The second type of T cell, the $CD4^+$ T cells, or helper T cells, will be the main focus of this thesis. Upon activation, naïve $CD4^+$ T cells can differentiate into various helper T cell (T_H) effector subsets, among these are the T_H1, T_H2, T_H17, T_{FH}, and T_{reg} subsets. T_H1 cells play a role in cellular immune responses, by expressing IL-2 and proinflammatory cytokines such as IFNγ along with helping in the activation of $CD8^+$ T cells, all leading to the clearance of intracellular pathogens (1-3). T_H2 cells play a role in humoral immune responses, by expressing cytokines such as IL-4, IL-5, IL-10, and IL-13, which help boost Ig production and lead to the production of immunoglobulin E antibodies, which are responsible for the clearance of extracellular parasites (1-3). T_H17 cells are involved in the production of IL-17 and in autoimmunity (4). T_{FH} cells (follicular B helper T cells) regulate the development of antigen-specific B cell immunity (5). T_{reg} cells (regulatory T cells) are involved in the suppression of an immune response (6). To become activated

and to differentiate into the effector $CD4^+$ T cell subsets, T cells require presentation of antigen (Ag) by a professional antigen-presenting cell (APC).

Ag presentation involves the expression of polymorphic MHC molecules loaded with specific antigenic peptide fragments on the APC membrane. The recognition of the specific MHC:peptide complex by the TCR induces a series of signaling cascades in the T cell leading to activation, differentiation, generation of effector function, and proliferation. TCR:pMHC engagement (called signal 1) is but 1 of 3 signals that are required for full $CD4^+$ T cell activation and differentiation. The second signal, costimulation, is induced by APCs recognizing Pathogen Associated Molecular Patterns (PAMPs). This "danger" signal (7, 8) leads to increases in the expression of costimulatory molecules, such as CD80 and CD86, which engage costimulatory receptors, such as CD28, on the surface of the T cell (8-10). The costimulatory signal augments TCR signaling (9), helping to increase activation, cytokine production, and proliferation. The final signal for full T cell activation and differentiation (signal 3) comes from the binding of cytokines to their receptors on the $CD4^+$ T cell. This induces signaling that drives proliferation and differentiation of naïve cells into one of the effector subsets.

The interacting molecules at the T-APC interface (including TCR:pMHC, costimulatory molecules, and adhesion molecules) along with intracellular signaling molecules and the T cell cytoskeleton, are spatially and temporally segregated in a structure termed the immunological synapse. The signaling through the synapse can lead to alterations in T cell function, activation of naïve and effector T cells (11), thymic selection (12), and/or cell death (13), and inactivation, also known as anergy (14).

When naïve T cells in the lymph nodes first encounter Ag, there is increased expression of CD69 (5) and downmodulation of the TCR (15-17). Increased CD69 expression, originally termed the "very early activation marker", is a sign of early activation and has been found to help in T cell proliferation, signal transduction, and is responsible for retention in the lymph nodes during T cell activation (18, 19). TCR downmodulation occurs during activation (16, 17) via proposed phagocytic mechanisms (20-22). TCR downmodulation is hypothesized to allow for serial TCR triggering (23, 24), where continuous TCR interactions with the pMHC can occur and desensitization of the activated T cell (16, 25). Increases in CD69 and downmodulation of the TCR precedes increased expression of CD25 (26), and the loss of CD62L (11) expression. The increase in CD25 (IL-2 receptor α) expression allows the cell to bind IL-2 with significantly higher affinity, which helps to increase T cell proliferation (26-28). The decrease in the adhesion marker CD62L, also known as L-selectin, prevents the cell from recirculating through 2° lymphoid organs, like the lymph nodes, after Ag recognition and activation (29, 30). T cell activation also leads to increased expression of CD4 and CD44 (31). CD4 binds to non-polymorphic regions of the MHC and brings the Src family kinase $p56^{Lck}$ (Lck) into close proximity to tyrosine containing substrates (16). CD4 can also help stabilize the interactions of the TCR with the MHC (32). CD44 is an adhesion marker commonly found on activated effector/memory cells that helps in lymph node retention by binding hyaluronan on the surface of the surrounding extracellular matrix (31, 33).

TCR signaling

The primary signal for T cell activation occurs through the engagement of the αβ TCR heterodimer by a specific MHC:peptide molecule present on the surface of an APC. TCR engagement initiates multiple signaling pathways that lead to the activation of three primary transcription factors: nuclear factor of activated T cells (NFAT) (30, 45, 46), activator protein 1 (AP-1) (45, 46), and nuclear factor kappa-light-chain-enhancer of activated B cells (NFκB) (48). Their activation results in T cell activation, proliferation, and development of effector functions. TCR:pMHC engagement leads to both TCR conformational changes (34) and aggregation (35, 36), which contribute to the initiation of signaling by recruiting cytoplasmic and membrane-bound kinases. These phosphorylate the immunoreceptor tyrosine-based activation motifs (ITAM) on the CD3 γ, ε, δ chains, and ζ dimer associated with the αβ TCR (37).

The kinase responsible for the initial ITAM phosphorylation is $p56^{Lck}$ (Lck) (34, 37). A recent report suggests that the main function of CD4 is the delivery of non-covalently associated Lck to the engaged receptor, rather than the previously hypothesized stabilization of the TCR:pMHC interaction (38). Lck knockout mice display a loss of active T cells in the periphery and the thymus of mice (39). The initial phosphorylation by Lck triggers the recruitment of a Syk-family kinase, zeta associated protein 70 kDa (ZAP-70) (37). ZAP-70 contains two SH2 (Src Homology 2) domains that bind the phosphorylated ITAMs. Upon ITAM binding, ZAP-70 is itself subsequently phosphorylated by Lck and activated (37).

The activation of ZAP-70 initiates several downstream signaling pathways. Phosphorylated ZAP-70 targets two important adapter proteins for phosphorylation: the Linker of Activated T cells (LAT) and SH2 domain containing leukocyte protein of 76 kDa (SLP-76) (40, 41). The loss of either LAT or SLP-76 results in the loss of nearly all signaling downstream of the TCR (42, 43). The phosphorylation of LAT at the plasma membrane recruits SLP-76 (which is also phosphorylated by ZAP-70) and GRB2-related adapter downstream of Shc (GADS). SLP-76 forms a stable interaction with LAT through GADS, forming a multimolecular signaling complex called the proximal signaling complex (40, 41). Even though these adaptor proteins lack enzymatic activity, they are responsible for the correct orientation and assembling of the proximal signaling complex to allow for the activation of multiple signaling pathways (44-46). The adapter molecules, LAT, SLP-76, and GADS, along with adapter protein, Nck, the guanine nucleotide exchange factor (GEF) Vav1, and the IL-2-induced tyrosine kinase (Itk), join together to recruit other secondary messengers that are critical in producing T cell effector function (fig. 1; purple box, fig. 2) (45).

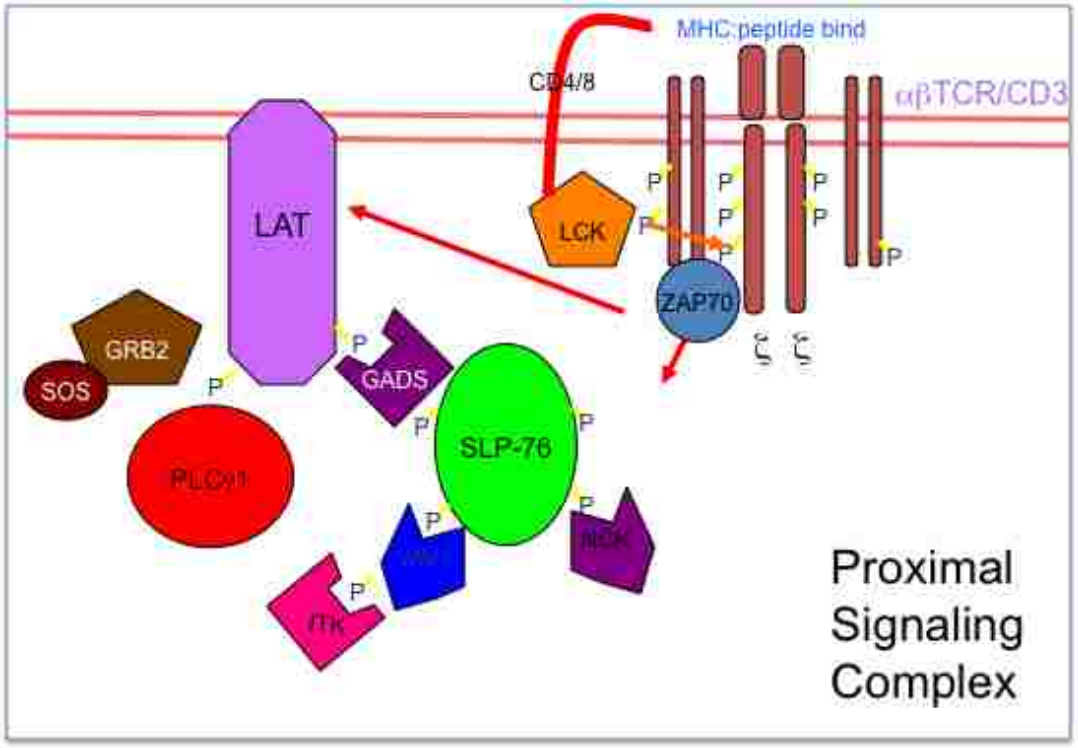

Figure 1: TCR proximal signaling complex.

One of the first signaling molecules recruited to the proximal signaling complex is phospholipase Cγ1 (PLCγ1) (47). PLCγ1 is phosphorylated by Itk, which is bound to the proximal complex by the protein Vav1 (48-50). After phosphorylation, PLCγ1 helps initiate calcium release from the endoplasmic reticulum (ER) in fig. 2 red box. PLCγ1 hydrolyzes membrane phosphatidylinositol-1,4-bisphosphate (PIP2) into the soluble sugar inositol-1,4,5-triphosphate (IP3) and the lipid diacylglycerol (DAG) (51, 52). IP3 binds IP3 receptors on the ER surface, leading to the release of Ca^{2+}. Increased intracellular Ca^{2+} leads to the activation of calcium release activated calcium (CRAC) channels (53, 54) (red box, fig. 2). The Ca^{2+} binds the regulatory protein calmodulin which activates the phosphatase calcineurin and dephosphorylates and subsequently activates the cytoplasmic transcription factor NFAT (55). The dephosphorylated NFAT

enters the nucleus and along with other transcription factors, activates T cell-associated activation genes (56). The release of Ca^{2+} during T cell activation can be easily monitored using imaging and flow cytometry (57, 58). PIP2 hydrolysis also produces DAG leading to the activation of the novel PKC family member protein kinase Cθ (PKCθ) (59), the guanine nucleotide binding protein Ras (through the guanine-nucleotide exchange factor (GEF) RasGRP) (60, 61), and the adaptor protein Carma1 (62). These molecules in turn activate three different downstream signaling pathways leading to the activation of the kinases ERK, JNK (63), and the transcription factor NFκB (62) (fig. 2).

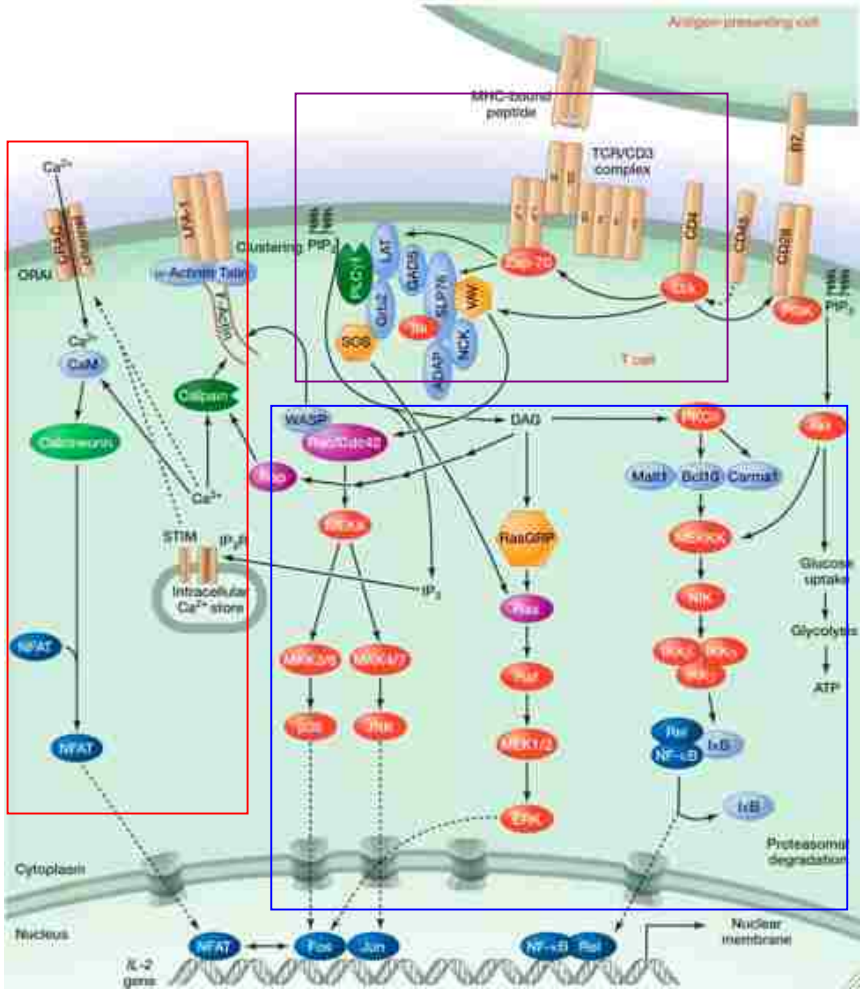

Figure 2. Overview of TCR signaling pathways. Taken from Samelson *et al*. (64)

Carma1 phosphorylation by PKCθ leads to the phosphorylation of mitogen-associated kinase kinase kinase (MEKKK), which releases the transcription factor NFκB from inhibitor of kappa B (IκB) by phosphorylating IκB for degradation. This allows NFκB to enter the nucleus (65). The phosphorylation of MEK1/2 by the kinase Raf and MEKK by the kinase Rac leads to the phosphorylation of kinases ERK, p38, and JNK. These, in turn, help dimerize the two transcription factors Fos and Jun into the AP-1 transcription factor (66) (blue box, fig. 2). Singular activation and translocation of NFAT without AP-1 leads to a hyporesponsive state in T cells, known as anergy (67). In addition, SLP-76 and Vav1 help to activate the kinase Rac which recruits Rho family GTPase Cdc42 and the Wiskott-Aldrich syndrome protein (WASP) to the signaling complex to initiate cytoskeletal rearrangements in the cell, allowing for continued proximal signaling and longer T-APC interaction (68, 69).

Costimulation and cytokines

In addition to signal 1, TCR engagement of the MHC:peptide complex, Ag presentation that leads to T cell activation also requires a second signal that is acquired through costimulation. TCR signaling in the absence of a costimulatory signal leads to anergy (8). Cytokines, as the third signal, leads to increased activation, proliferation, differentiation, and cell homing (70).

The prototypical costimulatory interaction involves the CD28 costimulatory receptor on the surface of the T cell engaging B7 family molecules CD80 (B7-1) and CD86 (B7-2) found on the surface of APC (71). According to the danger hypothesis,

microbial products or responses to cell damage induce the APC to upregulate expression of CD80 and CD86 (8-10). As shown in fig. 2, engagement of CD28 by CD80/CD86 at the immune synapse leads to the activation of PI3K (72), which augments the TCR-mediated activation of MEKKK via the kinase Akt (73), which contributes to the subsequent activation and translocation of NFκB (74).

The combination of TCR and costimulatory signaling leads to the induction of gene expression within the T cell associated with the production of cytokines and, ultimately, effector functions. One of the main cytokines produced during T cell activation is IL-2 (75, 76). IL-2 binds the high affinity CD25-containing IL-2 receptor on the surface of the T cell activating similar pathways involved in TCR and costimulation (27), and ultimately leading to proliferation and differentiation.

Immunological synapse

Ag recognition by T cells, and the subsequent signaling, leads to spatial and temporal molecular rearrangement at the T-APC interface to form a structure termed the immunological synapse. These molecular rearrangements involve the clustering and spatial segregation of molecules at the T-APC interface, including TCR:pMHC, costimulatory, and adhesion molecules, along with intracellular signaling molecules and the T cell cytoskeleton. This structure was first described by Kupfer *et al.* in 1987 (77), who showed when murine T cells were being presented Ag by a B cell, the TCR was concentrated at the cell-cell contact area. Kupfer *et al*. also found that T cells reorganized microtubules and membrane-bound cytoskeleton to the cell-cell contact area (77). In a

follow up paper in 1998, Monks *et al*. showed that surface receptors, like the TCR, segregated into specific areas on the T cells that were in contact with the APC, called supramolecular activation complexes (SMACs) (78). The initial studies of immune synapse formation found that the formation of an immune synapse coincided with T cell activation (78, 79).

Immunological synapse morphology

After the initial T-APC contact and subsequent Ag recognition occurs, the adhesion molecule leukocyte function-associated antigen 1 (LFA-1) on the T cell binds to intercellular adhesion molecule 1 (ICAM-1) on the APC, leading to the formation of microclusters containing both TCR:pMHC and LFA-1/ICAM-1(80). As shown in fig.3, these TCR/MHC microclusters are translocated to the center of the T-APC contact patch in an endosomal sorting protein, TSG101, dependent mechanism (81, 82). The area where TCR microclusters translocate to has been termed the central supramolecular activation complex (c-SMAC) (78). From fig. 3, it can best be seen that the c-SMAC contains not only TCR/MHC:peptide, but also costimulatory molecule interactions CD28/B7-1, adhesion molecule CD2, and the coreceptor CD4 (78, 83). The segregation of intracellular signaling molecules PKCθ, Lck, and Fyn also occurs at the c-SMAC (78, 83). Surrounding the interactions of the TCR with MHC at the c-SMAC is a peripheral ring of integrin adhesion molecules LFA-1/ICAM-1 (78, 83). This peripheral ring has been termed the peripheral SMAC, or p-SMAC. The p-SMAC has been shown as the location for accumulation of f-actin (84) and talin, which links integrins, like LFA-1, to

actin (78, 83). Once the defined p-SMAC and c-SMAC are spatially segregated, the synapse is termed a mature immunological synapse (84).

The prototypical mature T_H1 immune synapse can be characterized as a bull's-eye with the p-SMAC surrounding the c-SMAC, and after several minutes a third ring is formed termed the distal SMAC or d-SMAC. The d-SMAC discovered by Frieberg *et al.,* contains the phosphatase CD45 and, following 15 and 23 minutes of initial contact, both Lck and CD4 localize to the d-SMAC (85), repsectively. Fig. 3 shows the organization of the immune synapse into SMACs.

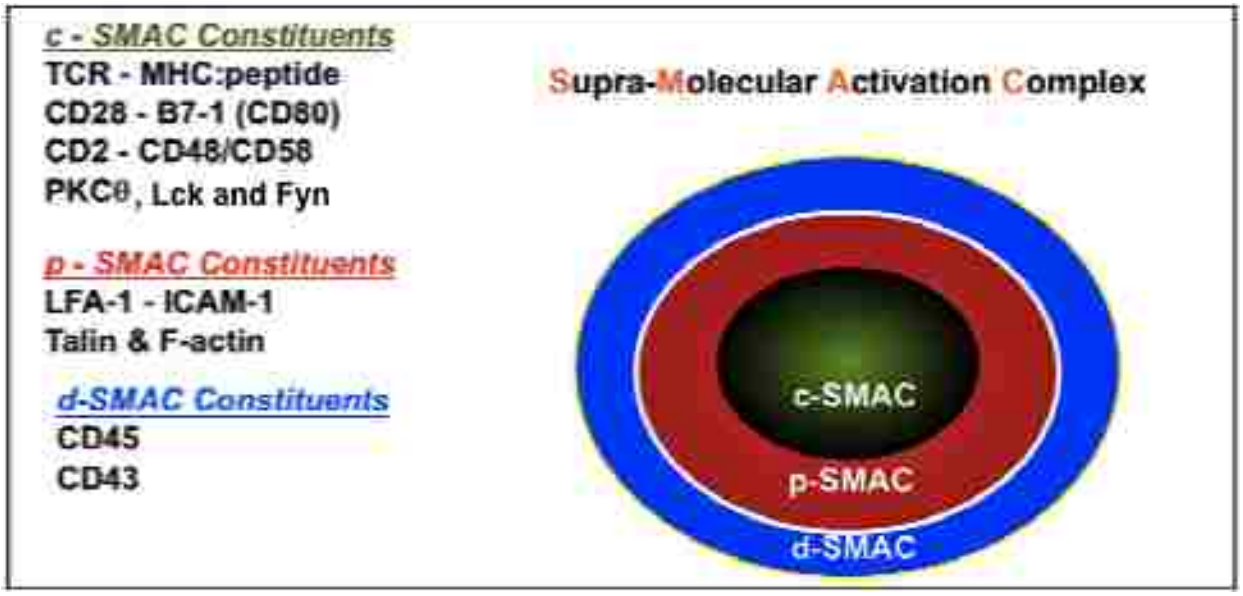

Figure 3. Immune synapse: supramolecular activation complex (SMAC) organization and content.

The morphology of a T_H1 synapse is different from the T_H2 synapse (86). The differences between a T_H1 and T_H2 cell synapse are the localization of adhesion molecule, ICAM-1. In T_H1 synapses, as shown above, a ring of ICAM-1 surrounds TCR:pMHC. In T_H2 synapses, ICAM-1 did not form a ring and colocalized with TCR:pMHC (86). The difference in distribution of ICAM-1 between T_H1 and T_H2

synapses suggest differences in the function of the synapse between these cells. T_H1 synapses could be used for cytotoxic functions (87), where the ring of ICAM-1 helps concentrate cytotoxic granules towards the target cell and prevent damage to bystander cells (88). T_H2 cells are not known to have cytotoxic functions (87, 89), so there may be less need for a ring of ICAM-1.

The organization of the c-SMAC and p-SMAC in T_H1 cells can be visualized using fluorescent microscopy, as shown in fig. 4. Using live-cell imaging and fluorescently labeled MHC:peptide and ICAM-1 attached to a planar lipid membrane, Grakoui *et al.* observed that when T cells interact with these molecules, large-scale molecular rearrangements occur leading to the formation of the immune synapse (79). Using time-lapse imaging, they showed that during the interaction of the T cell with molecules in the membrane, the surface molecules can be seen reordering into specific areas during a 60 minute time period, characterizing the c-SMAC and p-SMAC shown in fig. 4A (79). In fig.4B Dustin's group shows the localization of the TCR (red and green) to the c-SMAC surrounded by ICAM-1 (blue) in the p-SMAC (90).

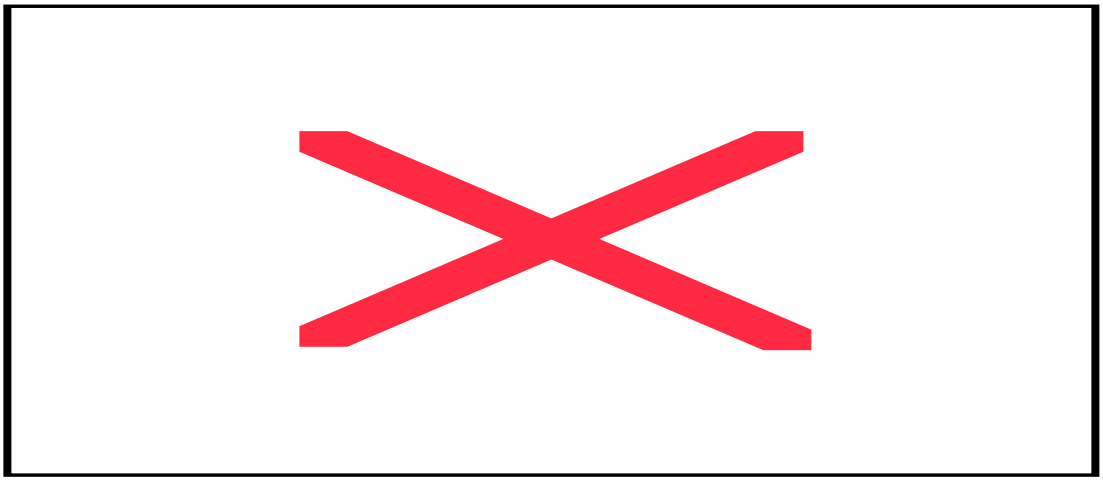

Figure 4. Immune synapse formation. (A) 60 minute time-lapse imaging showing the change in distribution of MHC (green) and ICAM-1 (red) receptors embedded in planar lipid bilayers when in contact with the T cell. From Grakoui *et al*. (79) (B) Fixed cell images showing the distribution of the T cell's TCR ζ (green) and β (red) chains corresponding to the c-SMAC and surrounded by ICAM-1 (blue) at the p-SMAC. From Roberts. J. (90)

Immunological synapse function

The formation and organization of the immune synapse has been well studied (78, 79, 84, 85, 91, 92), but the functions of the immune synapse remain unclear. The consensus from the last decade is that LFA-1/ICAM-1 interactions slow down rapidly migrating T cells, allowing for long sustained contacts with APCs (93, 94) which may lead to immune synapse formation and T cell activation. As the synapse is formed, the SMACs stabilize the T-APC contact and lead to the segregation of signaling molecules within the contact area. This allows for concentrated and continual TCR signaling (95)

leading to T activation (11). What remains unclear is the location of TCR signaling within the immune synapse.

Over the last decade controversy has arisen over whether TCR signaling localizes to the p-SMAC or c-SMAC, in a mature synapse. Recent results suggested that TCR signaling starts in the p-SMAC and ceases in the c-SMAC (81, 96, 97). Lee *et al*. showed as the TCR microclusters migrate from the p-SMAC to the c-SMAC, signaling associated with these microclusters decreased (97). During synapse formation signaling can initially be seen near the c-SMAC, but after one hour the signaling is gone (97). This can be seen in the images in fig. 5A showing that peripheral phosphotyrosine (green) is lost in the c-SMAC in an immune synapse after 60 min. Following entry into the c-SMAC the microclusters are hypothesized to be degraded due to the increase of lysobisphophatidic acid, a late endosomal marker in endosomes that are targeted for degradation (81). To sustain the signaling necessary for full T cell activation, continuous formation of signaling microclusters in the p-SMAC is required. These microclusters and the associated signaling appear to be degraded in the c-SMAC (81). This raises the possibility that the function of the c-SMAC may actually be to terminate TCR signaling. However, the role of the c-SMAC in signal termination is controversial because it has also been shown that signaling still occurs at the c-SMAC (78, 79, 98). In fig. 5B phosphotyrosine is localized to the c-SMAC after 60 min of T-APC conjugate formation (98). The images in fig. 5B are conflicting with the data shown by Lee *et al.* (97) in fig. 5A. These results are consistent with previous results showing signaling localized to c-SMAC (86).

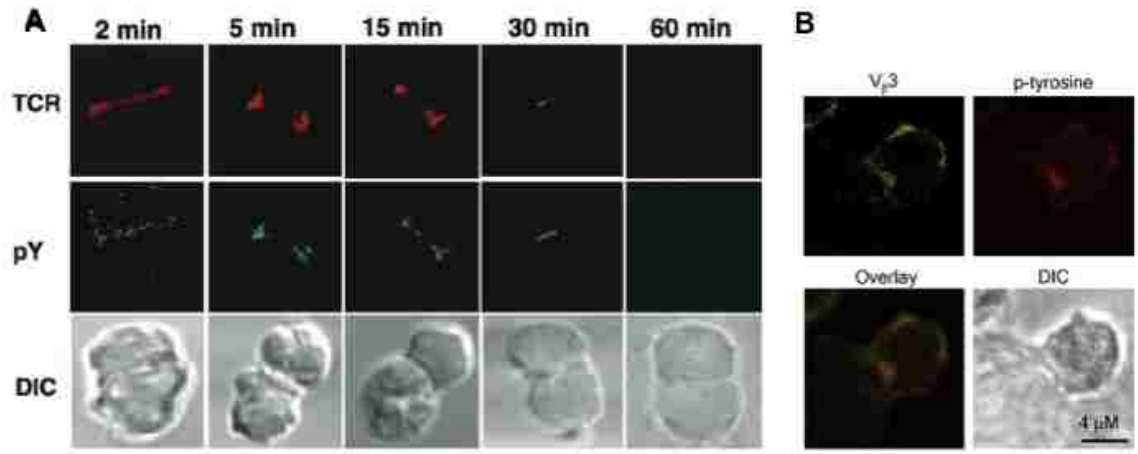

Figure 5. **TCR signaling at the c-SMAC.** (A) No c-SMAC signaling. T cell–APC conjugates stained TCR Vβ3 (red) and phosphotyrosine (green). AND TCR transgenic splenic T cells were conjugated with antigenic peptide–loaded splenic APCs from B10.BR mice. The lower row shows DIC images of the T cell–APC conjugates. Images show peripheral signaling as the synapse forms and by 60 min signaling has returned to basal levels. From Lee *et al.* (97), (B) Signaling at the c-SMAC. Rested AND T cells were stimulated with peptide-loaded CH27 B cells for 1 hr. Conjugates were then fixed, permeabilized, and stained with antibodies to Vβ3 (green) and phosphotyrosine (red). Images show phosphotyrosine concentrated at the c-SMAC, conflicting with the data show in (A). From Cemerski *et al.* (98).

In the last decade, other roles for the immune synapse have been elucidated in $CD4^+$ and $CD8^+$ T cells. In $CD8^+$ T cells, the p-SMAC is utilized as a barrier to help direct the release of cytotoxic granules towards the target cell (88, 99, 100). Stinchcombe *et al.* showed that $CD8^+$ T cells form a ring of adhesion with target cells, similar to the p-SMAC formed between a $CD4^+$ T cell and an APC (88). With the adhesion ring, lytic granules filled with perforin and granzymes were released onto the target cell (88). The immune synapse also plays a role in cytokine secretion. In 2006, Huse *et al.* showed IL-2 and IFN-γ accumulated at the synapse for release (101). Components of the immune synapse may play a critical role in the fate of the T cell. Recently, anergized T cells have

been shown to form an immune synapse with accumulated anergy-associated molecule, the E3 ubiquitin-protein ligase, Cbl-B (102). Anergized $CD4^+$ T cells formed distinct p- and c-SMACs, and both SMACs showed enhanced levels of c-Cbl and Cbl-B (102). Finally, and most relevant here, the immune synapse has been shown to be the site of intercellular membrane and membrane-associated molecule transfer from APC to T cell (88, 103-107).

Trogocytosis

Ag recognition by $CD4^+$ T cells and the formation of a mature immune synapse can lead to the acquisition of APC membrane lipids and membrane-bound proteins, including cognate MHC:peptide complexes (103, 107). This phenomenon of intercellular molecule transfer has been termed trogocytosis (108). Initially, the term was used to describe the injuring of mouse embryo cells by pathogenic amoeba, wherein the amoeba would acquire membrane from the mouse cells (109, 110). In 2003, Hudrisier and colleagues applied the term trogocytosis to define the swapping of membrane and membrane-associated molecules between immune cells (108, 111).

The discovery of immune cell trogocytosis came in the 1970's when Playfair's group discovered the presence of B cell-derived Ig molecules on the surface of T cells (112). Although there were several important publications in the 1980's (113-115), interest in trogocytosis and its potential immunomodulatory role was reignited in the late 1990s by the work of Mannie and colleagues (104, 116-121), Sprent *et al.* (105, 106, 122), and Hudrisier and Joly (107, 108, 111, 123-128). The general consensus of these,

and other studies, is that Ag recognition by T lymphocytes can lead to the trogocytosis of molecules from the surface of an APC. Trogocytosis requires TCR recognition of MHC:peptide ligands (103, 111, 129) and involves immune synapse formation (103) along with subsequent TCR signaling. In addition, costimulation and actin cytoskeletal rearrangements are required for efficient T cell trogocytosis (107, 108, 111, 123-128, 130).

While most studies have on focused on T cells; several other immune cells have been shown to perform trogocytosis. B cells (111, 129, 131, 132), dendritic cells (DC) (133, 134), and natural killer (NK) cells (135-138) have been shown to perform trogocytosis. B cells acquire tethered antigen from target cells via trogocytosis (132). *In vivo* studies have shown that DCs can capture MHC class I and II from other DCs (133, 134), and NK cells can acquire MHC class I *in vitro* and *in vivo* (135, 136, 138), along with membrane (137) from target cells. The requirements for trogocytosis by these cells appear to be less stringent than it is for T cells. B cells can perform trogocytosis without BCR signaling and can acquire molecules from dead or lysed cells (111, 129). Similarly DC have been shown to acquire MHC class I from apoptotic or necrotic tumor cells (139, 140), whereas T cells trogocytosis requires an intact APC (129). Unlike T cells, trogocytosis by NK, B, and DCs can does not require Ag recognition (111, 129, 139, 141).

The acquisition of APC-derived molecules via the immune synapse can be monitored using fluorescent microscopy, using fluorescently conjugated antibodies and tagged surface molecules. In fig. 6, live-cell microscopy images show the formation of several immune synapses, which can be seen as the accumulation of GFP-tagged

MHC:peptide at the T-APC interface. As each of the three T cells dissociate from the APC, the GFP:pMHC is trogocytosed onto the T cells (103).

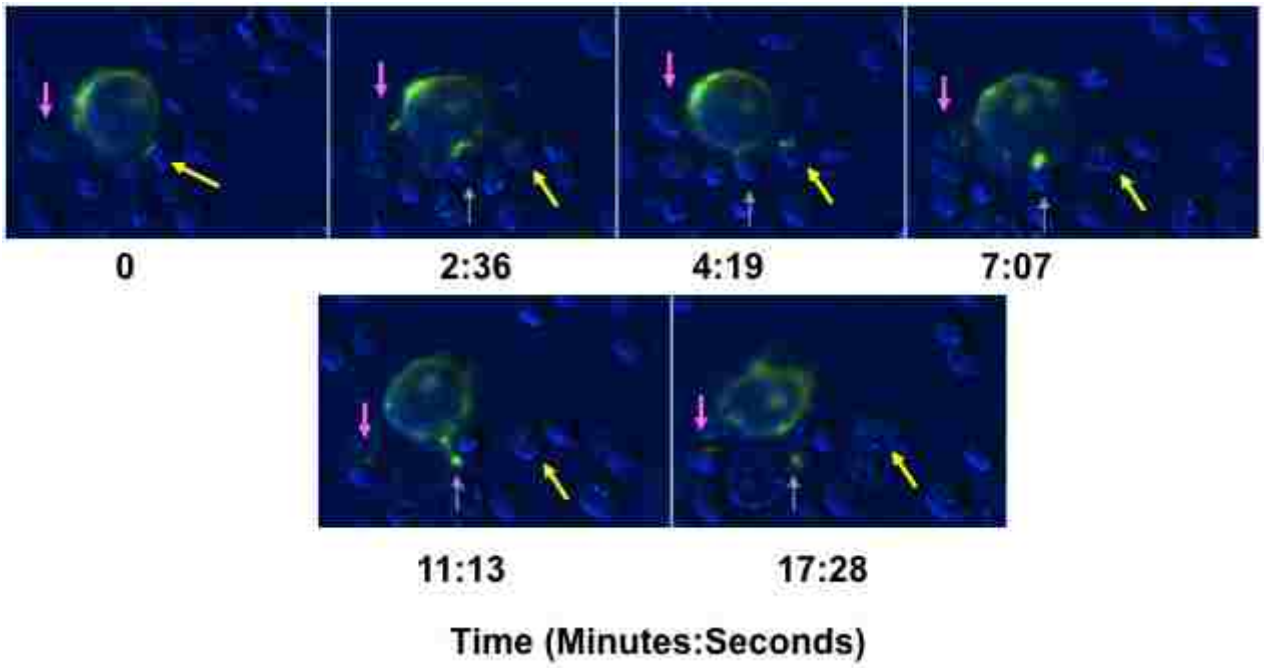

Figure 6. CD4$^+$ T cell trogocytosis via the immunological synapse. Time-lapse images showing immune synapse formation and upon dissociation from APC the T cell trogocytoses MHC:peptide. AD10 T cells were placed in culture with GFP-tagged MHC:peptide and live cell imaging was performed for the times shown above. GFP (green) is overlaid on DIC images (blue). From Wetzel *et al.* (103).

Molecules Trogocytosed and requirements for T cell trogocytosis

The process of trogocytosis occurs via the immune synapse in NK, B, and T cells, but only in T cells is the synapse and signaling an integral part of trogocytosis (103, 111, 129, 139, 141). Through the immune synapse, T cells trogocytose molecules from the c-SMAC, p-SMAC, and the d-SMAC. Among these are: costimulatory molecules

[including CD80 (103, 130, 142), CD86 (106), OX40 ligand (143), and programmed death ligand 1 (144)], adhesion molecules [including ICAM-1 (111)], and MHC:peptide complexes (103, 105-107, 119, 145-147). Also, T cells can acquire membrane lipids from the APC via the immune synapse (88, 107, 148).

Trogocytosis of membrane and membrane-bound molecules can also be measured using flow cytometry analysis. Fig. 7 shows histograms of $CD4^+$ T cells recovered from fibroblast APCs that had myristoylated-CFP membrane. In the left histogram, cells were antibody stained for trogocytosed MHC:peptide, and in the right histogram the trogocytosis of myristoylated-CFP-tagged APC plasma membrane is shown. The solid line represents T cells that were co-cultured with the myristoylated-CFP containing APCs. Both show a shift in the staining intensity for trogocytosed MHC:peptide and CFP membrane compared to the unstimulated sample (dotted line). These data show that one can monitor trogocytosis, such as the intercellular transfer of membrane proteins, along with plasma membrane using flow cytometry.

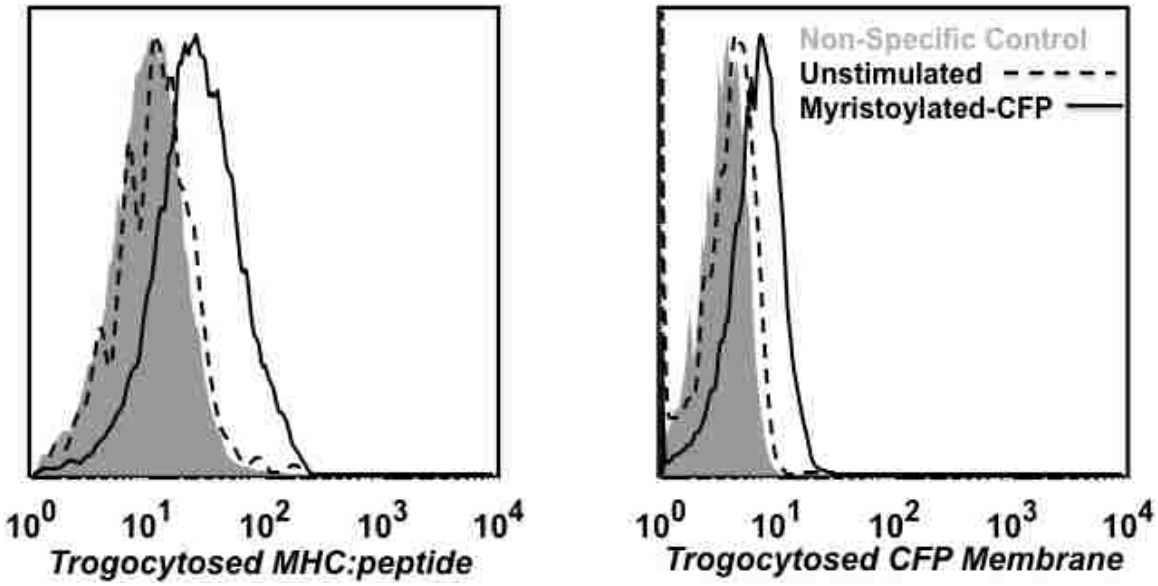

Figure 7. Measuring trogocytosis using flow cytometry. Flow cytometry can be used to measure receptor and membrane trogocytosis onto T cells. (left histogram) $CD4^+$ T cells recovered from myristoylated-CFP APC show increased staining for MHC:peptide on their surface (black line), compared to unstimulated T cells (dotted line), and non-specific antibody controls (shaded curve). (right histogram) Using the same $CD4^+$ T cells used in the left histogram, CFP fluorescence is measured showing higher levels of trogocytosed CFP membrane on the surface of T cells recovered from myristoylated-CFP APC (black line), compared to unstimulated cells (dotted line), and non-specific antibody controls. (Unpublished data by Dr. Scott Wetzel)

As mentioned above, an integral component of T cell trogocytosis is the engagement of the TCR by MHC:peptide (103, 111, 129). In the absence of TCR engagement, trogocytosis is significantly reduced or halted (103, 106, 122). Hudrisier *et al.* found that by blocking the initiation of TCR signaling using the Src kinase inhibitor, PP2, also blocked trogocytosis (107); as TCR signaling increased, trogocytosis also increased (107, 123), and that latruculin B, an inhibitor of actin polymerization, inhibits trogocytosis by T cells (107).

Our lab and others have shown that the amount and the specificity of the Ag being presented effects trogocytosis efficiency (103, 105-107, 119, 130, 142, 146, 149).

Trogocytosis efficiency is significantly lower in the absence of peptide (105-107) and is dose dependent (103, 105, 107, 130, 142). Wetzel *et al*. also found that $CD4^+$ T cell trogocytosis is peptide specific (103). Several other papers have confirmed that peptide specificity plays a role in trogocytosis (105, 107, 146).

Costimulatory molecules also play an important role in T cell trogocytosis. Using blocking antibodies or $CD28^{-/-}$ T cells, Hwang *et al.* found that T cells require interactions with costimulatory molecules, like CD80, on the APC for TCR mediated trogocytosis to occur (106). Their data give support to the hypothesis that the immune synapse is essential for trogocytosis, as it has been shown that CD80 is required for mature immune synapse formation (78, 150, 151).

The activation state of the T cell plays an important role in trogocytosis. One of the earliest T cell trogocytosis papers discovered that activated T cells performed trogocytosis better than naïve T cells (152). Since then, many others have found that resting or naïve T cells have reduced trogocytosis capabilities compared to activated T cells (104, 106, 124, 130, 142, 153). Hwang *et al.* and others have hypothesized that the increased expression of CD28 by activated T cells leads to increased adhesion that could result in this difference (106, 122, 130). Consistent with this hypothesis, activated T cells increase expression of their adhesion molecules, such as CD44 (31, 33), which could also lead to increased trogocytosis.

Trogocytosis mechanism

The mechanism of trogocytosis from APC to T cell remains unclear. Early data established that trogocytosis occurred via transsynaptic capture or directly from the immune synapse (120, 123). Using electron microscopy, Patel *et al.* observed that APC derived exosomes, which subsequently fused with the T cell, localized to the space between the T cell and the APC (120). Another method of transsynaptic capture was discovered by Stinchcombe *et al.,* where they showed that upon dissociation of a cytotoxic T lymphocyte (CTL) from its' target cell, small "membrane bridges" had formed between the cells (88). Resolution of the bridges lead to the transfer of MHC class I and YFP-tagged membrane onto the T cell from the APC (88).

More recently, TCR downmodulation and coincidental phagocytosis has been proposed as a mechanism for T cell trogocytosis. In 2011, Martin-Martin *et al.* found that phagocytic mechanisms, specifically involving the activity of the small GTPases TC21 and RhoG, drive TCR downmodulation at the c-SMAC (20). This is consistent with earlier data from Lee *et al.* and Cemerski *et al.,* showing the TCR is downmodulated at the c-SMAC (98, 154) and with the finding of Huang *et al*., who showed that $CD8^+$ T cells also perform trogocytosis by TCR downmodulation (105). These phagocytosed APC membrane fragments are delivered to endosomes (105) and it has been hypothesized that they fuse with the endosome membrane and upon recycling to the plasma membrane, the APC molecules are integrated into the T cell membrane in their native topology (20, 155). This model is depicted in fig. 8 (155).

Integration of trogocytosed molecules into the T cell plasma membrane

Imaging data by Wetzel *et al*. helped to confirm that trogocytosed molecules are integrated into the T cell plasma membrane. They showed that only after detergent permeabilizing the T cell membrane could they stain for the cytoplasmic GFP tail on trogocytosed GFP-tagged MHC:peptide (103). Other results from our lab also suggest that trogocytosed molecules are integrated into the T cells plasma membrane (fig. 9). After recovery of T cells from an *in vitro* trogocytosis assay, anti-I-E^k (I-E^k is the murine MHC class II) was added and the amount of trogocytosed GFP-tagged MHC:peptide was monitored over time. If the trogocytosed material were tethered, we would expect the antibody to disrupt and release the molecules from the surface of T cells, leading to a loss of GFP. In fig. 9, after 1 hr and up to 24 hrs with anti-I-E^k, there is still significant GFP on the surface of the recovered T cells (black line) suggesting the molecules have been integrated into the membrane. The presence of captured MHC:peptide and costimulatory molecules on the T cell surface, as a result of trogocytosis, suggests several potential roles for these molecules in T cell biology.

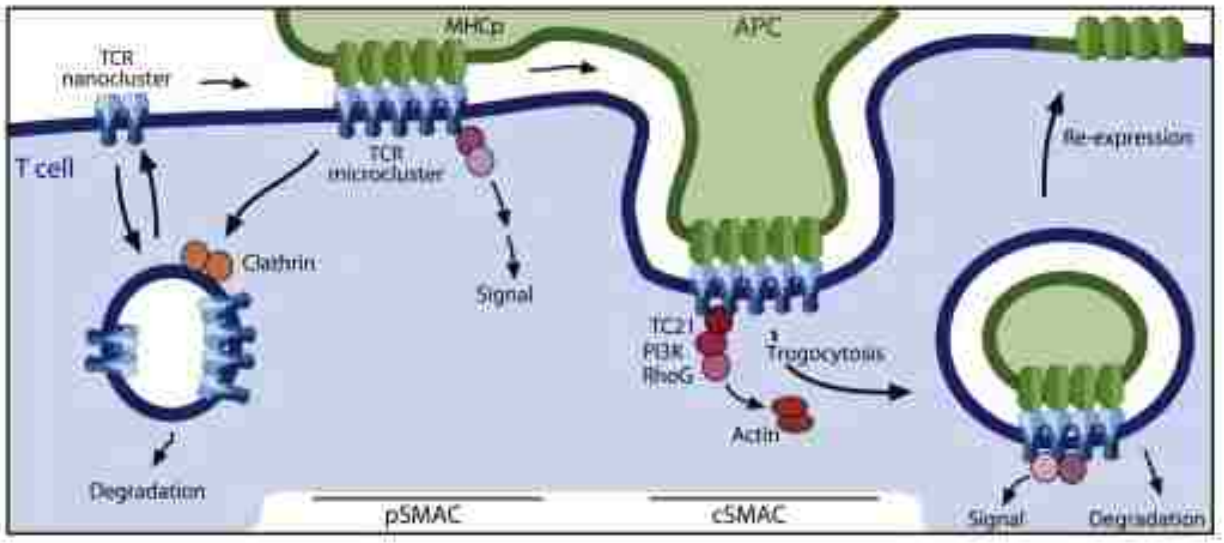

Figure 8. Proposed mechanism for trogocytosis. Two proposed mechanisms for TCR downmodulation. One occurs via clathrin dependent mechanisms in the p-SMAC and the second occurs via phagocytic mechanisms in the c-SMAC. The TCR internalization in the c-SMAC leads to the trogocytosis of APC molecules that are then re-expressed on the T cell surface. From Dopfer *et al.*(155).

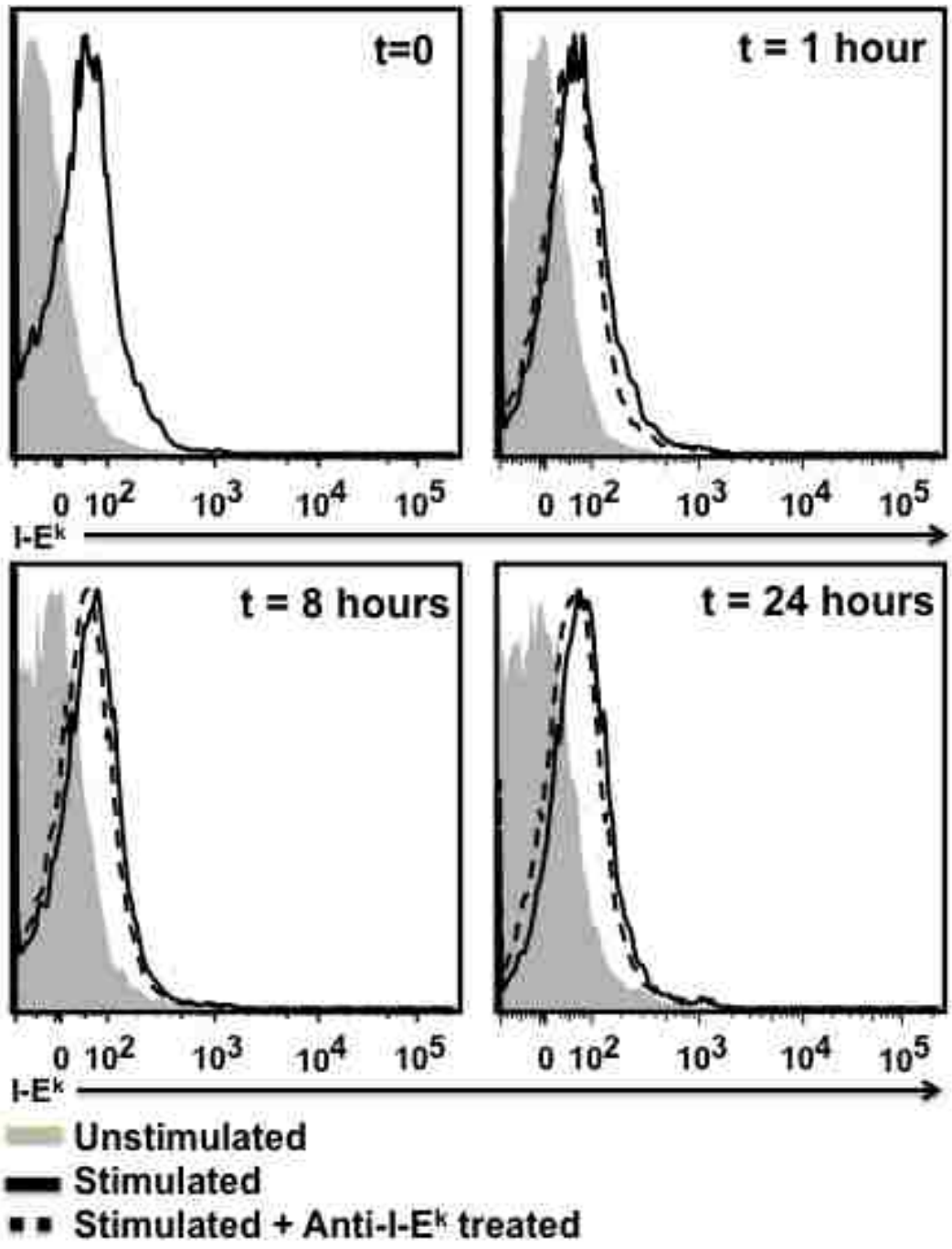

Figure 9. Trogocytosed molecules are integrated into the T cell membrane. After a 90 min co-culture with fibroblast APC, T cells were recovered and placed in culture with an antibody to I-E^k. Aliquots were taken at 1, 8, and 24 hours and stained for I-E^k. T cells with anti-I-E^k (black line) show higher levels of I-E^k staining compared to unstimulated T cells (shaded histogram) and similar to recovered T cells without anti-I-E^k (dotted line). (unpublished data by Dr. Scott Wetzel)

The function of trogocytosis

The biological significance of trogocytosis on $CD4^+$ T cells remains unclear. The potential role of trogocytosis in modulating immune responses falls into two broad categories: cell extrinsic and cell intrinsic. Extrinsic function relates to how the trogocytosis$^+$ ($trog^+$) T cell interacts with surrounding immune cells. The fact that trogocytosed molecules, including MHC:peptide and costimulatory molecules, are integrated into the T cell membrane in the correct orientation suggests that the $trog^+$ T cell may be able to present Ag (103, 107). As detailed below, several studies have observed that Ag presentation by $trog^+$ T cells can modulate the activation of responding T cells (146, 147, 156-160) (T-T Ag presentation). The intrinsic cellular function of trogocytosis relates to how trogocytosed material directly affects the individual $trog^+$ T cell biology. The few studies that have been done have shown that the trogocytosed material may continue to interact with surface receptors on the $trog^+$ T cell leading to continued activation and signaling in the absence of APC, a process called autopresentation (103, 161).

<u>$Trog^+$ T cells as APCs</u>

The presence of trogocytosed MHC:peptide and CD80 on the T cells has been shown in many studies to be involved in T cell to T cell Ag presentation (105, 107, 120, 130, 146, 150, 158, 159, 162-164) Analysis of T-T presentation first started in the 1970's with human T cells that endogenously express MHC class II, could be used to present Ag to other human T cells (165-174). The vast majority of these studies found that Ag

presentation by human or rat $CD4^+$ T cells (which also endogenously express MHC class II) leads to the induction of anergy in the responder T cells (165-167, 169-174). The induction of anergy in these responder T cells is likely due to a lack of costimulation on the surface of the presenting T cells. Of these studies, only two looked at T cell presentation of trogocytosed molecules (166, 168). One of the studies showed that $CD4^+$ T cells could pick up antigens of gp120, an HIV receptor, during Ag presentation with an infected T cell and use the antigens to help in the spread of HIV (168).

To study potential T-T Ag presentation as a result of trogocytosis, murine $CD4^+$ T cells are typically used because they don't endogenously express MHC class II (175). Several papers have examined the presentation of trogocytosed molecules by $CD4^+$ T cells (158, 159, 176). The initial studies of $CD4^+$ T cell trogocytosis and subsequent T-T presentation showed $CD4^+$ T cells presenting trogocytosed bystander MHC class I molecules and costimulatory molecules to $CD8^+$ T cells (147, 177, 178). Xiang *et al.* showed that $CD4^+$ $trog^+$ T cells can acquire bystander p:MHC class I with p:MHC class II at the synapse and act like T_H1 cells and activate $CD8^+$ T cells (147). The CD4-CD8 interaction leads to the clonal expansion and generation of effector functions in the $CD8^+$ T cells (147, 156, 177, 178). However, in the majority of trogocytosis-related studies, CD4-CD8 and CD4-CD4 Ag presentation have found that T-T presentation is a regulatory mechanism for inducing apoptosis, CTL killing (146, 178) or anergy (146, 158, 159, 179) in the responder T cells. Helft *et al*. found T-T presentation regulated responder T cells by inhibiting effector/memory cell activation, but allowed for naïve T cell survival (158). Most recently, Zhou *et al.* found that by adoptively transferring $trog^+$ T_H into TCR transgenic mice, the $trog^+$ T_H cells presented Ag to naïve T cells (159); this

increased CD25 expression in the responder. In contrast, when trog$^+$ T_{reg} cells were added with the effector cells, CD25 expression went down (159). These studies suggest that T cell Ag presentation has different effects on effector/memory cells and naïve T cells.

Trogocytosis intrinsic function

The presence of trogocytosed molecules may also have an effect on the biology of the individual trog$^+$ T cell. The presence of captured MHC:peptide and costimulatory molecules on T cells suggests the possibility of autopresentation, wherein the trogocytosed molecules on the surface of the T cell continue to engage receptors leading to signaling in the absence of APCs. Zhou *et al.* first studied the effects of autopresentation of CD4$^+$ T cells, by looking at the effects of antigen-presentasomes (APS), small exosomes derived from an APC tethered to the surface of T cells (161). They found that T cells with APC derived vesicles or APS attached to their surface, had increased levels of transcription factors NFκB and AP-1 which lead to proliferation and activation of the T cells in the absence of APC (161). However this study did not determine if the APS were responsible for signaling or if they just marked the cells that were signaling. In addition, this study did not involve actual "trogocytosis" because trogocytosis leads to the integration of trogocytosed molecules (103, 104, 152) and is not APC derived vesicles or APS tethered to the T cell surface (103, 155). Their experimental setup also strongly favored T-T presentation (161), casting further doubt on their results.

The study done by Wetzel *et al.* in 2005 was the first to examine signaling from trogocytosed molecules (103). Using fluorescent microscopy, they found that several TCR-associated signaling molecules, including phosphorylated tyrosine (pTYR) and Lck,

colocalized with the trogocytosed molecules on the surface of T cells recovered from APC (103). Their data suggest that there is sustained signaling occurring in the T cell due to autopresentation or continued engagement of the TCR with the trogocytosed molecules (103). Wetzel *et al*. and Zhou *et al*. studies were the only studies prior to the work detailed in this thesis analyzing intracellular signaling in trog^{+} CD4^{+} T cells. Autopresentation of trogocytosed molecules may play a role in signal "summing" (180) [i.e. repeated short-duration encounters that have been observed in T cell activation (181, 182)]. By continually engaging the TCR with trogocytosed MHC:peptide molecules may sustain intracellular signaling leading to continual activation, proliferation, and survival. An unresolved question regarding this potential autopresentation is whether trog^{+} T cells sustain signaling over time without the presence of APC and whether the sustained signaling is induced by the trogocytosed material, examining this question is the main focus of this thesis.

Rationale

The impact of trogocytosis on the biological function of T cells is unclear. In this thesis, I have examined the effects of trogocytosis on the individual $trog^+$ $CD4^+$ T cell. The goal of these experiments was to determine the role trogocytosis plays in $CD4^+$ T cell activation, sustained signaling, proliferation, and selective survival in the $trog^+$ T cells. A murine fibroblast cell line expressing an I-E^k molecule loaded with a covalently attached antigenic peptide (moth cytochrome C_{88-103}) and containing a GFP-tagged cytoplasmic tail was used as surrogate APCs and for T cells a peptide-specific TCR transgenic mouse was used. The GFP-tagged MHC:peptide on the APCs allows for the monitoring of trogocytosis by the presence of GFP on the surface of the T cells. Trogocytosis can also be monitored by antibody (Ab) staining, because murine T cells do not express MHC class II. Using a combination of high-resolution microscopy and flow cytometry, it was observed that the trogocytosed material is retained on the surface of the T cell.

The first aim was to determine what is required for the initial trogocytosis of molecules by T cells. Multiple studies have found that naïve T cells perform trogocytosis at reduced levels compared with activated T cells (104, 106, 124, 130, 142, 153), but none have looked at whether the initial interaction of the naïve T cell with APC leads to trogocytosis. Naïve T cells from AND x Rag-$1^{-/-}$ mice (mice with APCs that lack I-E^k) were use to determine if the initial Ag presentation was sufficient enough to induce significant trogocytosis. The data shows whether trogocytosis leads to the activation, proliferation, and selective survival of $trog^+$ $CD4^+$ T cells. Flow cytometry data will show

whether trog$^+$ T cells have an activated phenotype, proliferate, and survive longer in culture following recovery from APCs compared to trog$^-$ T cells.

The second aim was to assess whether trogocytosis leads to sustained signaling. Both Zhou *et al.* and Wetzel *et al.* have shown that signaling occurs in trog$^+$ T cells (103, 161), but neither has determined if the signaling persists over time in the absence of APC. Using wide-field microscopy, colocalization of several TCR associated-signaling molecules with the trogocytosed material was analyzed. Using flow cytometry, sustained signaling in trog$^+$ T cells, over several days, in the absence of APC to see if sustained signaling remained in trog$^+$ T cells and not in trog$^-$ T cells.

The final aim of this thesis was to determine whether sustained signaling observed in trog$^+$ T cells, is driven by the trogocytosed molecules. Zhou *et al*. showed that having tethered trogocytosed molecules on the T cell surface correlated with signaling in the trog$^+$ T cells (161), but they did not address if the trogocytosed molecules were responsible for the signaling. Using an inhibitor to TCR signaling, PP2, the role of trogocytosis in sustained signaling was examined. Using cultures of recovered T cells, PP2 was added for 10 min, duration long enough for TCR signaling inhibition, then washing out the inhibitor and incubate for 20 min to allow signal reinitiation. If TCR signaling rebounds it suggest there is continual engagement of the TCR by the trogocytosed material. Both flow cytometry and fluorescent microscopy data will determine if there is rebound in TCR signaling following removal of PP2 in recovered trog$^+$ T cells.

I conclude by showing preliminary T-T presentation data. Experiments were set up, using FACS sorted trog$^+$ AD10 T cells placed in culture with naïve AND x B10.BR T

cells, to determine if trog^{+} T cells present Ag to the naïve T cells. Ag presentation was confirmed by the activation of the naïve T cells by staining for activation markers (i.e. CD69 and CD25) using flow cytometry.

The findings from this dissertation will further help to elucidate the biological role of trogocytosis on CD4^{+} T cells by showing that trogocytosis leads to sustained signaling, proliferation, and selective survival of trog^{+} T cells. The data in this thesis suggest a possible role for trogocytosis in an immune response.

Chapter 2:

Materials and Methods

Animals

Heterozygous AD10 TCR transgenic mice ($V\beta3^+$), specific for pigeon cytochrome *c* fragment 88–104 (183) and reactive against moth cytochrome *c* (MCC) fragment 88–103 on a B10.BR ($H\text{-}2^k$) background, were kindly provided by S. Hedrick (University of California, San Diego, CA) by way of David Parker (OHSU, Portland, OR). This strain was maintained as heterozygotes by breeding to B10.BR mice, and transgenic mice were identified by PCR. Homozygous AND x Rag-$1^{-/-}$ TCR transgenic mice were purchased from Jackson Laboratory (Bar Harbor, Maine). AND x Rag-$1^{-/-}$ mice were maintained as homozygoytes. Heterozygous AND x B10.BR TCR transgenic mice were bred in the University of Montana Laboratory Animal Resources facilities Only F_1 animals resulting from breeding homozygous AND x Rag-$1^{-/-}$ mice with B10.BR mice were used in experiments. Mice were housed in the University of Montana Laboratory Animal Resources facilities and were allowed food and water *ad libitum*. All procedures were supervised and in accordance with the University of Montana IACUC.

Antibodies and staining reagents

The following conjugated or unconjugated Abs were purchased from BD Pharmingen (San Jose, CA): anti-TCR Vβ3 (clone KJ25), anti-ZAP70 PO_4 (Y319 ; clone 17 A/P-ZAP-70), anti-ERK PO_4 (MAPK p44/42 T202/Y204; clone 20a). CFSE, chicken anti-rabbit IgG AlexaFluor 647, AlexaFluor 647-conjugated streptavidin, Pacific Blue-

conjugated streptavidin, AlexaFluor 488-conjugated streptavidin, and Vybrant® CM-DiI cell solution were purchased from Life Technologies (Eugene, OR). Biotin conjugated anti-phosphotyrosine (4G10) was purchased from Upstate Biotechnology (Lake Placid, NY). Rabbit polyclonal antibodies specific for phosphorylated Lck (Y505; #2751) and phosphroylated ZAP-70 (Y319 Syk PO_4 Y352; #2701) along with a mouse IgG1 monoclonal anti-phosphroylated ERK 1/2 (MAPK p44/42 T202/Y204; #E10) were purchased from Cell Signaling Technology (Beverly, MA). Secondary staining reagents, including Aminomethylcoumarin Acetate (AMCA)-conjugated streptavidin, Cy5-conjugated polyclonal goat anti-armenian hamster IgG H+L, Texas Red-conjugated polyclonal goat anti-armenian hamster IgG H+L, Texas Red-conjugated polyclonal donkey anti-rabbit IgG H+L, and Texas Red-conjugated anti-mouse IgG H+L were purchased from Jackson ImmunoResearch Laboratories (West Grove, PA). Purified anti-CD3 (145.2C11), along with fluorescently conjugated anti-CD69 (H1.2F3), anti-CD4 (RM4-5), anti-C25 (PC61), anti-CD11c (N418), anti-F4/80 (BM8), and CD80 (16-10A1) were purchased from BioLegend (San Diego, CA). PE-conjugated anti-CD45R (B220) (RA3-6B2) was purchased from eBioscience (San Diego, CA). Anti-I-E^k (17-3-3) was purchased from Southern Biotechnology (Birmingham, AL). EZ-link® Sulfo-NHS-biotin (sulfosuccinimidobiotin) to label the cell surface was purchased from Pierce (Rockford, IL).

Antigen presenting cells

MCC:GFP fibroblasts expressing enhanced GFP-tagged I-E^k β-chain with covalently attached antigenic $MCC_{88\text{-}103}$ were described previously (184). A second

transfected fibroblast line, MCC:FKBP, has the MCC:I-E^k β-chain fused to three repeats of the FK506-binding protein (FKBP) (Ariad Pharmaceuticals, Cambridge, MA) in place of the GFP tag (103). The MCC:GFP and MCC:FKBP express nearly identical levels of CD80, ICAM-1 and surface MCC:I-E^k. A third transfected fibroblast cell line, P13.9H expresses CD80 and ICAM-1 similar to the other fibroblast cell lines, but it expresses I-E^k without antigenic peptide attached. P13.9 cells were provided by Dr. Ron Germain (NIAID, National Institutes of Health). Cells were maintained in "complete DMEM" containing high glucose DMEM (Life Technologies, Carlsbad, CA) supplemented with 10% FBS (Atlanta Biologicals, Atlanta, GA), 1 mM L-glutamine, 100 mg/ml sodium pyruvate, 50 μM 2-ME, essential and nonessential amino acids (Life Technologies, Carlsbad, CA), 100 U/ml penicillin G, 100 U/ml streptomycin, and 50 μg/ml gentamicin (Sigma, St. Louis, MO.).

In vitro T cell priming

Single cell suspensions of splenocytes from 6- to 12-wk-old AD10 transgenic mice or AND x B10.BR F_1 mice were depleted of erythrocytes by hypotonic lysis in Gey's solution and resuspended in "complete RPMI" containing RPMI (Life Technologies) supplemented with 10% FBS (Atlanta Biologicals, Atlanta, GA), 1 mM L-glutamine, 100 mg/ml sodium pyruvate, 50 μM 2-ME, essential and nonessential amino acids (Life Technologies), 100 U/ml penicillin G, 100 U/ml streptomycin, and 50 μg/ml gentamicin (Sigma, St. Louis, MO.). Cells were used directly *ex vivo* or were activated *in vitro* for 6 days by addition of 2.5 μM $MCC_{88\text{-}103}$ peptide to splenic cell suspensions at ~4 x 10^6 cells/ml . Lymphocytes were isolated from priming cultures by density

centrifugation using Lympholyte M (Cedarlane Laboratories, Burlington, NC). T cells were resuspended at 5 x 10^6/ml in phenol red-free complete RPMI and kept at 4°C until used.

Standard in vitro trogocytosis assay

To assess trogocytosis by the $CD4^+$ AD10 T cells, we used our previously described standard *in vitro* trogocytosis assay (103). Briefly, 1 x 10^6 MCC:GFP or MCC:FKBP cells were plated into individual wells of a six-well tissue culture plate (Greiner, Monroe, NC) and incubated overnight at 37°C. For cell surface labeling and to measure trogocytosis, either 2.5 x 10^7 MCC:GFP or MCC:FKBP cells/ml were placed in PBS (pH 8.0) and stained using 10 mM solution of EZ-link® Sulfo-NHS-biotin at room temperature for 30 min. These cells were washed three times in PBS with 100 mM glycine, resuspended in DMEM, and then plated at 10^6/well. In some experiments, 5 μM Vybrant® CM-DiI cell solution was also used to stain the cell surface of MCC:GFP or MCC:FKBP. For this staining, 5 μl/ml of CM-DiI was added to 10^6 MCC:GFP or MCC:FKBP cells/ml in Hank's Balanced Salt Solution (HBSS, Life Technologies) for 20 min at 37°C, washed in complete DMEM, and then the cells were incubated overnight 37°C. A total of 2.5 x 10^6 *in vitro* primed T cells were added to each well and the plates were centrifuged briefly (30 seconds at 200 x g) to promote T-APC interaction. The cells were then incubated for 90-minutes at 37°C. After the 90-minute incubation, T cells were recovered from the cultures by rinsing with PBS. No additional dissociating reagents were added (e.g., EDTA or trypsin) to aid in T cell recovery. In this way, only cells that had spontaneously dissociated from the APC were collected. After two PBS washes,

recovered T cells (containing both trogocytosis$^+$(trog$^+$) and trogocytosis$^-$ (trog$^-$)) were used immediately in microscopy or flow cytometry experiments, or were resuspended in complete RPMI at very low density (10^4/ml) and cultured for additional times up to 6 days. At the end of the incubation period, cells were resuspended at 10^6/ml before staining and fixation for flow cytometry experiments or addition to poly-L-lysine-coated LabTek II chambered coverslips for imaging, as described below.

In vitro naïve T cell trogocytosis assay

To assess trogocytosis by naïve T cells, AND x Rag-1$^{-/-}$ mice were used. In these experiments, 1 x 10^6 biotin labeled MCC:FKBP cells were plated into individual wells of a six-well tissue culture plate (Greiner, Monroe, NC) and incubated overnight at 37°C. A total of 2.5 x 10^6 AND x Rag-1$^{-/-}$ T cells were added to each well and the plates were centrifuged briefly (30 seconds at 200 x g) to promote T-APC interaction. The cells were then incubated for 6-24 hours at 37°C. After the 6-24 hour incubation, T cells were recovered from the cultures by rinsing with PBS, as described for the standard trogocytosis assay. Similar to the standard trogocytosis assay, after two PBS washes, recovered T cells (containing both trog$^+$ and trog$^-$) were used immediately in microscopy or flow cytometry experiments or were resuspended in complete RPMI at very low density (10^4/ml) and incubated for additional times up to 6 days. In some experiments, after 2 days T cells were restimulated using fresh biotin-labeled MCC:FKBP cells using the standard *in vitro* trogocytosis assay described above. To differentiate between trogocytosis that occurred in the primary stimulation compared to the restimulation, two different secondary staining reagents were used: AF488-conjugated and AF647-

conjugated streptavidin. Prior to the restimulation, T cells were stained with AF488-conjugated streptavidin to identify biotin that had been trogocytosed from the primary stimulation. Following the restimulation, the T cells were stained with AF647-conjugated streptavidin to identify biotin trogocytosis from the restimulation culture.

Flow cytometry

Cells were recovered from the cultures and resuspended at 10^6/ml in FACS buffer (PBS, pH 7.4 containing 2% BSA Fraction V (Sigma) and 0.1% NaN_3). The T cells were stained with the indicated reagents for 30-minutes at 4°C in FACS buffer. When necessary, after three washes, cells were stained for 20-minutes with secondary reagents in FACS buffer. To measure activation, cells were stained for the activation marker CD69 and CD25, along with the TCR (Vβ3) and CD4. Following a final set of three washes in FACS buffer, cell were resuspended in 500µl of FACS buffer and stored on ice protected from light until analyzed using a FACSAria II (BD Biosciences) in the UM Fluorescence Cytometry Core. Alternatively, after the final wash cells were fixed by addition of ice-cold fixative (4% paraformaldehyde and 0.5% glutaraldehyde) followed by a 45-minute incubation at room temperature. Following an additional set of FACS buffer washes, cells were resuspended in 500µl FACS buffer and were stored at 4°C in the dark for up to 3 days until analysis. To examine proliferation, cells were labeled with 5 mM CFSE in PBS prior to establishment of the *in vitro* priming cultures.

Examination of trogocytosis associated intracellular signaling by flow cytometry

To assess the activation state of TCR proximal (ZAP-70) and distal (ERK) intracellular signaling molecules, we modified the phosphorylation (phosflow) protocol of Chow *et al.* (185). After staining surface molecules on live cells, as described above, cells were fixed for 10-minutes in ice-cold fixative (4% paraformaldehyde and 0.5% glutaraldehyde in PBS). After two washes in PBS plus 5% FBS, cells were permeabilized/fixed for between 10-30 minutes with ice-cold 50% methanol in PBS and washed twice in PBS prior to staining. Cells were then stained with primary staining reagents for 30 min at 4°C in FACS buffer at a 1:100 dilution (2 μg/ml). After three washes, cells were stained for 20-minutes with secondary reagents in FACS buffer at a 1:200 dilution (2 μg/ml). After a final set of washes, cells were analyzed immediately or were stored at 4°C for up to 3 days before analysis on a FACSAria II. Data were analyzed with FlowJo 8.8.7 software (Tree Star, Ashland, OR) on a Macintosh iMac (Apple, Inc). As a positive control, AD10 T cells were activated using phorbol 12-myristate 13-acetate (PMA) (Sigma, St. Louis, MO.) or anti-CD3 (145-2C11). For PMA stimulation, following a 6 day *in vitro* T cell priming, 40 nM PMA was added to the cells for 10 min at 37°C, and then washed out immediately before the cells were stained. For anti-CD3 stimulation, following a 6 day *in vitro* T cell priming, 5 μg/ml anti-CD3 was added to the cells in solution for 30 min at 4°C. Following a wash with PBS, 10 μg/ml Texas Red-conjugated polyclonal goat anti-armenian hamster IgG H+L was added for 15 min at 4°C to cross-link the anti-CD3, unbound Ab washed out before the cells were stained.

Immune synapse microscopy

To examine the immune synapse, one day prior to imaging 2.5×10^4 MCC:GFP cells were added per well in #1.5 LabTek II eight-chambered coverslips (Nunc, Rochester, NY) and incubated overnight at 37°C. The next day 10^5 T cells were added to each well and the dishes were spun at 200xg for 30 sec to initiate contact between T cells and APCs. After a 30-minute incubation at 37°C, cells were fixed by addition of ice-cold fixative (4% paraformaldehyde and 0.5% glutaraldehyde in PBS) and incubated for 45-minutes at room temperature in the dark followed by permeabilization with 0.2% Triton X-100 in PBS for 10-minutes. Cultures were stained with primary Abs at concentrations of 10 μg/ml in imaging buffer (PBS plus 2% BSA Fraction V) for 2 h at room temperature in a humidified chamber. After three 5-min PBS washes, cells were incubated with secondary Abs (1:200 dilution in imaging buffer) for 2 h at room temperature. After three additional PBS washes, SlowFade Gold antifade reagent (Life Technologies) was added to the wells. Samples were stored at 4°C and protected from light until imaged.

T cell–APC conjugates to be imaged were chosen based upon their characteristic morphology in differential interference contrast (DIC) of T cells in tight contact with and flattened against an APC. A stack of 50–90 fluorescent images spaced 0.2 μm apart in the *z*-axis was obtained with a 60X, 1.4 NA, oil immersion lens on the Applied Precision (API) DeltaVisionRT image restoration microscopy system (Issaquah, WA).

Microscopic analysis of trogocytosis

To examine trogocytosis by microscopy, T cells were recovered from the standard *in vitro* trogocytosis assay after the 90-minute incubation by vigorous rinsing with PBS cells were immediately stained or incubated for up to 72 hrs before staining. For imaging of cells directly from the trogocytosis assay, 10^6 recovered T cells were placed in each well of Poly-L-Lysine pre-coated #1.5 LabTek II eight-chambered coverslips for 10-minutes at 37°C. For time course experiments, recovered T cells (containing both trog$^+$ and trog$^-$) were incubated at very low density (10^4/ml) for the indicated times before being placed in the Poly-L-Lysine coated chambered coverslips. Cells were fixed by addition of ice-cold fixative (4% paraformaldehyde and 0.5% glutaraldehyde in PBS) and incubated for 45-minutes at room temperature in the dark followed by permeabilization with 0.2% Triton X-100 in PBS for 10-minutes. Cells were antibody stained as described above, then imaged using an Applied Precision DeltaVisionRT microscopy system (Issaquah, WA). Cells were chosen for imaging in DIC by identifying isolated, individual T cells in the field (and without regard to potential fluorescence). T cells were imaged in the same manner as the T-APC conjugates, as described above.

Image analysis

Constrained, iterative deconvolution was performed using the API SoftWorx software package. Using SoftWorx the integrated intensity of GFP, which is a measure of the amount of fluorescently-labeled molecules accumulated, was obtained for areas ≥ 2-fold above background fluorescence. Background fluorescence was measured using a region of interest (ROI) that encompassed areas away from the cell. For the analysis of

phosphorylated signaling molecules, the integrated intensity and mean fluorescent intensity was obtained for areas ≥6 fold above background, again using ROI to measure background, unless otherwise noted. Maximum intensity projections (MIP) were used to create three-dimensional (3D) reconstructions for image analysis using the API SoftWorx software. Line profiles were used to measure pixel intensity and distances using the API SoftWorx software. For both recovered T cells and T-APC conjugates, 20-25 cells or conjugates were imaged for each treatment group in each of the six experiments. Integrated intensity and mean fluorescence intensity (MFI) were measured using single optical sections. Both MFI and integrated intensity were measured using ROIs that encompassed the trogocytosed molecules or intracellular signaling molecule. Co-localization between trogocytosed molecules and intracellular signaling molecules was assessed by the Pearson's correlation coefficient and overlap coefficients using the JACOP plug-in (186) in ImageJ (187).

TCR signaling inhibition

To determine if sustained signaling was due to engagement of the TCR by trogocytosed material, TCR signaling inhibition experiments were performed similar to those of Faroudi *et al.* (188). Cells incubated at very low density (10^4/ml) were treated for 10 or 30 minutes with 20 μM PP2, a Src-family tyrosine kinase inhibitor (189) (Life Technologies). Three treatment groups were set up for the TCR signaling inhibition experiments. In the first group, cells were incubated for 30-minutes in media only to serve as an untreated control. In the second group, cells were incubated with 20μM PP2 for 10-minutes followed by three washes to remove the PP2. Cells were incubated for 20

additional minutes in media. In the final positive-control group, cells were incubated for 30-minutes in the presence of 20μM PP2, to confirm that the PP2 treatment inhibited both TCR proximal and distal signaling events. After incubation, cells were fixed and stained for phosphorylated ZAP-70 (TCR proximal signaling) and phosphorylated ERK 1/2 (TCR distal signaling) for flow cytometry and imaging, as described above.

T-T presentation

To examine the potential of $trog^+$ T cells to present Ag, $trog^+$ T cells were FACS sorted and incubated with naïve AND x B10.BR T cells as potential responders. To generate the $trog^+$ cells, AD10 T cells were incubated with surface biotinylated and CFSE stained MCC:FKBP cells in the standard *in vitro* trogocytosis assay. The CFSE stain and lineage markers were used to identify and remove fibroblast, other contaminating cells. $Biotin^+$ $CFSE^-$ ($trog^+$) and $biotin^-$ $CFSE^-$ ($trog^-$) T cells were sorted using the FACSAria II in the UM Fluorescence Cytometry core. The cultures were also stained for the following lineage markers, B220 (B cells), F4/80 (Mθ), CD11c (DC). For each of the four experiments performed, ~10^7 $trog^+$ and $trog^-$ T cells were collected. To assess sort purity, 10^6 $trog^+$ and $trog^-$ T cells were stained with PerCP-conjugated anti-CD4 and analyzed by flow cytometry. To assess the ability of the $trog^+$ and $trog^-$ cells to present Ag, the sorted $trog^+$ or $trog^-$ T cells were placed in culture with CFSE-labeled naïve AND x B10.BR T cells at a 1:1 ratio overnight at 37°C. The CFSE staining allowed for identification of the naïve T cells. After the overnight coculture, T cells were recovered, stained, and analyzed using flow cytometry. $CFSE^+$ and $CFSE^-$ cell populations were compared using stains for activation markers CD69 and CD25, and trogocytosed biotin.

Peptide affinity

To assess whether antigenic peptide affinity affects trogocytosis by either $CD4^+$ AD10 or AND x B10.BR T cells, we used our previously described standard *in vitro* trogocytosis assay (103). Briefly, P13.9H cells were plated at 10^6/well into individual wells of a six-well tissue culture plate and incubated overnight at 37°C with peptides. Three peptides with varying TCR affinity were loaded onto P13.9H cells: a high-affinity agonist peptide MCC (ANERADLIAYLKQATK) (Sigma, Woodlands, TX), intermediate-affinity peptide MCC-A (AAAAAAAIAYAKQATK) (New England Peptide, Gardner, MA), or a very weak agonist altered peptide ligand MCC-K99A (ANERADLIAYLAQATK) (Sigma, Woodlands, TX). During the initial plating of the P13.9H cells, 2.5 μM of each peptide was added to the cell cultures. A total of 2.5 x 10^6 *in vitro* primed T cells were added to each well and the plates were centrifuged briefly (30 seconds at 200 x g) to promote T-APC interaction. The cells were then incubated for 90-minutes at 37°C. After the 90-minute incubation, T cells were recovered from the cultures by rinsing with PBS. No additional dissociating reagents were added (e.g., EDTA or trypsin) to aid in T cell recovery. In this way, only cells that had spontaneously dissociated from the APC were collected. After two PBS washes, recovered T cells (containing both trogocytosis$^+$($trog^+$) and trogocytosis$^-$ ($trog^-$)) were used immediately in flow cytometry experiments. Recovered T cells were resuspended at 10^6/ml before staining and fixation for flow cytometry experiments, as described above.

qRT-PCR

Quantitative RT-PCR was used to analyze the differences in gene expression between trog^{+} and trog^{-} T cells. Using the same cell sorting technique as described above, 10^{6} trog^{+} and trog^{-} T cells were placed in 1 ml Trizol overnight at 4°C to digest the cells and to recover mRNA and then sent to the Molecular Biology core at the University of Montana to perform qRT-PCR on the BioRad iCycler 5 (Hercules, CA). qRT-PCR was run using selected primers, shown in Table 1. Primers for T cell cytokines, *IL-2, IFNγ, IL-4,* expression were used to determine which T cell subsets, T_H1 or T_H2 performed trogocytosis. Primers for pro-apoptosis molecule *Bad* and anti-apoptotic molecule BCL_2, were used to determine if there is an increase or inhibition of apoptosis. Primers for cell cycle molecules $p27^{KIP1}$, which is involved in G1 cell arrest, *c-Fos*, and *cyclin D2,* which play a role in cell cycle progression, were used to determine if the cells are preparing for proliferation. Primers were purchased from Integrated DNA Technology (Coralville, IA). Data was returned from the core and analyzed by the $\Delta\Delta C_t$ method to determine fold changes in gene expression using Microsoft Excel.

Table 1. qRT-PCR primer sets:

Gene	5' Primer	3' Primer
IL-2	GCTGTTGATGGACCTACAGGA	TTCAATTCTGTGGCCTGCTT
IFNg	ATCTGGAGGAACTGGCAAAA	TTCAAGACTTCAAAGAGTCTGAGG
IL-4	GAGAGATCATCGGCATTTTGA	AGCCCTACAGACGAGCTCAC
Bad	AAGTCCGATCCCGGAATCC	GCTCACTCGGCTCAAACTCT
Bcl-2	GTGGGATGCTGGAGATGC	GGCATTGGGTTGCTCTCA
p27	TCAAACGTGAGAGTGTCTAACG	CCGGGCCGAAGAGATTTCTG
c-Fos	CGGGTTTCAACGCCGACTA	TTGGCACTAGAGACGGACAGA
Cyclin D2	GAGTGGGAACTGGTAGTGTTG	CGCACAGAGCGATGAAGGT

Statistical analysis and graphing

Statistical analysis (student's *t* test) and graphing were performed using Prism 4 (GraphPad Software, La Jolla, CA). Significance was defined as $p \leq 0.05$.

Chapter 3:

Results

The presence of APC-derived molecules on the surface of T cells, as a consequence of trogocytosis, raises the possibility that these molecules play a role in immune modulation. It has previously been shown that trogocytosis may allow T cells to act as antigen presenting cells (146, 147, 156, 158, 190), but the biological effect of trogocytosis on the individual T cell remains unclear. In support of a potentially biologically significant role of trogocytosis on individual cells, our lab previously reported that the acquired MHC:peptide molecules co-localized with elevated phosphorylated tyrosine (pTyr) and the TCR-proximal kinase $p56^{Lck}$ (Lck) (103). This suggests that the trogocytosed molecules are associated with sustained intracellular signaling after dissociation from APC. In this thesis, I examine the biological effects of trogocytosis on individual $CD4^+$ T cells, specifically looking at sustained signaling, proliferation, and cell survival.

Measuring Trogocytosis

To identify $trog^+$ T cells, several different cell-labeling methods were used. Our previous studies relied upon the detection of GFP-tagged MHC:peptide molecules trogocytosed from APC. In addition, we have observed APC plasma membrane transfer onto the T cells by monitoring the trogocytosis of myristoylated-CFP (fig. 7). To compare trogocytosis efficiency of different markers, T cells were incubated with fibroblast APCs and stained using several different staining protocols. Histograms for

several trogocytosed markers are shown in fig. 10. Trogcytosis was measured using GFP-tagged MHC:peptide (fig. 10A) and fluorescently conjugated antibodies (Ab) to I-E^k (fig. 10B). Murine T cells do not express MHC class II, so the presence of MHC signifies that trogocytosis has occurred. In fig. 10A, GFP mean fluorescence intensity (MFI) is measured on the surface of the T cell using flow cytometry. AD10 T cells recovered from fibroblast APC expressing GFP-tagged MHC (blue line) have a ~30 fold higher MFI than T cells placed in culture without APC (red line). Using Abs specific for trogocytosed MHC (fig. 10B) there is significant transfer of MHC detected (~6 fold higher MFI), but the Ab staining is not as sensitive a measure of trogocytosis compared to the GFP-tagged MHC:peptide (fig. 10A). In fig. 10C, lipophilic dye CM-DiI is used to stain the surface of APC prior to co-culture with T cells. To measure membrane trogocytosis, T cells were recovered from CM-DiI stained fibroblast APCs. The histogram in fig. 10C shows that T cells recovered from CM-DiI stained APC (dotted line) have a 31 fold higher MFI than the unstimulated T cell control (black line). The final method tested was to biotinylate the surface of the APCs prior to incubation with T cells. T cells were stained with streptavidin (SA) conjugated to fluorophore Pacific Blue (PB) to detect biotin trogocytosis. The results in fig.10D show that biotinylated APC membrane proteins are trogocytosed by the T cells and are easily detected by flow cytometry. Biotin trogocytosis was not as significant as CM-DiI trogocytosis, showing only a 24 fold increase in MFI for the recovered T cells compared to the unstimulated control.

As with the I-E^k data in figures 10A and 10B, there is significant transfer of biotin from APC to T cells. This verifies that this method is able to efficiently detect

trogocytosis. The data in fig. 10 show that each of these methods can be used to assess trogocytosis.

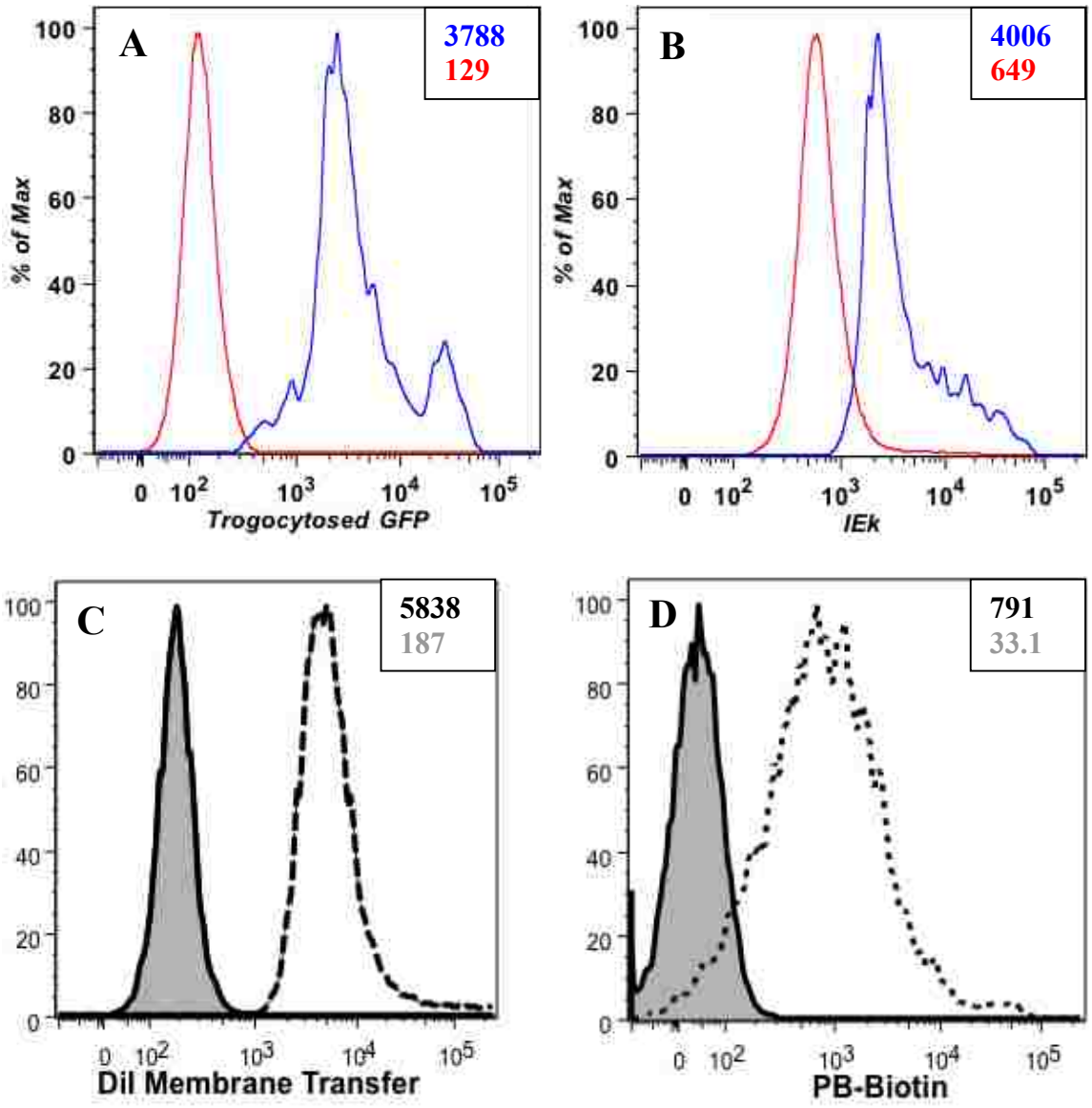

Figure 10. Measuring Trogocytosis using different APC-labeling methods. Multiple protocols were used to measure trogocytosis from the APC to the $CD4^+$ T cells. (A) The detection of GFP-tagged MHC:peptide trogocytosed from APCs is shown. (B) Similarly, the detection of I-E^k trogocytosed from APC shown by anti-I-E^k staining is displayed. (A and B) Blue lines represent T cells recovered from APC and red lines represent T cells cultured in the absence of APC. (C) The detection of CM-DiI stained membrane

trogocytosed from APC. (D) The detection of biotin trogocytosed from APC. To measure biotin trogocytosis, a secondary antibody specific for biotin, streptavidin-Pacific Blue, was used to stain (D). (C and D) Dashed lines represent T cells recovered from APC and the solid filled-in curve represents T cells cultured in the absence of APC. Black number represents recovered T cells and the gray letter represents the T cells minus APC. Data are representative of twelve separate experiments.

Naïve T cell Trogocytosis

The experiments shown in fig.10 used T cells that had been primed *in vitro* with peptide and before use in the *in vitro* trogocytosis assay. It is unclear how efficient naïve T cells can carry out trogocytosis. To address the question of whether T cells require previous Ag recognition to efficiently perform trogocytosis, naïve $CD4^+$ T cells from an AND x Rag-$1^{-/-}$ mouse were used. The cells were placed in culture with biotinylated fibroblast APC for 6-24 hours (primary stimulation), which has been shown to induce naive T cell activation (11). The AND x Rag-$1^{-/-}$ mice were used because the T cells were naïve due to the fact that their APCs do not express I-E^k. To determine the extent of naïve T cell trogocytosis, following recovery from APCs the T cells were either stained immediately and analyzed using flow cytometry or were placed in culture and aliquots were taken and stained daily for up to 6 days. After a 6 hour co-culture, naïve T cells were $CD69^{lo}$, suggesting they were not activated (fig. 11A). In a parallel set of experiments, the naïve T cells recovered from an initial *in vitro* trogocytosis assay were restimulated 2-3 days following recovery from the primary stimulation. To differentiate between the trogocytosis that occurred during the primary stimulation with the trogocytosis that occurred in the secondary stimulation, T cells were stained for trogocytosed biotin from the primary stimulation using SA-AlexaFluor 488 (AF488) before restimulation, while trogocytosis occurring in the secondary culture was detected using SA-AlexaFluor 647 (AF647). Trogocytosis was compared between the primary

stimulation of 6-24 hrs to the secondary stimulation occurring at 2-3 days following recovery.

Fig. 11 shows that naïve T cells require a second round of stimulation for efficient trogocytosis to occur. Following a six-hour co-culture with fibroblast APC (primary stimulation), the recovered naïve T cells (blue line) showed a 15% increase in biotin on their surface, which is similar to the unstimulated T cells (red line; fig. 11B). In contrast, when cells had been Ag stimulated and then rested for 3 days prior to restimulation, there was a 16 fold increase in trogocytosis (fig.11C). These results show that the initial 6 hr incubation does not result in T cell activation (as measured by CD69 and TCR staining). The level of trogocytosis, while detectable, is minimal (15% increase in MFI). In fig. 11D scatter plots of trogocytosis from the primary stimulation (AF488) versus trogocytosis from the secondary stimulation (AF647), shows the significant difference in trogocytosis that occurred between the two stimulations. 69.1% of the T cells are $AF647^{hi}AF488^{lo}$ and only 4.54% of the T cells are $AF647^{hi}AF488^{hi}$, suggesting more trogocytosis occurred after the secondary stimulation. This shows that a majority of the trogocytosis occurred by naïve T cells that did not trogocytose biotin during the primary stimulation.

After resting 3 days, the cells have significantly higher levels of trogocytosis. This data suggest that prior Ag stimulation significantly enhances T cell trogocytosis potential. The increase in trogocytosis could be due to T cells increasing their avidity for APCs.

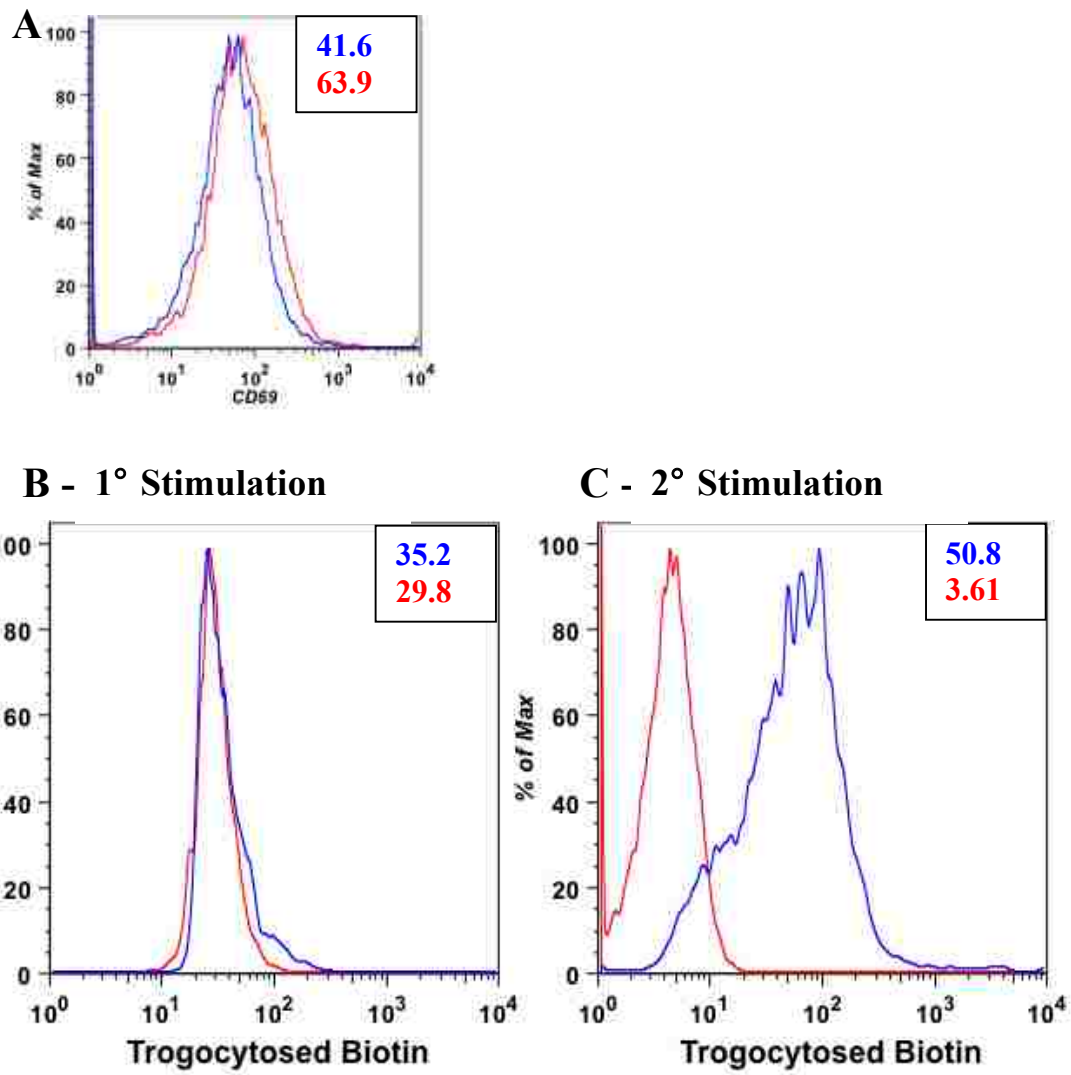

Figure 11. Primary vs. secondary stimulation of naïve T cell shows increased trogocytosis during the secondary stimulation with APCs. Using the naïve T cell *in vitro* trogocytosis assay, trogocytosis of surface biotin by naïve AND x Rag-1$^{-/-}$ T cells was measured. (A and B) Primary stimulation: gated naïve CD4^{+} T cells recovered after 6-hour co-culture with fibroblast APC stained for CD69 and trogocytosed biotin. (C) Secondary stimulation: following a 3 day rest, T cells were placed with APC and recovered after a second 90 min co-culture. Blue lines represent recovered T cells and the red lines represent T cells placed in culture without APC. (D) Secondary stimulation: gating primary vs. secondary stimulation trogocytosis, using SA-AF488 and SA-AF647. Data are representative of four separate experiments.

Trogocytosis correlates with naïve T cell proliferation

The difference in trogocytosis between the primary stimulation and secondary stimulation of naïve $CD4^+$ T cells can be seen in fig. 11. The limited amount of trogocytosis in the 6 hr primary stimulation of the naïve T cells, seen in fig. 11B may be due to the length of the primary stimulation. To determine whether extended stimulation of naïve T cells could result in enhanced trogocytosis, naïve T cells were Ag stimulated for 24 to 96 hours. This time interval has previously been shown to allow enough time for the naïve T cells to initiate proliferation (11). To induce activation of primary naïve AD10 T cells *in vitro*, $MCC_{88\text{-}103}$ peptide was added to an AD10 whole spleen suspension culture. The physiologic APC in the spleen cell suspension serves as an APC in this experiment. Proliferation of the $CD4^+$ T cells was monitored by CFSE dilution over four days and daily proliferation vs. trogocytosis results for $CD4^+$ $V\beta3^+$ T cells are shown in fig. 12. Before the cultures were established (day zero) the naïve T cells were bimodal with respect to trogocytosed I-E^k, with approximately 25% of the cells being I-E^{k+} directly *ex vivo*. While the frequency number of $trog^+$ cells varies between the 20 separate experiments, the frequency of MHC^+ TCR transgenic cells directly *ex vivo* ranges between 10 and 25%. This has also been observed in 4 other TCR transgenic and non-transgenic strains our lab has tested (OT-II, 3.L2, AND x B10.BR, B10.BR). The nature of this *in vivo* trogocytosis by naïve cells is unknown, but it is potentially the result of positive selection events (121) or tonic stimulation *in vivo* by selecting ligands in the periphery (191). By day one, the frequency of $trog^+$ T cells almost doubled to 46.5%. Of note, only the $trog^+$ population had begun to divide, with 57.8% of the $trog^+$ cells dividing

on day one. Thus, the earliest cell division correlates with cells being trog$^+$, although it is unclear whether this proliferation is driven by trogocytosis.

The results on day two showed that both the trog$^+$ cells and the trog$^-$ population were proliferating, but the frequency of dividing cells was still significantly higher for the trog$^+$ population. By day three, both trog$^+$ and trog$^-$ populations were clearly dividing. The trog$^-$ population was bimodal with 91% of the cells dividing up to 4 times, while 9.0% remained undivided. The proliferation of the trog$^-$ cells surpassed that of the trog$^+$ cells by day three; however, the frequency of trog$^+$ cells had decreased between days two and three. The remaining trog$^+$ cells had 4.77-fold higher surface I-E^k than the trog$^-$. The reduction in the trog$^+$ cells on day three was likely not due to activation induced cell death, as measured by staining cells with Annexin V and 7-AAD (data not shown). This raises the possibility that an alternative, such as dilution by proliferation by distribution onto daughter cells, was responsible for the decrease in the trog$^+$ cells. By day four, more than 92% of the CD4$^+$ cells had divided and few trog$^+$ cells remain. Of the proliferating cells, more than 82% were trog$^-$. Taken together, the data in fig. 12 suggest that it is the trog$^+$ cells that initially divide upon Ag stimulation, followed by the proliferation of trog$^-$ cells. Additionally, fig. 12 raises the possibility that as the trog$^+$ cells divide, the trogocytosed I-E^k may be diluted among daughter cells, reducing the apparent frequency of trog$^+$ cells and significantly increasing the apparent number of dividing trog$^-$ cells. Thus, by day four the dividing cells appear to be overwhelmingly trog$^-$. The data in fig.12 shows that initially naïve T cells do have trogocytosed I-E^k on their surface (day zero), which differs from the data shown in fig. 11. This difference is likely due to differences in the experimental systems. For fig. 11, naïve T cells are from I-E^k negative TCR Tg

mice, whereas in fig. 12 T cells are taken from mice that have I-E^k positive APCs, which allow for Ag presentation to occur. From the data in fig. 12, naïve T cells from *in vitro* priming cultures show a correlation between trogocytosis and proliferation.

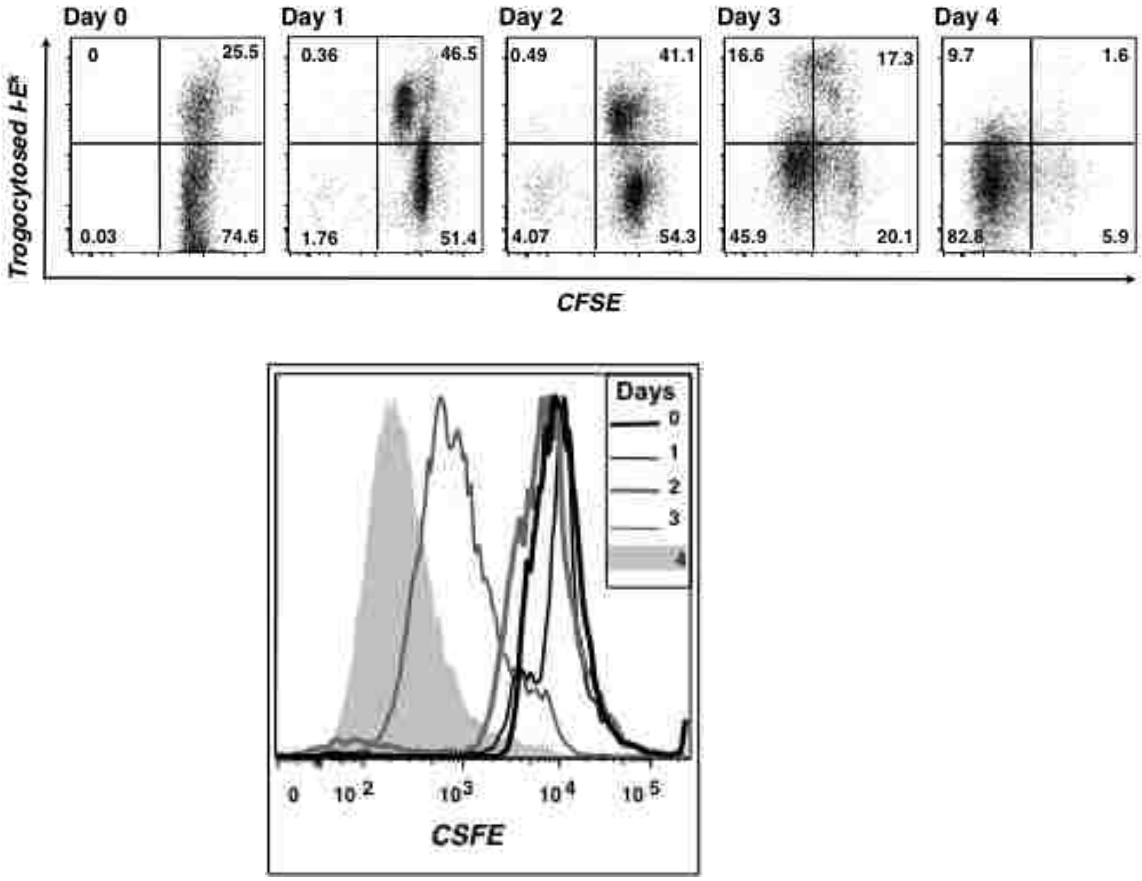

Figure 12. *In vitro* trogocytosis is associated with more rapid proliferation of naïve T cells. (Top) T cells were removed from *in vitro* priming cultures daily for 4 days and $CD4^+V\beta3^+$ cells were analyzed for trogocytosed I-E^k and CFSE dilution. CFSE histogram overlay (bottom) comparing T cell proliferation over the course of the 4-day experiment. Data are representative of three separate experiments.

Trogocytosis negative cells recognize antigen and are activated similar to trogocytosis positive cells

After recovery from the *in vitro* trogocytosis assay, T cells are clearly $trog^+$ or $trog^-$. It is unclear whether this reflects differences in activation or the ability to perform

trogocytosis. To examine the hypothesis that *in vitro* Ag recognition by trog$^-$ cells was not as efficient by the trog$^+$ cells, the standard *in vitro* trogocytosis assay was used to characterize the activation state of trog$^+$ and trog$^-$ cells. The activation state of trog$^+$ and trog$^-$ T cells was assessed by TCR (Vβ3) downmodulation and CD69 upregulation. As predicted, the trog$^+$ T cells had elevated CD69 expression along with substantial TCR downmodulation (fig. 13), indicating that they recognized Ag and were activated. These results are consistent with our previously published data (103). Somewhat unexpectedly, the trog$^-$ T cells also expressed high levels of CD69 and TCR downmodulation, clearly showing that the trog$^-$ T cells also interacted with APCs and were activated. There were small experiment-to-experiment variations in the levels of CD69 and TCR downmodulation, but over the course of 6 separate experiments, these differences were not significant.

The results in fig. 13 suggest that the difference between trog$^+$ and trog$^-$ cells is not simply the lack of Ag recognition by the trog$^-$ cells since it appears that both trog$^+$ and trog$^-$ T cells are similarly activated. To determine if there are biological differences between trog$^+$ and trog$^-$ T cells, CD69 expression was monitored following recovery from APC co-culture for several days.

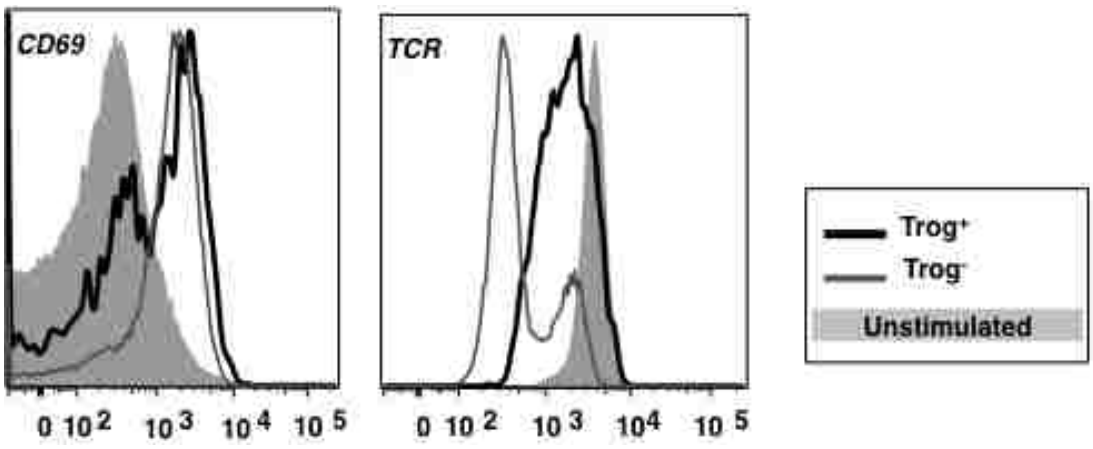

Figure 13. Trog$^+$ and trog$^-$ T cells have an activated phenotype. Both trog$^+$ and trog$^-$ AD10 T cells are activated during standard *in vitro* trogocytosis assay using MCC:FKBP APCs. CD69 (left) and TCR (right) expression on T cells recovered from fibroblast APC. Data are representative of six separate experiments. (192)

Sustained CD69 expression in trog$^+$ T cells

In fig. 13, immediately following recovery, both trog$^+$ and trog$^-$ T cells have recognized Ag and, based upon CD69 expression, have become activated. Since trogocytosis does not appear to differentiate activated and non-activated T cells, it is unclear whether this phenomenon is physiologically significant. To examine whether there is an advantage to the individual T cell to carry out trogocytosis, changes in CD69 expression overtime in the recovered T cells were examined. After the 90-minute co-culture, recovered T cells were placed in culture dishes at low density to limit potential T-T antigen presentation events. Aliquots were removed from the cultures at different time points up to three days. As shown in fig. 14, there are significant differences in the expression of CD69 between trog$^+$ and trog$^-$ CD4$^+$ T cells. Immediately after removal from APC (time 0), the MFI of CD69 is 4.18 fold higher for trog$^+$ cells (thick black line) than in the trog$^-$ T cells (thin black line). The trog$^-$ cells are nearly identical to unstimulated T cell controls (shaded histogram). In fig. 13 CD69 expression is similar

between trog$^+$ and trog$^-$ T cells. The reason for the difference seen at t=0 in fig. 14 could be due to experiment-experiment variations. By 30 min, the CD69 MFI of the trog$^+$ T cells is 4.9 fold higher than the trog$^-$ T cells and is similar to the anti-CD3-stimulated positive control (thick gray line). Over the next two hours, CD69 MFI for trog$^+$ cells remains nearly the same with CD69 levels staying at 3-4 fold higher than trog$^-$ cells. After 3 hours, the level of CD69 steadily decreases in the trog$^+$ cells, but remains 5.5 fold higher than trog$^-$ cells. The level of CD69 in the trog$^+$ cells remains very similar to the anti-CD3 positive control during this time frame. From twenty-four to seventy-two hours, the trog$^+$ T cells still have significantly higher CD69 levels, 2-4 fold higher MFI, compared to the trog$^-$ T cells, which remain similar to the unstimulated control cells. Thus, there is sustained CD69 expression only in trog$^+$ T cells.

The CD69 results in fig. 14 suggest that there are differences between trog$^+$ and trog$^-$ cells following T cell recovery from APC. The higher CD69 levels in trog$^+$ T cells over time suggests sustained activation in these cells. Since CD69 requires continued signaling for its expression (193), the sustained CD69 on the trog$^+$ T cells could be due to sustained signaling by the continued engagement of T cell receptors by the trogocytosed molecules. In the remainder of this thesis I will assess whether there are other potential biological advantages for the individual T cells that perform trogocytosis.

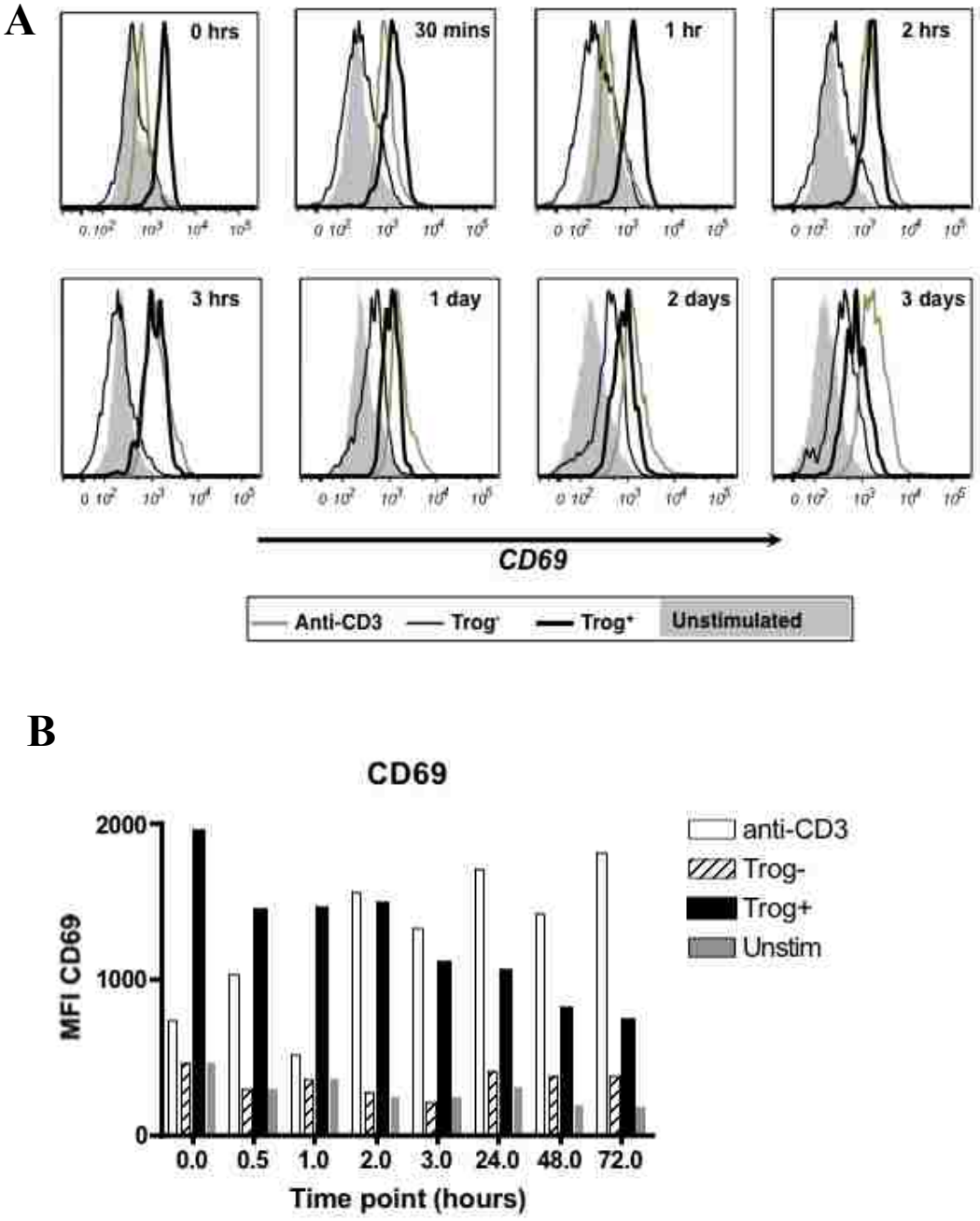

Figure 14. Sustained CD69 expression in trog$^+$ CD4$^+$ T cells. (A) AD10 T cells were recovered from the standard *in vitro* trogocytosis assay using MCC:FKBP APCs and fixed immediately (0 h) or were cultured for the indicated times before fixation and Ab staining. The levels of CD69 in CD4$^+$Vβ3$^+$ gated trog$^+$ (thick black line), trog$^-$ (thin black line), and unstimulated cells (shaded histogram) are shown for each time point. Cross-linked anti-CD3 (gray line) was used to stimulate TCR signaling as a positive control. (B) Mean fluorescence intensity values for the CD69 flow cytometry data in (A). Data are representative of six separate experiments.

Selective survival of trogocytosis$^+$ CD4$^+$ T cells in vitro after removal of APC

As shown in figures 13 and 14, both trog$^+$ and trog$^-$ cells recognize Ag and become activated, but only the trog$^+$ cells sustain CD69 expression. To examine whether this difference correlated with any selective advantages for the trog$^+$ T cells, I examined the fate of the trog$^+$ and trog$^-$ cells over several days after removal from GFP-tagged MHC:peptide expressing APCs. T cells recovered from the standard *in vitro* trogocytosis assay were placed in culture dishes at low density to limit potential T-T Ag presentation events. The frequency of trog$^+$ (GFP$^+$) and trog$^-$ (GFP$^-$) cells was monitored daily over five days by flow cytometry. On day zero, the trog$^+$ T cells made up roughly 35.1% of the T cells in the cultures, while 64.8% of the CD4$^+$ T cells were trog$^-$ (fig. 15). By day one a significant change in the proportion of trog$^+$ and trog$^-$ T cells in the culture occurred, with the trog$^+$ T cells more than doubling to 72.7% of the CD4$^+$ cells. This trend continued on days two and three, where the trog$^+$ cells represented 78.8% and 82.2% of the viable CD4$^+$ cells in culture. By day three the trog$^-$ T cell population represented only 17.5% of the viable CD4$^+$ T cells. The population of trog$^+$ cells peaked on days three and four at 82.2% of the viable CD4$^+$ cells and decreased slightly on day five to 73.9%. While there is an overall reduction of viable CD4$^+$ cells over the five-day culture period, the proportion of trog$^+$ to trog$^-$ cells changes dramatically. The results in fig. 15 strongly suggest that trog$^+$ cells selectively survive in culture after removal from APCs. There is a slight reduction in the GFP levels between day zero and one, but the level remains fairly constant after day one. This is consistent with our previously published data (103). Interestingly, the trog$^+$ cells do not appear to be proliferating significantly in this culture

because the level of GFP on the trog$^+$ cells is not significantly reduced on days four and five, as would be expected if the GFP was equally distributed among daughter cells as a result of proliferation. Taken together, the results in figures 12-15 suggest that the trog$^+$ cells are activated, proliferate, sustain activation, and selectively survive after removal from APCs.

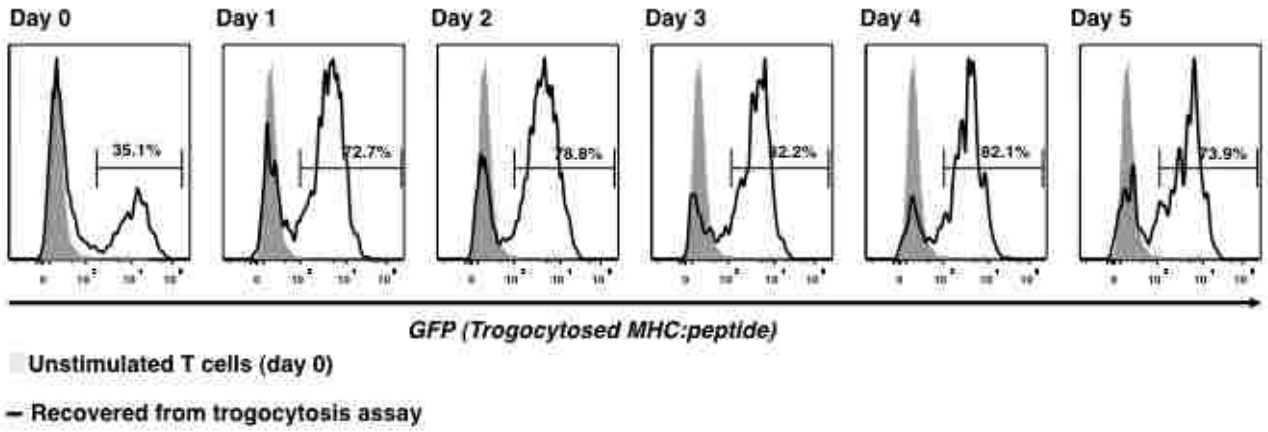

Figure 15. Selective survival of trog$^+$ T cells. AD10 trog$^+$ T cells preferentially survive after removal from GFP-tagged MHC:MCC expressing APCs. T cells were recovered from standard *in vitro* trogocytosis assay and cultured at low density (10^4/ml). At indicated time points, the presence of trogocytosed GFP-tagged MHC:peptide on CD4$^+$Vβ3$^+$ gated cells was determined by flow cytometry. The levels of trogocytosed MHC:peptide on day 0 unstimulated (gray shaded) and on recovered T cells at the indicated time point (black line) are shown. Horizontal region markers indicate the frequency of trog$^+$ cells in the cultures. Data are representative of four separate experiments. (192)

Sustained TCR-proximal intracellular signaling in trogocytosis$^+$ T cells

The results in figures 12-15 suggest that trog$^+$ cells have sustained activation and selective survival after removal from APCs compared to trog$^-$ cells. It is unclear whether trogocytosed molecules drive this T cell activation and survival or simply mark differentially activated cells that survive. One potential explanation consistent with a

direct role for the trogocytosed molecules in the selective survival of trog$^+$ cells is that these molecules are engaging the TCR and costimulatory receptors on the T cell surface and sustaining intracellular signaling. Consistent with this possibility, we have previously shown that pTyr and the Src kinase Lck accumulate with trogocytosed molecules on T cells after removal of APC (103). To examine the hypothesis that the trogocytosed molecules sustain intracellular signaling leading to T cell activation and survival, TCR signaling in T cells recovered from APC was assessed by flow cytometry and imaging.

As a measure of TCR signaling events, the phosphorylation and activation state of the TCR-proximal Syk family kinase, ZAP-70 and the TCR-distal MAP kinase, ERK were examined. To measure the phosphorylation of molecules in T cells recovered from the standard *in vitro* trogocytosis assay, phospho-specific Abs and phosflow (185, 194) were used. This technique is as sensitive as traditional biochemical methods (194) and requires significantly fewer cells. To establish the method for analysis of pERK and pZAP-70 levels, AD10 T cells were pharmacologically stimulated. For pERK, T cells were treated with 5 nM phorbol myristate acetate (PMA), which has a structure analogous to diacylglycerol (DAG), to activate PKC and induce the activation of the ERK. To increase intracellular pZAP-70, T cells were treated with 5 μg/ml anti-CD3 in solution, followed by a secondary Ab, to crosslink CD3, leading to ZAP-70 phosphorylation. In fig. 16, T cells show elevated pERK (dotted line) and pZAP-70 (black line) staining following activation with PMA and anti-CD3 compared to the untreated cells (shaded histogram). T cells stimulated with PMA showed a 2.2 fold increase in pERK MFI compared to unstimulated cells, while anti-CD3 stimulated cells showed a 3.1 fold increase in pZAP-70 MFI compared to the unstimulated sample. These

results confirmed that phosflow analysis can be used to measure intracellular signaling in trog^{+} and trog^{-} T cells.

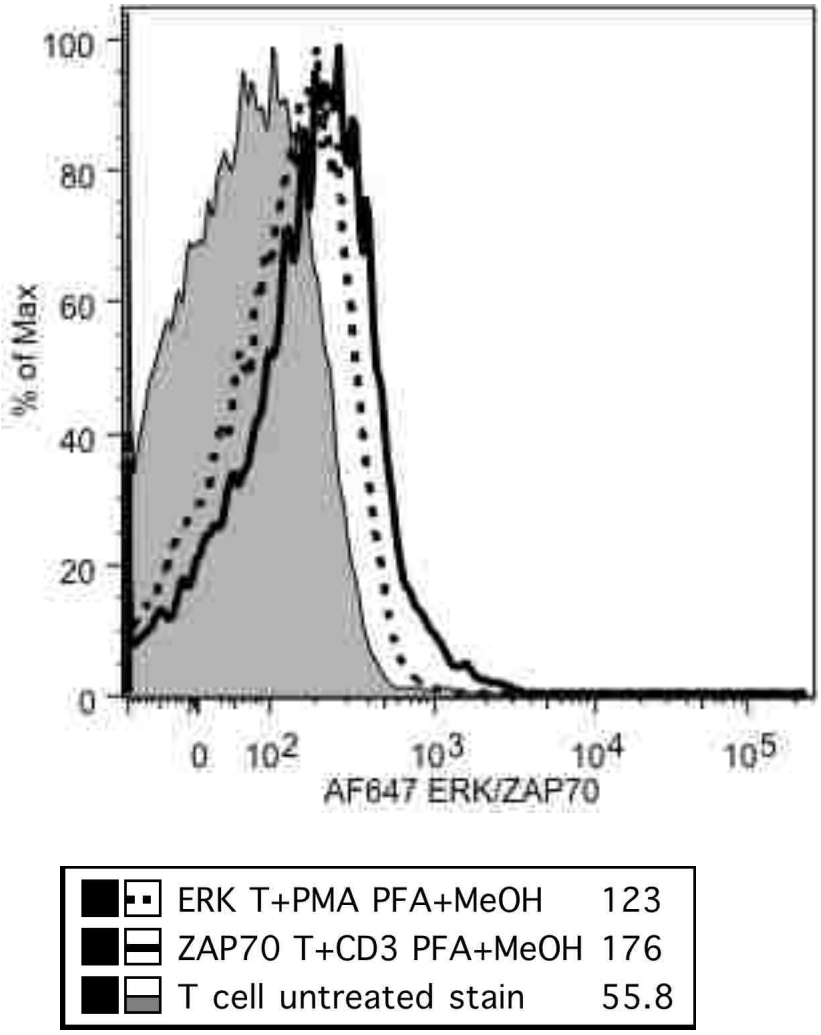

Figure 16. Testing phosflow. Using the phosflow protocol of Chow *et al.*, pERK and pZAP-70 signaling can be measured following the activation of AD10 T cells. (dotted line) CD4^{+} T cells were stimulated with 5 nM PMA and then stained with AF647-conjugated pERK antibodies. (solid line) T cells were stimulated with 5 μg/ml anti-CD3 and then stained for AF647-conjugated pZAP-70 antibodies. Data is representative of 3 separate experiments.

After validating this approach, both TCR-proximal and TCR-distal signaling were measured after the recovery of T cells from the *in vitro* trogocytosis assay. As shown in fig. 17, there are significant differences in the phosphorylation and activation state of ZAP-70 between $trog^+$ and $trog^-$ $CD4^+$ T cells. Immediately after removal from APC (time 0), the MFI of pZAP-70 is 3.03 fold higher for $trog^+$ T cells (thick black line) than in the $trog^-$ T cells (thin black line). The $trog^-$ cells are nearly identical to unstimulated T cell controls (shaded histogram). By 30 min, the pZAP-70 MFI of the $trog^+$ T cells is 4.2 fold higher than the $trog^-$ T cells and is nearly identical to the anti-CD3-stimulated positive control (thick gray line). Over the next twenty-four hours, there is a steady decrease in the pZAP-70 MFI for $trog^+$ cells, but pZAP-70 remains 2.3 fold higher than $trog^-$ cells. During this time frame, the level of pZAP-70 in the $trog^+$ cell remains very similar to the anti-CD3 positive control. At seventy-two hours, the $trog^+$ T cells still have significantly higher pZAP-70 levels (2.8 fold higher MFI) compared to the $trog^-$ T cells, which remain similar to the unstimulated control cells. Thus, there is sustained TCR-proximal signaling in $trog^+$ T cells, which were shown to preferentially survive in culture after recovery from APCs (fig. 15).

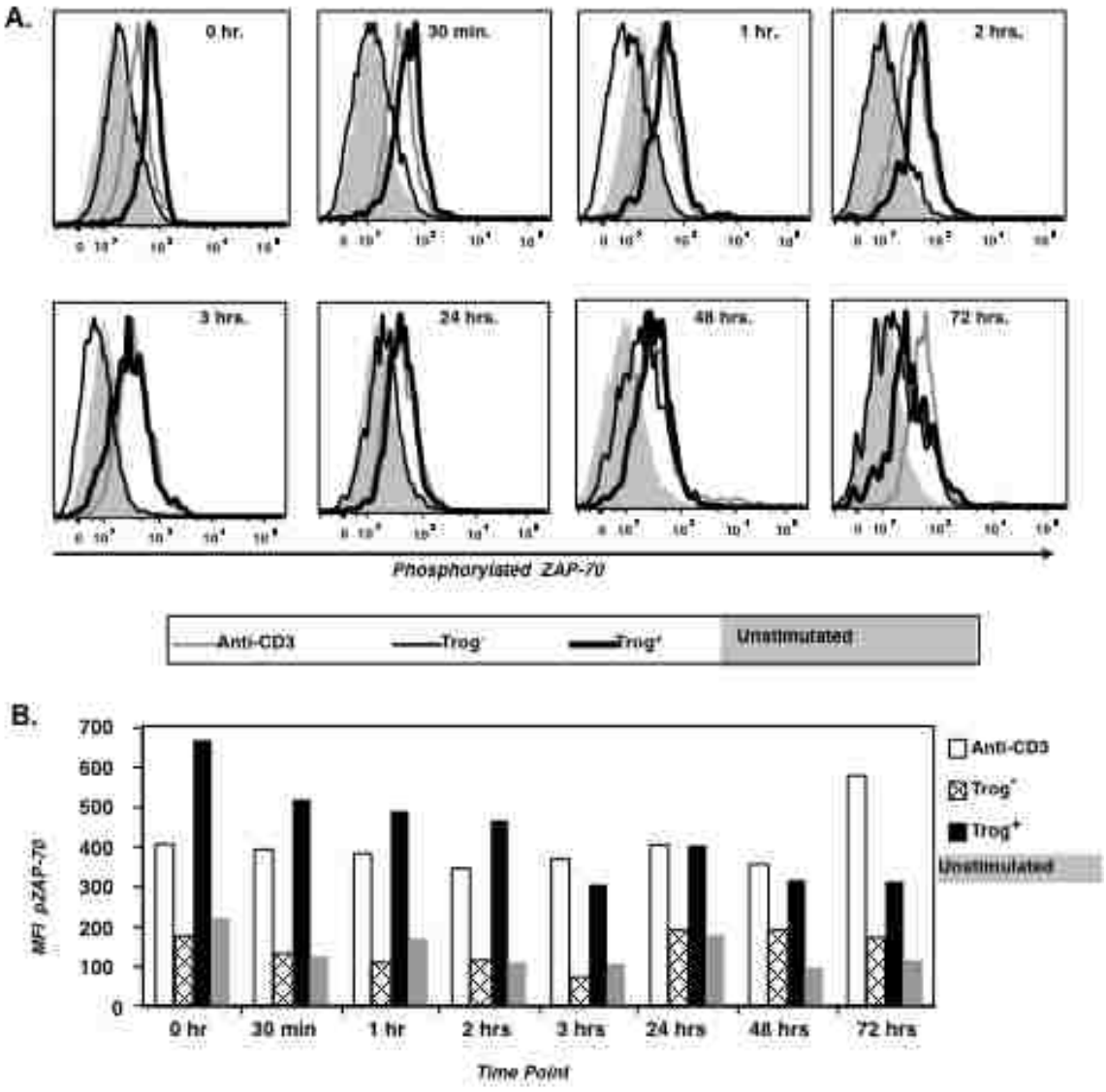

Figure 17. TCR-proximal signaling is sustained in trogocytosis$^+$ CD4$^+$ T cells using phosflow. (A.) AD10 T cells were recovered from the standard *in vitro* trogocytosis assay using MCC:FKBP APC and fixed immediately (0 hr) or were cultured for the indicated times before fixation and antibody staining. The level of pZAP-70 in CD4$^+$Vβ3$^+$ gated trog$^+$ (thick black line), trog$^-$ (thin black line), and unstimulated cells (shaded histogram) are shown for each time point. Cross-linked anti-CD3 (grey line) was used to stimulate TCR signaling as a positive control. (B.) Mean fluorescence intensity values for the phospho-ZAP-70 flow cytometry data in (A). Data are representative of 6 separate experiments. (192)

Trogocytosed MHC:peptide molecules co-localize with TCR-proximal signaling molecules in trog$^+$ T cells

The flow cytometry data show that TCR-proximal signaling is maintained in the trog$^+$ cells after removal of APC (fig. 17). To determine whether the elevated pZAP-70 was associated with the trogocytosed molecules on the surface of the T cells, high-resolution microscopy was used to determine the spatial distribution and potential co-localization of TCR-proximal signaling molecules with trogocytosed, GFP-tagged MHC:peptide. To begin, the spatial distribution of the TCR, pZAP-70, total phosphotyrosine (pTyr) and GFP-tagged MHC:peptide molecules were characterized at the immune synapse formed between AD10 T cells and MCC:GFP fibroblast APC. At the T-APC interface, cognate MHC:peptide (green) and the T cell antigen receptor (top-row, blue) are accumulated and colocalized (fig.18), indicating the presence of a mature immune synapse (IS) (184). At the T-APC interface, there is also significant enrichment of pZAP-70 (red) and total phosphotyrosine (blue, bottom). These images are consistent with previous reports characterizing signaling at the IS (97, 102, 154, 184, 195, 196). Interestingly, there is a small spot of trogocytosed MHC:peptide on the distal pole of the T cell (opposite the IS). The presence of trogocytosed MHC:peptide complexes (≥2x background) was observed in 24% of the T-APC conjugates imaged. These trogocytosed molecules accumulated at the distal pole on more than 82% of the trog$^+$ T cells in T-APC conjugates. Images of T-APC conjugates displaying accumulation of trogocytosed MHC:peptide complexes at the distal pole of the T cell, showed that these molecules colocalized with the TCR (blue) and were associated with elevated pZAP-70 (red) and total pTyr (blue) more than 99% of the time.

Line profiles were used to measure pixel intensity and staining thickness at the synapse and the distal membrane to determine if there was TCR signaling at the trogocytosed molecules (figures 19 and 20). Measuring pixel intensity across the line profile will show where the highest pixel fluorescence occurs for different TCR signaling and trogocytosed molecules staining. Line thickness is used to measure the distance across staining for TCR signaling molecules ≥2x above background fluorescence. In fig. 19, T-APC were imaged for IE^k (green) and pLck (red), similar to the conjugates in fig. 18. pLck was used because it is a TCR-proximal signaling molecule and is found near the TCR during its engagement with MHC. Two lines were drawn across the synapse and the distal membrane of the T cells to measure pLck pixel intensity and staining thickness or distances across stains. Fig. 19B line 1 shows a line drawn across the synapse and the distal membrane lacking trogocytosed IE^k. Fig. 19B line 2 is drawn across the synapse and the distal membrane containing trogocytosed IE^k. When comparing the two lines (fig. 20), the pixel intensity increases at the immune synapse with similar staining thickness for both lines 1 and 2 (bottom fig. 19B). When comparing the distal pole with (line 2) or without (line 1) trogocytosed IE^k, line 1 has increased pLck pixel intensity (fig. 20) and a 7.67 fold increase in staining thickness compared to line 2 (bottom fig. 19B). The staining pattern in the images in fig. 18 and 19 are very similar to that of the immunological synapse at the T-APC interface and strongly suggests that these trogocytosed molecules sustain/initiate TCR signaling after transfer onto the T cell.

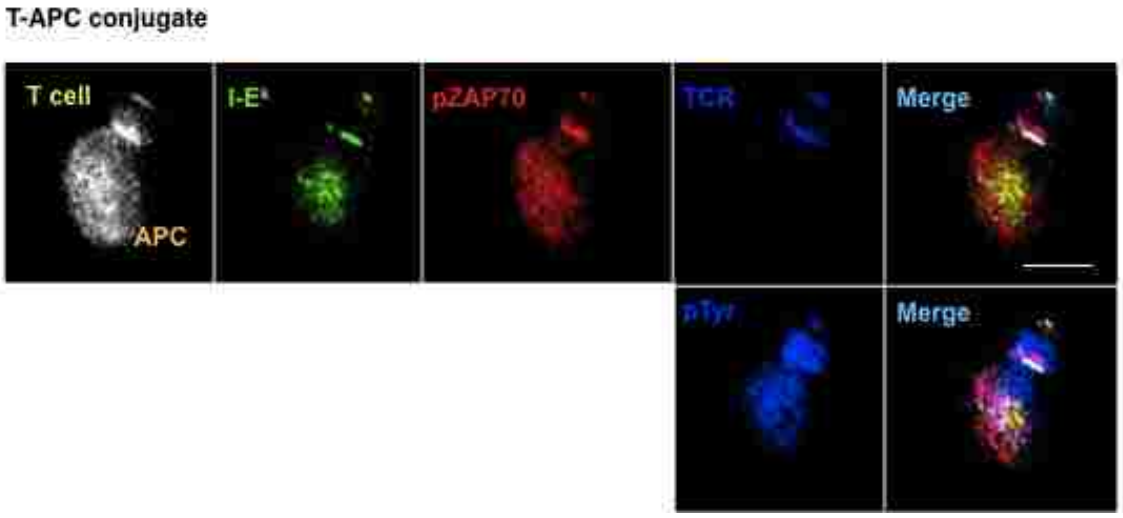

Figure 18. TCR signaling-associated molecules are associated with trogocytosed molecules on the T cell surface in conjugate with APC. AD10 T cells in conjugate with GFP-tagged MHC:MCC expressing APCs were fixed and stained for the indicated molecules, as described in the Methods section. Elevated pZAP-70 (red) and pTyr (blue, bottom row) levels co-localize with GFP-tagged MHC:peptide (green) and the TCR (blue, top row) at the immune synapse. These molecules also co-localize with trogocytosed MHC:peptide on the distal pole of the T cell. Fluorescence composite image shows position of T cell and APC. For each condition, more than 100 individual T cells were imaged. Images were collected with a 60X objective. Scale bar = 10 μm. (192)

A

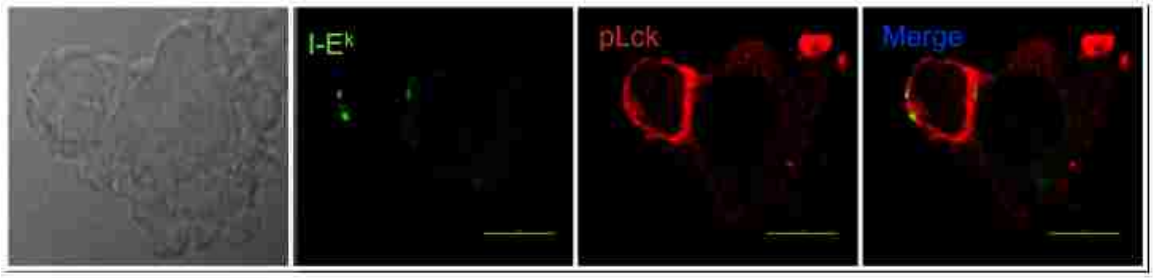

B

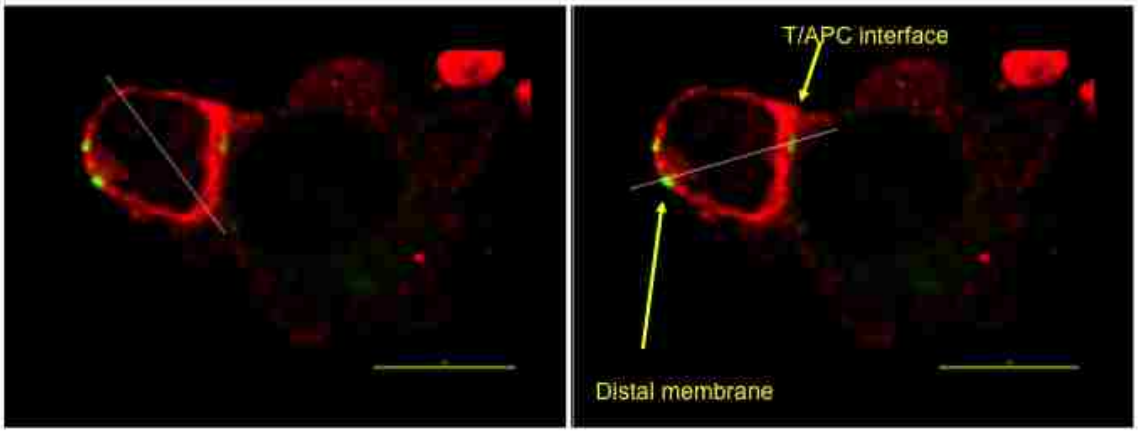

Line 1 Line 2

Line 1	Distal membrane = .3 μm	T/APC interface = 1.30 μm
Line 2	Distal membrane = 2.3 μm	T/APC interface = 1.35 μm

Figure 19. Measuring the thickness of TCR signaling-associated molecules across the distal T cell surface and T-APC interface. Cells were fixed and stained for the indicated molecules, as described in the Methods section. (A) Elevated pLck (red) levels co-localize with GFP-tagged MHC:peptide (green) at the immune synapse. These molecules also co-localize with trogocytosed MHC:peptide on the distal pole of the T cell. Fluorescence composite image shows position of T cell and APC. (B) pLck accumulation at the distal membrane near transferred MHC:peptide is significantly higher than on other regions of the cell. Line profiles were performed, which measure pixel intensity and staining thickness across a line. Lines 1 and 2 measure pLck MFI across the cells. Table shows the thickness of membrane-associated pLck signal ≥ 2x background intensity. More than 100 individual T cells were imaged. Lines profiles were created using API SoftWorx software. Images were collected with a 60X objective. Scale bar = 10 μm.

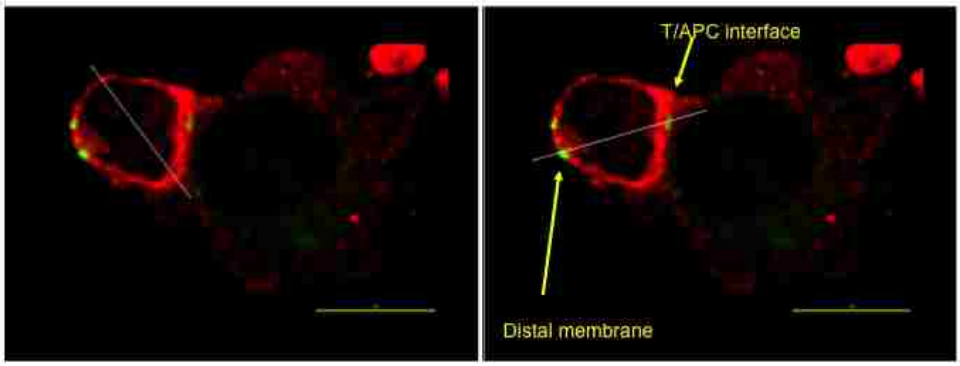

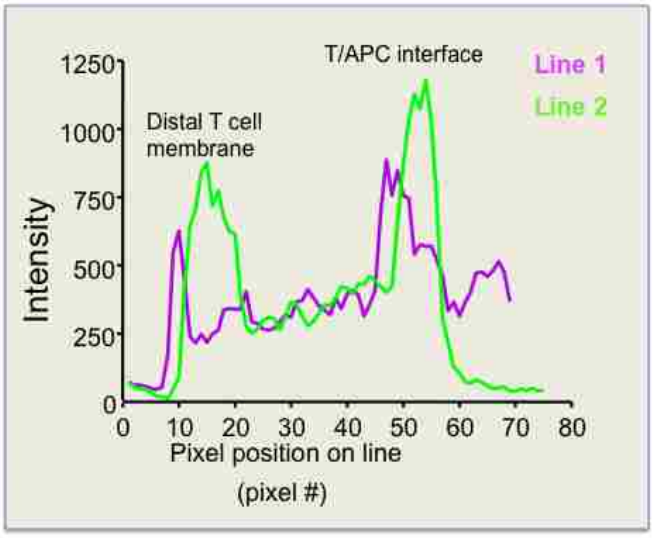

Figure 20. Measuring pLck staining intensity across the distal T cell surface and the T-APC interface. Graph of the line profiles from fig. 18B measure the pixel intensity of pLck across the T cell distal pole and the T-APC interface. Line 1 measures pLck pixel intensity across the T-APC interface and the distal pole of the T cell with trogocytosed GFP-tagged MHC absent. Line 2 measures pLck pixel intensity across the T-APC interface and the distal pole of the T cell with trogocytosed GFP-tagged MHC. Line profiles were created using API SoftWorx software.

Sustained TCR-proximal signaling in trog$^+$ T cells

The imaging data in figures 18-20 shows that the trogocytosed MHC:peptide appears to co-localize with the TCR and signaling associated molecules and raises the possibility that there is sustained TCR signaling from trogocytosed molecules in T-APC conjugates. To examine the possibility that the trogocytosed molecules sustain TCR signaling in T cells after dissociation from APC, recovered T cells from the standard *in vitro* trogocytosis assay were fixed and stained after an additional 30-minute incubation in the absence of APC. The relationship of the localization of the TCR to signaling molecules, using the TCR-proximal signaling molecules pLck and total pTyr, were examined in 111 T cells. Representative images are shown in fig. 21. Trogocytosis, defined as the presence of GFP-tagged MHC:peptide at least >2x above background fluorescence, was observed in 36% of the T cells imaged. The cell imaged in fig. 21 has two regions of trogocytosed MHC:peptide (indicated by the orange and yellow arrows). These are similar in size and total MHC:peptide accumulation, but the bottom region appears smaller because this image is a single optical section and the bottom spot is axially-centered in a separate focal plane. For both regions, the trogocytosed MHC:peptide localizes with both pLck and pTyr. This staining pattern was observed in 45% of trog$^+$ cells. These results are similar to our previously published data (103). The localization of TCR-proximal signaling molecules with transferred GFP in fig. 21 suggests that after recovery from APCs the trogocytosed molecules on the T cells sustain TCR-proximal signaling.

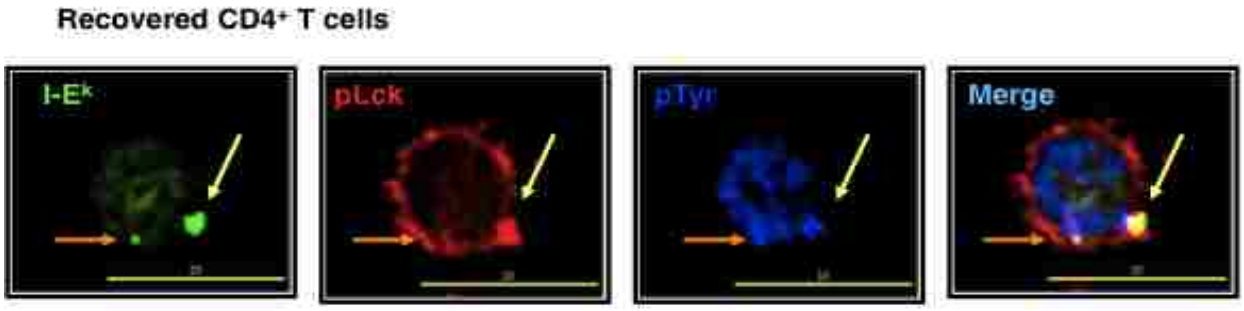

Figure 21. Proximal TCR signaling-associated molecules are associated with trogocytosed molecules on the recovered T cell surface. Recovered AD10 T cells were fixed and stained for the indicated molecules, as described in the Methods section. pLck (red) and total pTyr (blue) co-localize with two trogocytosed MHC:peptide spots (green) (indicated by yellow and orange arrows) on T cells recovered from the *in vitro* trogocytosis assay. Images are from a single focal plane. More than 100 individual T cell were imaged. Images were collected with a 60X objective. Scale bar = 10 μm. (192)

Sustained TCR-distal signaling in trog$^+$ T cells

To examine whether the trogocytosis-associated TCR-proximal signaling observed in figures 17-21 leads to downstream signaling, the accumulation of phosphorylated ERK1/2 (red) and its spatial distribution relative to the TCR(Vβ3) (blue) and trogocytosed MCC:MHC:GFP (green) were analyzed. As in fig. 21, the cells in fig. 22A have two distinct trogocytosed spots (green) that are ≥2x above background fluorescence. These spots co-localize with accumulated TCR in 96.6% of the 111 trog$^+$ T cells imaged. The TCR-distal signaling molecule pERK is also accumulated to the region adjacent to the trogocytosed molecules. While there is little actual pERK co-localization with the TCR or MHC:peptide, this staining pattern is very similar to what has been previously reported for pERK accumulation at the mature immunological synapse (102)

and is consistent with sustained TCR-distal signaling initiated by the trogocytosed molecules.

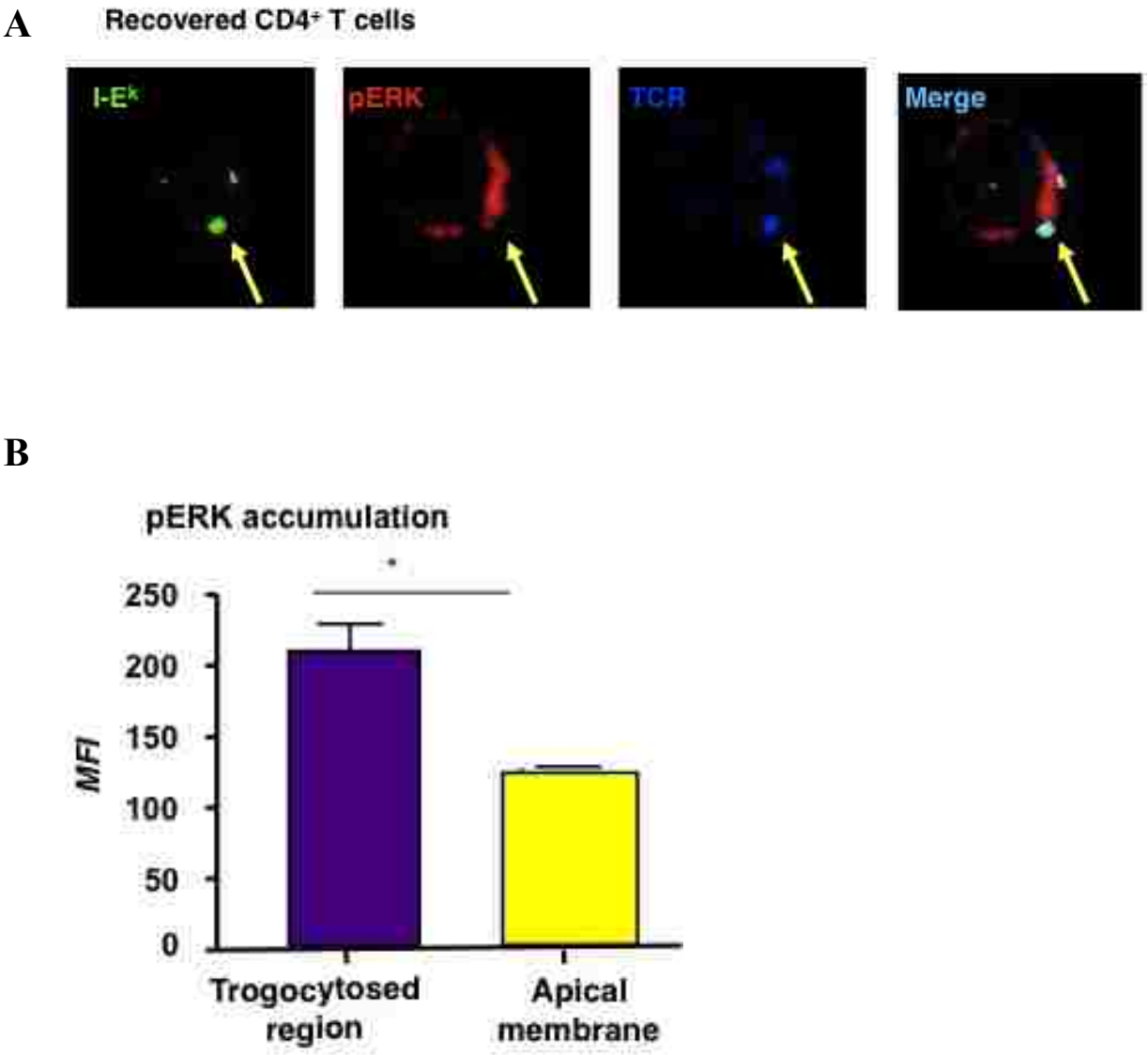

Figure 22. Distal TCR signaling-associated molecules are associated with trogocytosed molecules on the recovered T cell surface. Recovered AD10 T cells were fixed and stained for the indicated molecules, as described in the Methods section. (A) pERK (red) co-associates with trogocytosed MHC:peptide (green) and TCR (blue) on the recovered trog^{+} cells. pERK and TCR localize with the trogocytosed MHC:peptide molecule (green) region (indicated by the yellow arrow) on T cells recovered from the *in vitro* trogocytosis assay. Images are from a single focal plane. (B) Mean fluorescent intensity of pERK associated with the trogocytosed MHC:peptide compared to the apical membrane on the same cell. More than 100 individual T cells were imaged. Images were collected with a 60X objective. Scale bar = 10 μm. (192)

To further analyze the potential relationship between trogocytosed molecules and T cell intracellular signaling, the MFI of elevated pERK adjacent to trogocytosed molecules was compared to the amount at a region of the T cell apical membrane devoid of transferred material. The bar graph in fig. 22B shows that the regions adjacent to the trogocytosed molecules have a 56% increase in the level of pERK staining compared to the apical membrane. Taken together, the flow cytometry and imaging data in figures 17-22 suggest that after the trogocytosis event, the transferred MHC:peptide may continue to engage the TCR and sustains intracellular signaling. These results also correlate with the selective survival of T cells, by showing that the $trog^+$ cells could survive longer than $trog^-$ cells, due to sustained signaling and activation (fig. 15).

While examining the accumulation of the TCR and pERK with the trogocytosed MHC:peptide complexes, a correlation between the area of the MHC:peptide and the frequency of TCR and pERK co-accumulation was unexpectedly observed. Using three-dimensional image reconstruction, 228 different GFP regions on 47 T cells were analyzed to further assess this potential relationship between the area of the GFP-tagged MHC:peptide (>6x above background) with the TCR and enhanced pERK (≥2x over background). We observed that ~80% of larger GFP regions, defined as being ≥6x6 pixels in size, co-localized with elevated TCR and ~60% had adjacent elevated pERK staining. In comparison, small GFP regions (<6x6 pixels in size) co-localized with TCR only ~20% of the time and only ~22% were adjacent to elevated pERK (fig. 23). These data suggest a correlation between the size of the trogocytosed patches of APC molecules

on the T cell, and the engagement of the TCR, leading to increased levels of TCR-distal signaling.

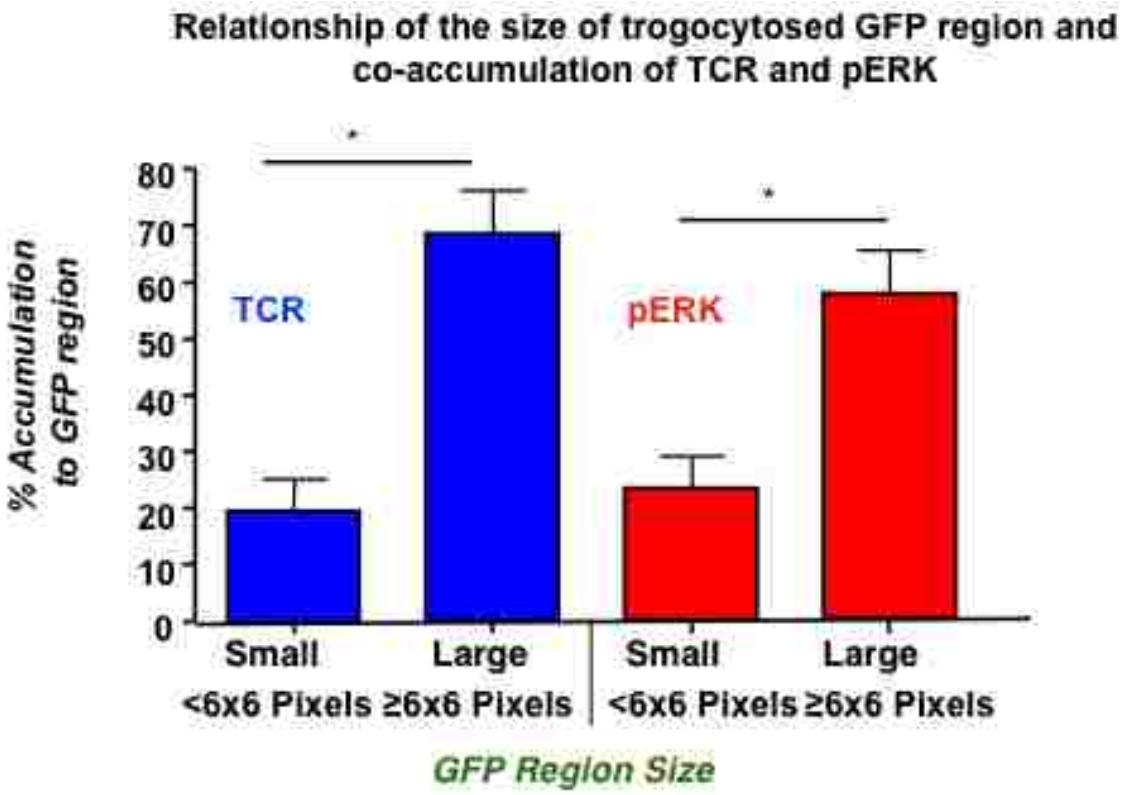

Figure 23. Correlation between the size of trogocytosed MHC:peptide and TCR/pERK staining. The relationship of the size of the trogocytosed MHC:peptide region on the T cell with the co-accumulation of TCR (blue) and pERK (red) from images in *fig. 22*. Small regions were defined as < 6x6 pixels and large ≥ 6x6 pixels. Data based off of more than 100 individual T cells imaged. (192)

Trogocytosed molecules induce sustained signaling in trog$^+$ T cells

The results in figures 17-23 suggest that trogocytosed molecules sustain TCR signaling in T cells after the removal of APCs. However, these results could also be attributed to residual signaling initiated at the immune synapse when T cells initially interacted with APCs. To determine whether the trogocytosed molecules were initiating TCR signaling, the PP2 interruption technique of Faroudi *et al* (188) was modified. PP2 is a reversible Src family kinase inhibitor that prevents the phosphorylation and activation of Lck during TCR engagement and terminates TCR signaling (188, 189). If the signaling detected by flow cytometry and imaging resulted from residual signaling from the immune synapse, it would be extinguished by PP2 and would not resume after the removal of this inhibitor. However, if the trogocytosed molecules were engaging their receptors on the T cell and sustaining/initiating intracellular signaling, this signaling would be expected to resume upon removal of PP2. To test this hypothesis, T cells were recovered from the standard 90-minute trogocytosis assay and incubated for an additional 30-minutes followed by flow cytometry and imaging analysis of potential TCR-proximal and TCR-distal signaling. Control cultures were treated with 20μM PP2 or were left untreated for the entire 30-minute culture period. In parallel cultures, cells were incubated with 20μM PP2 for 10-minutes at 37°C before the PP2 was washed out. These cells were incubated for an additional 20-minutes in the absence of PP2 before analysis. The results of these experiments are shown in figures 24-28.

In the first set of experiments, TCR-proximal signaling was examined by assessing the level and localization of phosphorylated ZAP-70 in more than a 100 PP2 treated cells by imaging. In addition to representative images seen in fig. 24, quantitative

data analysis of the imaging is shown in the bar graphs in fig. 25. The images in the top row of fig. 24, contained the untreated cells that were incubated in media alone for 30-minutes after removal from APC. There are three distinct GFP-tagged MHC:peptide spots (green) on this particular T cell. These spots co-localized with the TCR Vβ3 (blue) and phosphorylated ZAP-70 (red). In contrast, when cells were cultured in 20μM PP2 for the 30-minute incubation period (bottom row), the MHC:peptide and TCR co-localized normally, but there was minimal pZAP-70 staining and essentially none was associated with either the trogocytosed MHC:peptide or the accumulated TCR. This shows that PP2 treatment extinguishes TCR-proximal signaling, but does not alter TCR-MHC:peptide interactions. Cells treated with PP2 for 10-minutes showed a reduction of total pZAP-70 and no pZAP-70 co-localization with either MHC:peptide or TCR, which was similar to the 30-minute PP2 treatment group (data not shown). The cells treated with PP2 for 10-minutes followed by an additional 20-minute incubation after PP2 removal, displayed a single distinct GFP spot on the cell that was co-localized with both the TCR and elevated pZAP-70.

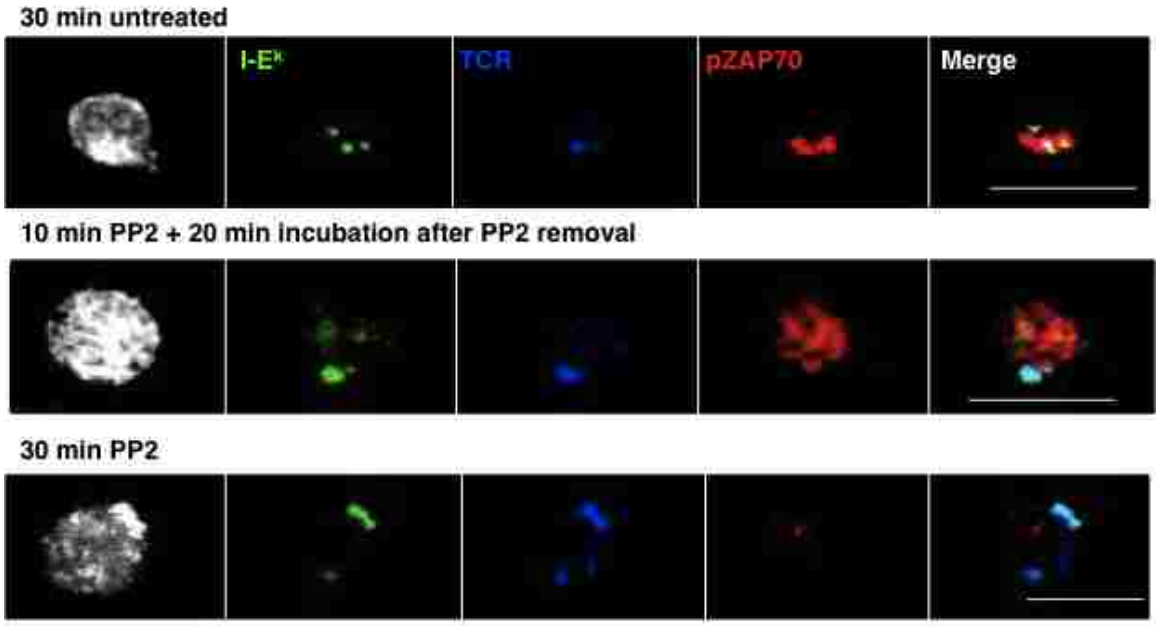

Figure 24. TCR-proximal signaling is sustained by trogocytosed molecules in trog$^+$ T cells. *Top:* T cells were incubated for 30-minutes after recovery from standard trogocytosis assay before fixation and staining. In untreated cells, pZAP-70 (red) and the TCR (blue) co-localize with the trogocytosed MHC:peptide on the T cell surface. *Bottom:* The TCR and MHC:peptide co-localize on T cells treated with the Src-inhibitor PP2 during the 30-minute incubation period, but there is minimal pZAP-70 detected. *Middle:* For cells with a 10-minute PP2 treatment to extinguish signaling and before incubation for 20-minutes after PP2 removal, the pZAP-70 level rebounds and it co-localizes with the trogocytosed MHC:peptide and TCR. More than 110 individual T cells were imaged using a 60X objective. Left image for each group is a fluorescence composite image to show the position of the T cell. Scale bar = 10 μm. (192)

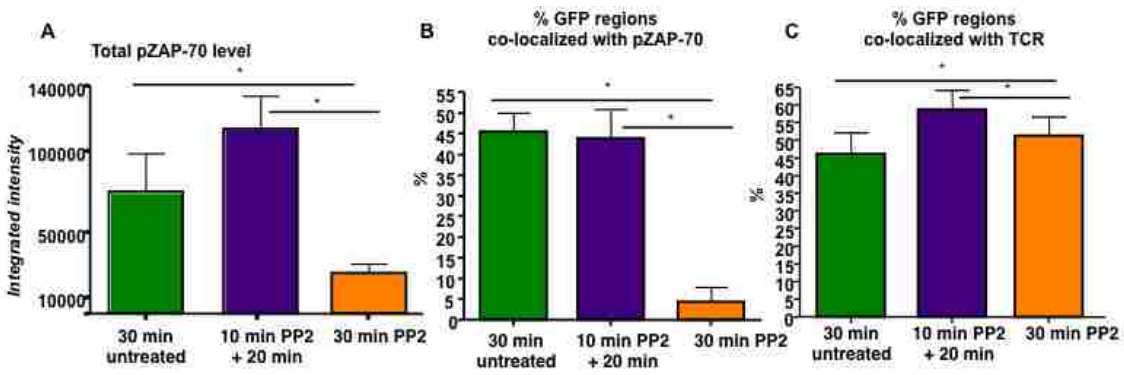

Figure 25. pZAP-70 rebounds and localized with trogocytosed GFP-MHC in trog$^+$ T cells following the removal of PP2. (A) Integrated intensity of pZAP70 ≥6-fold above background from images in *fig. 24.* 30-minute untreated T cells (green bar), T cells incubated with PP2 for 30-minutes (orange bar) or T cells treated for 10-minutes then incubated for 20-minutes after removal of PP2 (purple bar) are shown. (B) The frequency of pZAP-70 co-localizing with trogocytosed MHC:peptide for each treatment group is shown. (C) The frequency of TCR co-localizing with the TCR. Bars represent mean ± SEM. Horizontal lines indicate statistical comparison between indicated groups; * $p \leq$ .05. (192)

The bar graph in fig. 25A shows the integrated intensity of pZAP-70 (a measure of fluorescence intensity and accumulation of stains) in areas ≥6x above background on trog$^+$ cells. After imaging more than 110 trog$^+$ cells, the 30-minute PP2 treated cells had significantly reduced levels of pZAP-70 staining compared to the 30-minute untreated cells. For the 10-minute PP2 plus 20-minute incubation group, the level of pZAP-70 was restored. Interestingly, the levels were consistently higher for the 10-minute PP2 plus 20-minute incubation group than that found in the untreated cells. The trog$^-$ T cells showed an absence of pZAP-70 staining in all of the treatments (data not shown), consistent with the flow cytometry data in fig. 17. Thus, elevated pZAP-70 seen in the trog$^+$ 10-minute PP2 treatment plus 20-minute incubation group is not simply due to PP2 treatment and removal, but also requires the presence of trogocytosed molecules.

To confirm that the observed signaling was being initiated at the location of the trogocytosed molecules, I examined the spatial relationship between elevated pZAP-70 and trogocytosed MHC:peptide molecules on the T cell surface for the different treatment groups (fig. 25B). For approximately 45% of both the 30-minute untreated cells and the 10-minute PP2 plus 20-minute incubation cells, pZAP-70 co-localized with the trogocytosed MHC:peptide complexes. In contrast, less than 5% of the cells treated with PP2 for 30-minutes showed MHC:peptide co-localization with pZAP-70. The significant reduction in total pZAP-70 and co-localization with the TCR or MHC:peptide for the 30-minute PP2 treatment group is likely due to the biochemical effects of PP2 on Lck activation and is not due to inhibition of TCR-MHC:peptide interactions, since these molecules co-localized equally in the presence or absence of PP2 (fig. 25C). The results in figures 24-25 strongly support the hypothesis that the trogocytosed molecules continue to engage their receptors on the T cell surface and sustain TCR-proximal signaling.

After showing that the trogocytosed molecules induced TCR-proximal signaling upon removal of PP2, TCR-distal signaling was examined using the phosphorylation and activation of ERK1/2 as a readout. T cells were recovered from the standard trogocytosis assay and treated with PP2 following the same regimen for the ZAP-70 studies described above. The extent of ERK phosphorylation in the 3 treatment groups was examined by phosflow. Similar to the pZAP-70 data, 30-minute PP2 treatment significantly reduced the amount of phosphorylated ERK in the cell (fig. 26, orange line) compared to the untreated cells (fig. 26, green line). The pERK1/2 MFI for the 30-minute PP2 treatment group was 1.6 fold lower than the untreated control. In contrast, the cells treated with PP2 for 10 min followed by an additional 20-minute incubation in the absence of PP2 (fig. 26,

purple line) showed a restoration of pERK1/2 staining. Reminiscent of the pZAP-70 imaging data, the MFI for the 10-minute PP2 plus 20-minute incubation group was 30% higher than the untreated controls and was 1.9 fold higher than the 30-minute PP2 treatment group. It was also 2.4 fold higher than the unstimulated T cell controls. These results are consistent with the TCR-proximal signaling seen in fig. 24 and show that after PP2 inhibition of TCR signaling is removed, TCR-distal signaling is re-initiated within the trog^{+} T cells.

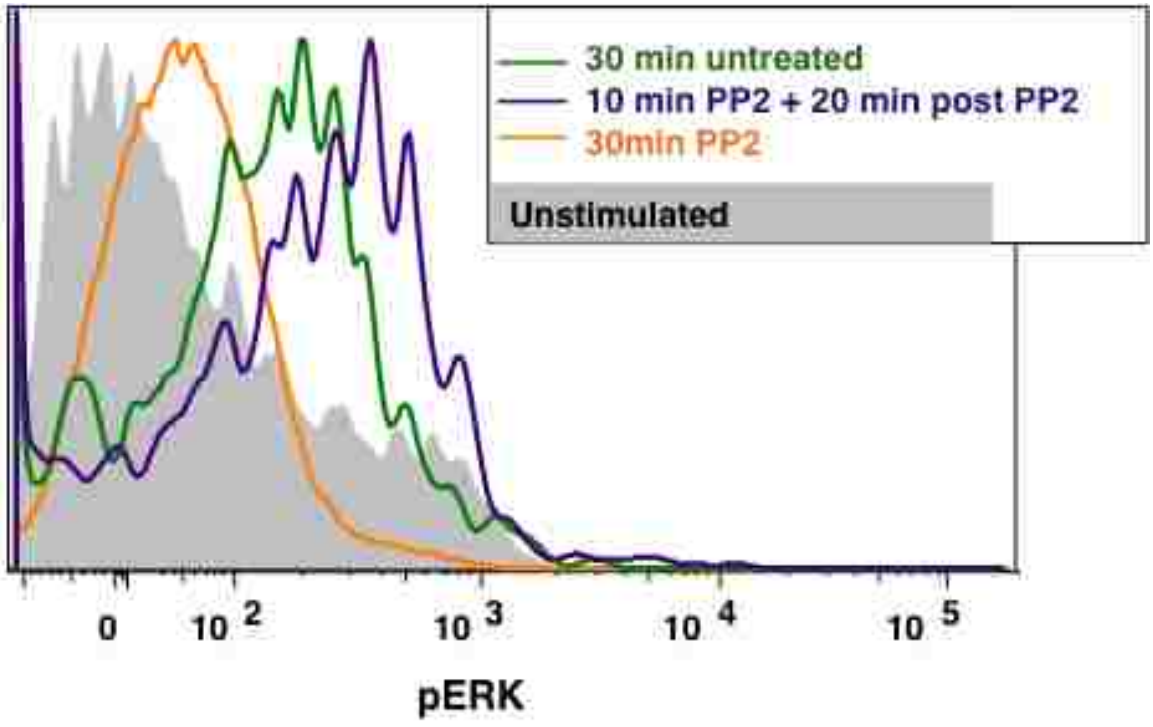

Figure 26. TCR-distal signaling is sustained by trogocytosed molecules in trog^{+} CD4^{+} T cells using phosflow. Phosflow data showing the level of pERK1/2 in untreated cells (green line), cells treated with PP2 for 30-minutes (orange line), and cells treated with PP2 followed by a 20-minute incubation after PP2 removal (purple line). Unstimulated cells (shaded histogram) are shown as a control. Data are representative of six separate experiments. (192)

To confirm that the recovery of TCR-distal signaling after PP2 removal is associated with the trogocytosed molecules, imaging experiments were performed. In each row of images in fig. 27, the trogocytosed GFP-MHC:peptide (green), TCR Vβ3 (blue), and pERK1/2 (red) are seen; the right column shows merged images of all three. The untreated group in the top row has several distinct MHC:peptide spots on the recovered T cell. Each of these spots co-localize with the regions of elevated TCR (blue). Adjacent to these TCR-MHC:peptide regions, there is accumulation of elevated pERK. Similar to fig. 22, the pERK does not co-localize with either the MHC:peptide or TCR, but rather is adjacent to these molecules on the T cell. The spatial distribution of the pERK in these $trog^+$ cells is very similar to our previous report regarding pERK accumulation at the immunological synapse (102). When PP2 was present for the entire 30-minute incubation period, the trogocytosed MHC:peptide co-localized with the TCR. Similar to the pZAP-70 data, there was minimal pERK1/2 staining in the 30-minute PP2 group. In the cells incubated for 10-minutes with PP2 followed by an additional 20-minute incubation in the absence of PP2, there were several regions of trogocytosed MHC:peptide complexes that co-localized with the TCR. This is similar to the untreated control (fig. 27, top row). There was also accumulation of pERK1/2 adjacent to the trogocytosed molecules. This complements the flow data (fig. 26) by showing that removal of PP2 allows resumption of TCR-dependent distal signaling from the trogocytosed molecules.

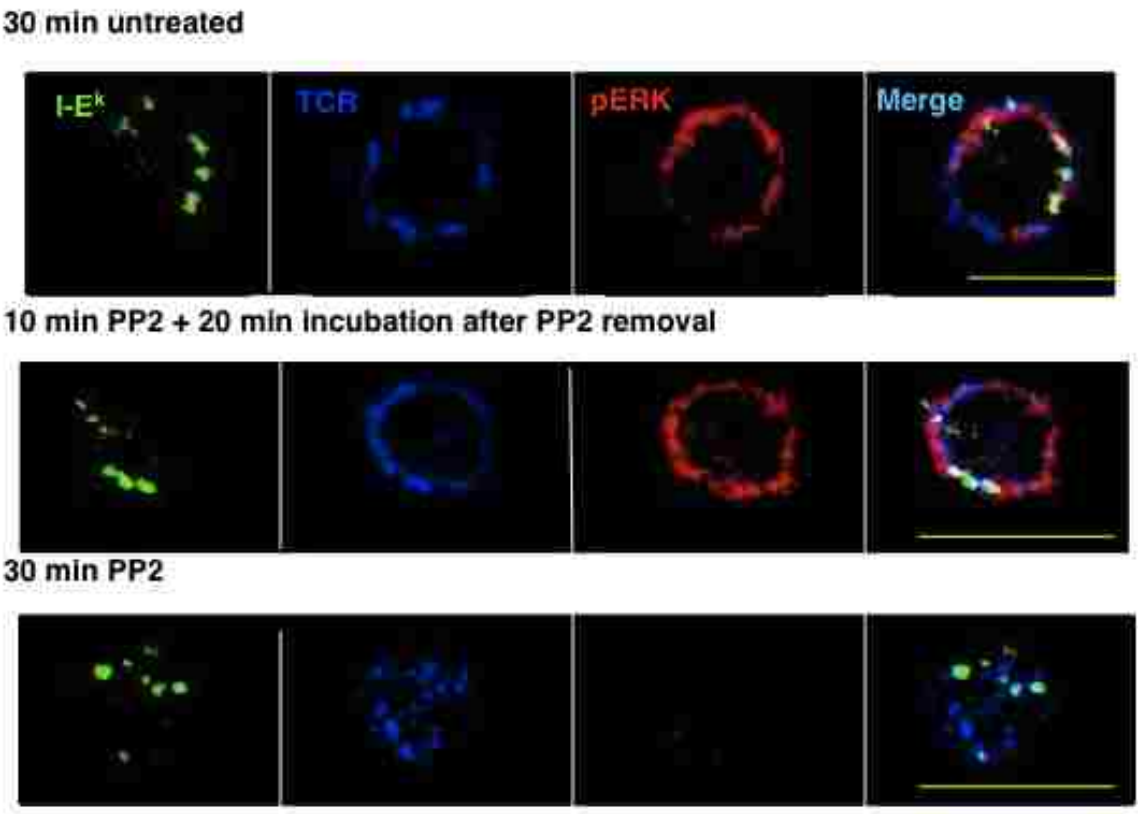

Figure 27. TCR-distal signaling is sustained by trogocytosed molecules in trog$^+$ CD4$^+$ T cells. Recovered T cells were incubated for 30-minutes, as described in *fig. 24,* before staining and imaging. The location of TCR (blue), MHC:peptide (green), and elevated pERK (red) are shown for each treatment group. Data are representative of three separate experiments with more than 100 cells imaged for each treatment group. Images were collected using a 60X objective. Bar = 10μm. (192)

As with the pZAP-70 imaging data, the integrated intensity of pERK (fig. 28A) and the frequency of pERK association with trogocytosed MHC:peptide (fig. 28B) were calculated for more than 100 cells in each treatment group. As expected from the representative images in fig. 27, the cells treated with PP2 for 30-minutes showed an absence of pERK1/2 staining, in contrast to the untreated group. Cells treated for 10-minutes were identical to the 30-minute PP2 treatment (data not shown). The 10-minute

PP2 plus 20-minute incubation group displayed a significant recovery in the integrated intensity for pERK1/2, similar to pZAP-70 results. The pERK integrated intensity for cells treated for 10-minute with PP2 treatment followed by a 20-minute post-PP2 incubation was 10-fold higher than the 30-minute PP2 treatment and 1.6 fold higher than the untreated control. The frequency of elevated pERK adjacent to the trogocytosed MHC:peptide was also quantified for each of the treatment groups (fig. 28B). In 39% of untreated samples and 47% of 10-minute PP2 plus 20 minute post-wash samples, the trogocytosed GFP-tagged MHC:peptide was associated with elevated pERK staining. In contrast, only 8% of the 30-minute PP2 cells showed association of pERK with the trogocytosed molecules.

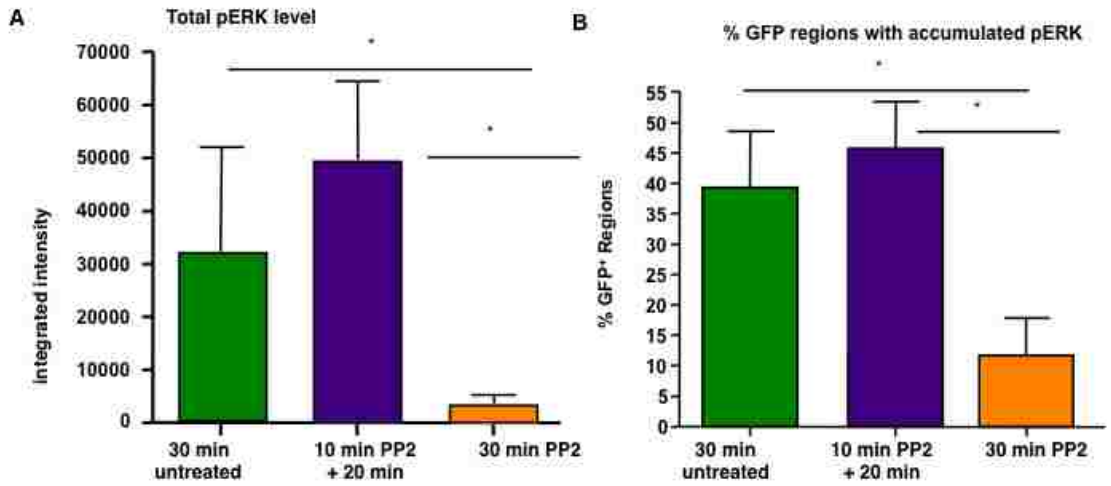

Figure 28. pERK1/2 rebounds and localizes with trogocytosed GFP-MHC in trog^{+} T cells following the removal of PP2. (A) Total pERK integrated intensity for areas ≥6-fold above background for each treatment group. (B) The frequency of trogocytosed MHC:peptide molecules that co-associate with elevated pERK (≥2-fold above background) is shown. Bars represent mean ± SEM. Horizontal lines indicate statistical comparison between indicated groups; * $p \leq .05$. (192)

Taken together, the results in figures 24-28 show that a 30-minute treatment with PP2 significantly reduces both pERK1/2 and pZAP-70 levels in the trog$^+$ cells. After a 10-minute PP2 treatment, both TCR-proximal (pZAP-70) and TCR-distal (pERK1/2) signaling is re-initiated upon PP2 removal. This re-initiated signaling is dependent upon the trogocytosed molecules. These results strongly suggest that these trogocytosed molecules are engaging their receptors on the T cell surface and are sustaining intracellular signaling after dissociation from the APC. Beyond the TCR:pMHC interactions, the participation of other trogocytosed molecules (i.e., costimulatory and adhesion) is currently unknown.

T-T Ag presentation

To examine the cell extrinsic effects of trogocytosis, the potential of trog$^+$ T cells to present Ag was examined. The work of Zhou *et al.* showed that CD4$^+$ T cells could present trogocytosed Ag to naïve T cells, inducing CD25 expression and proliferation of the responder naïve T cells (159). They also showed that when trog$^+$ regulatory T cells were present, immune suppression of the T cells occurred (159). To examine potential T-T Ag presentation following trogocytosis, experiments were set up to analyze the phenotype of the responder naive T cells. Fig. 29 shows the results of T-T presentation to naïve T cells. Following the T-T presentation assay, trog$^+$ and trog$^-$ FACS sorted AD10 T cells were used as APCs. Responder CFSE-labeled naïve AND x B10.BR T cells become activated and also performed trogocytosis when incubated with the trog$^+$ T cells, but not with the trog$^-$ cells. In fig. 29A and B, naïve T cells with trog$^+$ T cells (thick black line) had a 1.5 fold increase in CD69 expression and a 2.7 fold increase in CD25 expression compared to naïve T cells with trog$^-$ T cells (thin black line). Naïve T cells with trog$^+$ T

cells also showed a 20 fold decrease in the expression of the TCR compared to the naïve T cells with trog^{-} T cells (fig. 29C), showing they had downmodulated their TCR. In contrast, the naïve T cells placed with trog^{-} and unstimulated T cells (shaded histogram) showed similar expression of CD69, CD25, and TCR. Interestingly, naïve T cells with trog^{+} T cells showed a 2.2 fold increase in biotin expression compared to naïve T cells with trog^{-} T cells, suggesting these cells had performed trogocytosis. These results show that T-T presentation may play a role in stimulating naïve T cells during an immune response.

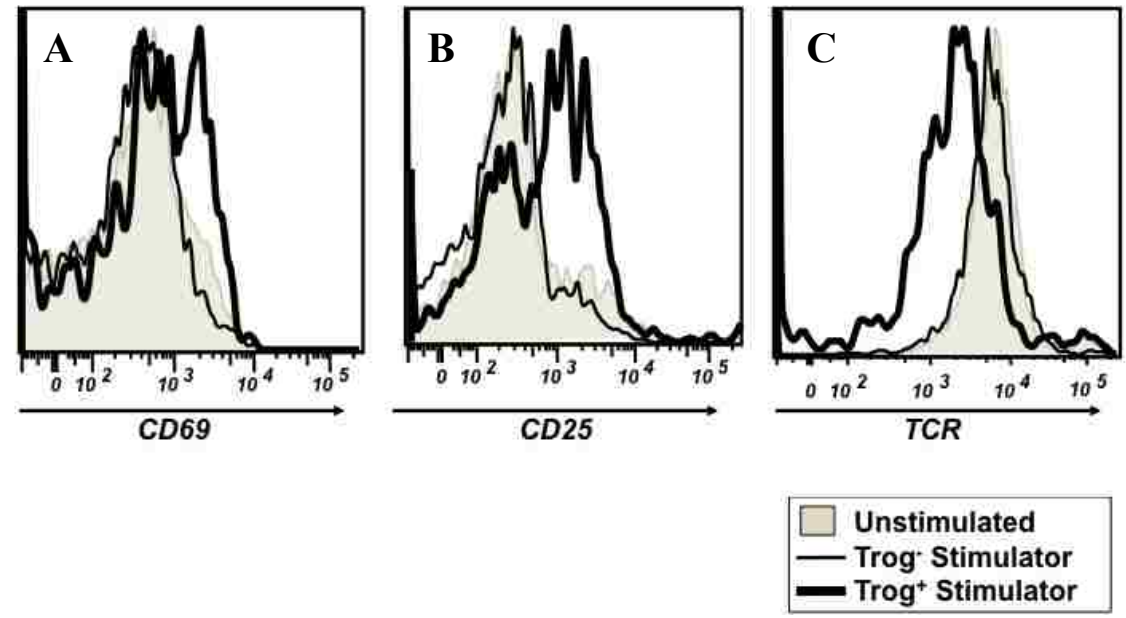

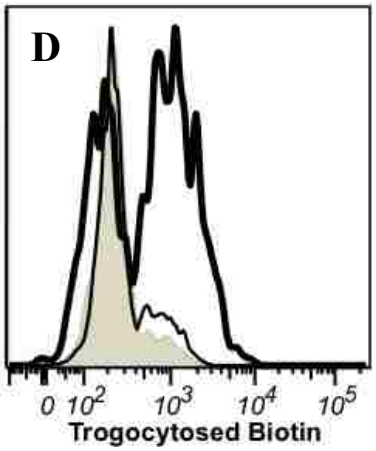

Figure 29. T-T presentation. Trog^{+} and trog^{-} AD10 T cells were sorted and placed with naïve AND x B10.BR T cells at a 1:1 ratio. Naïve cells were CFSE labeled to distinguish from sorted T cells. (A-C) Naïve T cells stimulated with trog^{+} T cells (thick black line) compared to naïve T cells stimulated with trog^{-} T cells (thin black line) and unstimulated naïve T cells (shaded) using CD69, CD25, and TCR staining. (D) Trogocytosed biotin was compared between the three naïve T cell setups. Data are representative of 1 experiment.

Chapter 4:

Discussion

During antigen (Ag) recognition by $CD4^+$ T cells, three signals are required for the T cells to become activated. The first signal involves the engagement of the T cell receptor (TCR) by cognate MHC:peptide. The TCR binds and recognizes MHC class II and antigenic peptide bound to the MHC. TCR recognition of specific peptide residues and the MHC leads to TCR crosslinking with CD3 and activation of the kinases Lck and ZAP-70. The activation of these molecules leads to a series of signaling cascades that ultimately leads to activation of several transcription factors. The transcription factors activate genes that produce IL-2 and induce activation and proliferation. The second signal involves the engagement of costimulatory molecules, like CD28 on the surface of the T cell. Costimulatory engagement activates kinases leading to a cascade of signaling molecule activation, similar to TCR engagement. In combination with TCR signaling, costimulation leads to increased IL-2 production, activation, and proliferation. The final signal comes from cytokines binding to their specific receptors on the surface of the T cell leading to signaling and gene activation similar to TCR and costimulation engagement.

During Ag recognition by $CD4^+$ T cells, spatial and temporal rearrangements of the TCR, costimulatory, and adhesion molecules results in the formation of an immunological synapse between the APC and the T cell. The molecules accumulate at the immune synapse and are arranged into distinct supramolecular activation complexes (SMACs) (78). The prototypical T_H1 immune synapse is characterized as a bull's-eye with TCR-MHC:peptide, TCR signaling associated molecules, and CD28/CD80 localized

to the center (the cSMAC). Adhesion molecules, such as ICAM-1/LFA-1, are found in a surrounding peripheral ring (the pSMAC) (78, 79, 86). The overall function of the immunological synapse is unclear; past results have shown that the immune synapse is the site of cytokine secretion (101, 197), cytolytic granule secretion (88), and TCR down-modulation and signaling (154). Our lab has shown that the immune synapse is also the site of APC to $CD4^+$ T cell trogocytosis (103). As T cells dissociate from APCs, MHC:peptide complexes (103, 107), costimulatory molecules (106, 130, 142), plasma membrane lipids (111, 148), and other membrane-bound molecules found on APCs are trogocytosed by the T cells via the immunological synapse (103, 108, 124).

Over the past decade, there have been numerous studies that have examined the mechanism of trogocytosis and the complement of molecules that are transferred, but relatively little is known about the potential biological significance of the capturing of these molecules by the $trog^+$ T cell. The presence of APC-derived molecules on the T cell raises the potential that they could engage receptors on the T cell and sustain intracellular signaling. Sprent's group has published several papers looking at the ability of APC-derived exosomes to stimulate T cells (198-201), but attachment of exosomes to the surface of the cell is fundamentally different from the integration of these molecules into the plasma membrane via trogocytosis. Using fluorescent microscopy, Wetzel *et al.* showed that staining for the cytosolic tail of the trogocytosed MHC class II required permeabilization of the T cell membrane (103), suggesting the trogocytosed MHC was integrated into the T cell plasma membrane in its topologically native form. These results are consistent with the results in fig. 9. This finding also correlates with the hypothesis by Martinez-Martin *et al.* (20) and Dopfer *et al.* (155), that endosomes containing

trogocytosed APC membrane and membrane molecules fuse with the T cell plasma membrane resulting in the integration of these molecules in the correct orientation. This raises the possibility that sustained signaling via trogocytosis results from trogocytosed molecules engaging their receptors on the T cell surface.

A few studies have looked at the correlation between trogocytosis and sustained T cell signaling, but the correlation remains unclear. In 2005 Zhou *et al.* showed that $CD80^+$ T cells had sustained NFκB activation and production of selected cytokines (161). However, their results were most likely the result of T-T antigen presentation, not cell autonomous signaling (161). Other reports have looked at the constitutively activated receptor tyrosine kinases (202) and the Ig-like Transcript 2 (ILT2) signaling after trogocytosis (203) in $CD8^+$ T cells, but none have actually addressed sustained signaling in T cells from trogocytosed APC-derived molecules. In this thesis, I have examined the hypothesis that trogocytosed MHC:peptide complexes sustain intracellular signaling within $CD4^+$ T cells after dissociation from APC, leading to sustained T cell activation, proliferation, and survival.

Kinetics, activation, proliferation, and selective survival of trog$^+$ T cells

Since murine $CD4^+$ T cells cannot express MHC class II endogenously (175), the presence of these molecules on T cells is due to trogocytosis. I initially examined trogocytosis by testing different cell labeling protocols to determine which was the most efficient at measuring trogocytosis (fig. 10). GFP-tagged MHC class II and the use of anti-I-E^k have been previously shown to be a good measure of trogocytosis (103). These were compared with membrane (CM-DiI) and total protein (surface biotinylation)

trogocytosis to determine which has the best dynamic range when measured by flow cytometry. Both CM-DiI and biotin were more sensitive measures of trogocytosis compared to staining for just MHC. These results are consistent with past results showing significant lipid trogocytosis from APCs onto the T cell (88, 107). The transfer of APC membrane lipids may be the result of membrane fusion between the T-APC, as suggested by Stinchcombe *et al.* (88). Hudrisier *et al.* proposed that T cells pull off membrane to use in proliferation and metabolism and, in return, the T cell provides protection for the target cell (108), but there are currently no published data to support this hypothesis.

To further examine trogocytosis, I addressed whether T cells require previous Ag recognition to efficiently perform trogocytosis. Past results have shown that trogocytosis is antigen dose-dependent (105, 107), peptide-specific (105, 107), and requires the immune synapse (103, 108, 124), but very little research has looked at the length of stimulation required for naïve T cell trogocytosis. Using AND x Rag-1$^{-/-}$ naïve T cells, it was observed that two rounds of stimulation with APCs lead to T cells that are efficient at naïve T cell trogocytosis. During the primary stimulation with APCs for 6-24 hr, little to no trogocytosis occurred (fig. 11B). Following T cell recovery from the primary culture and two additional days in culture, the naïve T cells showed significant trogocytosis after a secondary 90 min stimulation with APC (fig. 11C). Previous studies have reported that naïve T cells have a reduced ability to perform trogocytosis (104, 106, 130, 142, 153), but none has restimulated these cells to examine their trogocytosis capacity upon the secondary challenge. Our results suggest that following the primary stimulation, the T cells increase avidity for the APC, by increased expression of adhesion molecules and integrin activation, allowing for more stable T-APC interactions and, thus, increased

trogocytosis. CD28 expression is also increased in activated T cells and has been linked to increases in transfer (106, 122, 130).

Using *in vitro* primed naïve T cell cultures, I found that $trog^+$ T cells do proliferate. Approximately 25% of naïve $CD4^+$ T cells from AD10 TCR transgenic mice were MHC class II positive directly *ex vivo* (fig. 12). Since murine $CD4^+$ T cells cannot express MHC class II endogenously (175), the presence of these molecules was due to a trogocytosis event *in vivo*. The nature of this *in vivo* trogocytosis by naïve cells is unclear; it could be the result of tonic stimulation by positively selecting ligands in the periphery (191) and/or thymic positive selection events (121). When the AD10 splenic suspensions were stimulated by addition of exogenous $MCC_{88\text{-}103}$ antigenic peptide, the frequency of MHC^+ ($trog^+$) T cells doubled by day 1 (fig. 12). The $trog^+$ cells were also the first $CD4^+$ cells to proliferate. This raises the intriguing possibility that trogocytosis may lower the threshold for activation and proliferation of naïve T cells upon antigen stimulation. The lack of proliferation and activation from the primary stimulation of the naïve T cell could be due to the cells not performing trogocytosis (fig. 11). Several possibilities could explain this observation, including alterations in intracellular signaling and/or increased avidity of the T cells, which could be due to signaling from the trogocytosed molecules.

When trogocytosis by *in vitro* primed AD10 T was examined, the $trog^+$ T cells were found to have increased TCR-downmodulation and higher levels of CD69 (fig. 13). This suggests that the cells were activated and is consistent with our previously published results (103). It is interesting to note that both $trog^+$ and $trog^-$ T cells have a similar activation phenotype suggesting that both cell populations recognize Ag and are

activated. It is unclear why the trog$^-$ cells did not perform trogocytosis when even anergic T cells efficiently trogocytosed molecules from APC (102). It is not likely due to differences in activation because both populations are similarly activated upon antigen recognition. It is possible that it reflects differences in the avidity of the T cells, their adhesion molecule concentrations, activation states, and/or additional uncharacterized attributes of the two populations of cells.

The significance of trogocytosis becomes clearer once the cells are recovered and placed in culture away from APC. Analyzing sustained expression of CD69 in recovered AD10 T cells over time, the trog$^+$ T cells continue to express CD69, while trog$^-$ T cells do not. In fig. 14, trog$^+$ T cells (thick black line) have high levels of CD69 similar to the anti-CD3 positive control (gray line) for up to one day following recovery. Continual CD69 expression on the surface of the T cell requires TCR:pMHC engagement (19) and TCR signaling (193). I hypothesize that the continued expression of CD69 on the surface the T cells is due to the trogocytosed material engaging receptors on the surface of the T cell after recovery from APC.

This hypothesis is supported by fig. 15, which shows that trog$^+$ T cells survive longer in culture following recovery. When cells were recovered from the standard *in vitro* trogocytosis assay and incubated at low density, a significant change in the frequency of trog$^+$ and trog$^-$ cells was observed over several days. Immediately after recovery from the APC, the trog$^-$ T cells represented almost two-thirds of the CD4$^+$ cells. Over the course of several days, the frequency of trog$^+$ and trog$^-$ cells had reversed so that by day three, the trog$^+$ cells made up more than 82% of the viable CD4$^+$ T cells and the trog$^-$ represented less than 18% of the viable CD4$^+$ cells. The level of GFP-tagged MHC

remained fairly constant on the trog$^+$ cells over 5 days, which suggests that the cells weren't dividing, because proliferation would result in the dilution of trogocytosed molecules onto daughter cells. These results suggest that the trog$^+$ cells were selectively surviving in the cultures, while the trog$^-$ cells were dying.

Sustained signaling by the trogocytosed material

One explanation for the preferential survival of the trog$^+$ cells is that the trogocytosed molecules were sustaining intracellular signaling. It would be expected that TCR signaling would cease in recovered cells unless there is continued TCR-MHC:peptide engagement. By flow cytometry it was observed that after the acquisition of cognate MHC:peptide complexes and other APC membrane molecules, there was elevated phosphorylation and activation of both TCR-proximal (pZAP-70) and TCR-distal signaling molecules (pERK1/2) over several days. Using high-resolution light microscopy, it was observed that these TCR-associated signaling molecules accumulated with the TCR and trogocytosed molecules. pERK1/2 was found to co-associate with the trogocytosed material, meaning that pERK1/2 was near the trogocytosed molecules but did not colocalize. This is consistent with Adams *et al.* and our previous results showing ERK was sequestered and localized near the plasma membrane where the TCR is in activated T cells (102, 204). These data support the hypothesis that the trogocytosed molecules continued to engage their receptors on the T cell and that this "autopresentation" sustained intracellular signaling.

While the detection of phosphorylated and activated signaling molecules in trog$^+$ cells and the co-localization of these molecules with both the TCR and trogocytosed

MHC:peptide supports this model, it does not prove that the trogocytosed molecules are driving the observed signaling. It is possible that the sustained signaling is actually due to residual signaling carried over from the immune synapse between the APC and T cell. To show that this signaling was due to sustained signaling from the trogocytosed molecules, the approach of Faroudi *et al.* (188) was used. Following the addition of the Src-family of tyrosine kinase inhibitor, PP2, TCR-mediated signaling, both proximal (pZAP-70) and downstream (pERK1/2), ceased. Upon removal of the PP2 and a subsequent 20-minute incubation, both pZAP-70 and pERK1/2 were detected and localized with the TCR and trogocytosed MHC:peptide molecules. This signaling was observed only in the $trog^+$ cells, not in the $trog^-$ cells. Since the $trog^-$ cells were capable of recognizing antigen and responding (fig. 13), the lack of detectable signaling within these cells leads me to the conclusion that the signaling in the $trog^+$ cells was cell autonomous and driven by the trogocytosed molecules. If this signaling had been the result of T-T presentation events, there would have been detectable signaling within the $trog^-$ cells, as well, since the $trog^-$ cells make up the majority of the population and are more likely to encounter the $trog^+$ cells in T-T conjugates. The role of specific trogocytosed molecules (i.e. MHC:peptide, costimulatory molecules, etc.) in the sustained signaling is currently unclear.

These results show that the trogocytosed molecules are responsible for initiating and sustaining signaling by engaging the TCR, suggesting that this leads to the activation and selective survival of $trog^+$ T cells. The result of trogocytosis could, therefore, play a role in immune modulation. This sustained signaling might lead to clonal exhaustion or activation-induced cell death, helping to turn off an ongoing immune response. Alternatively, this sustained signaling could result in selective survival and to

alterations/increases in T cell effector functions. Further analysis of effector function and cytokine production by trog^{+} T cells will help clarify the potential role of trogocytosis in immune control.

The imaging experiments shown in fig. 18 demonstrate that in T-APC conjugates a significant accumulation of the TCR and signaling-associated molecules with trogocytosed molecules. Interestingly, the trogocytosed molecules move to a region of the T cell directly opposite the immune synapse more than 82% of the time. This area has been termed the distal pole complex (205, 206). The trogocytosed patches of APC membrane are usually arranged in a circular pattern at the distal pole forming a "trogocytosis crown". The reason for this segregation of the trogocytosed molecules when conjugated to APC is unclear, but it raises the intriguing possibility that the trogocytosed molecules could play a role in asymmetric T cell division. Asymmetric T cell division involves the segregation of proteins and signaling molecules in a bipolar manner resulting in the differential cell fate (effector versus memory) of daughter cells (207). It is possible that the T cells integrate differential signaling from the immune synapse and from trogocytosed molecules, which may play a role in setting up the observed asymmetric T cell division and differential development of T cell fate.

Sustained signaling after trogocytosis could also resolve an apparent paradox between the duration of Ag stimulation necessary to fully activate CD4^{+} T cells. Iezzi *et al.* found that T cell activation required sustained Ag stimulation for up to 6 hours (11). However, intravital microscopy has shown that the duration of initial T-DC interactions are on the order of minutes inside an intact lymph node (208). A pair of previous *in vitro* studies has shown that T cells form multiple short lived interactions with APC, and that

signals are "summed" to fully activate the T cells (181, 182). These results are consistent with the signaling summation model proposed by Lanzavecchia and colleagues (180). However, Lanzavecchia's model requires that the summed signaling events temporally overlap. The interval between successive T-APC encounters in both *in vivo* (208) and *in vitro* studies is on the order of minutes, during which time signaling would likely be terminated. Partially phosphorylated/activated signaling cascades are refractory to further stimulation leading to inactivation of the cells; a phenomenon underlying the TCR antagonism phenomenon (209, 210). Thus, during the short duration, repeated T-APC interactions observed by others are not strictly in line with the Lanzavecchia model. I propose that trogocytosis could function to sustain intracellular signaling between successive APC interactions allowing for full activation of the T cells via signal summing. The proposed mechanism for how trogocytosis could lead to sustained intracellular signaling is shown in fig. 30.

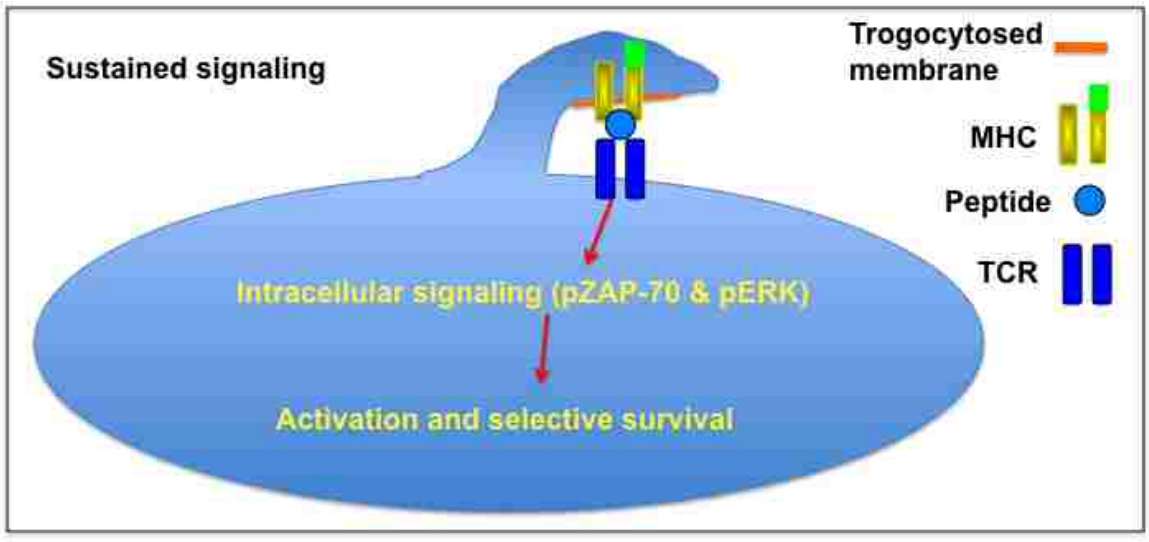

Figure 30: Autopresentation: proposed hypothesis for how trogocytosis leads to sustained intracellular signaling.

Trogocytosis signaling and spots

Imaging done in this thesis and by many others have shown that trogocytosed molecules are usually found in punctate spots on the surface of the T cell (20, 103, 105, 106, 120, 122). In T-APC conjugate images (figures 18-19), trogocytosed GFP:MHC can be seen as one to two spots at the distal pole, as discussed above. It is unclear why trogocytosis leads to punctate spots. The accumulation of trogocytosed molecules into distinct spots suggest that the T cell is concentrating the molecules to accumulate signaling in the area, which is consistent with the sustained signaling imaging data. When the TCR becomes engaged with MHC:peptide, the TCR forms aggregates (35, 36), this could explain why distinct spots form if there is continual engagement of the TCR by trogocytosed MHC:peptide. Wetzel *et al.* showed in recovered cells that the trogocytosed spots are surrounded by actin cytoskeleton (103), which could help maintain the spots. Fig. 23 is the first data to look at how spot size could correlate to intracellular signaling levels. Spots trogocytosed GFP ≥6x6 pixels showed higher staining for TCR and pERK compared to spots <6x6 pixels. These data suggest that increasing the size of the trogocytosed spot could lead to increased accumulation of intracellular signaling and cytoskeleton keeping the punctate spot together.

T-T presentation

The work of Zhou *et al.* showed that $CD4^+$ T cells could present trogocytosed antigen to naïve T cells, showing increases in CD25 and proliferation in the responder naïve T cells (159). They also showed that when $trog^+$ regulatory T cells were present,

immune suppression of the T cells occurred (159). To further Zhou *et al*. work, experiments looking at the phenotype of the responder T cells and the effect of T-T presentation on different responder T cells would help determine a role T-T presentation in an immune response. Using trog^{+} and trog^{-} sorted T cells as potential APCs, it was observed that naïve T cells incubated with trog^{+} and not trog^{-} T cells became activated. Naïve T cells cultured with trog^{+} T cells showed increases in CD69, CD25, and downmodulation of the TCR compared to naïve T cell placed in culture with trog^{-} T cells. Interestingly, naïve T cells trogocytosed biotin from the trog^{+} T cells, as shown in fig. 29D. Trogocytosis by responder naïve T cells during T-T Ag presentation may play a role in sustained activation and signaling in these cells. Further experiments are needed to determine this and whether an immune synapse forms at the interface. Understanding the role of T-T presentation to naïve T cells (fig. 29) and effector T cells is important in determining the overall role that trogocytosis may play in an immune response.

In conclusion, for the first time, the data presented here demonstrate that trogocytosed molecules continue to engage their receptors on the surface of trog^{+} T cells to cause sustained intracellular signaling. The selective survival of the trog^{+} T cells after recovery from the APC co-culture suggests this is most likely due to sustained signaling associated with trogocytosed molecules and provides strong evidence that trogocytosis provides a selective advantage for trog^{+} T cells.

Chapter 5:

Future Directions:

Peptide affinity

For this thesis, trogocytosis has been monitored during Ag presentation using a strong agonist peptide, MCC, to the TCR. Results by Wetzel *et al.* have shown that using non-specific peptide-loaded APCs does not lead to T cell trogocytosis (103). What has not been analyzed is the effects on trogocytosis efficiency using varying Ag affinity for the TCR. If trogocytosis occurs with specific Ag recognition, is trogocytosis dependent upon the strength of the TCR-MHC:peptide interaction? Very preliminary peptide affinity experiments have been performed using the fibroblast cell line P13.9H, loaded with an high-affinity agonist peptide (MCC), intermediate-affinity peptide (MCC-A) or a very weak agonist altered peptide ligand (MCC-K99A) (fig. 31A). Using this system we can examine trogocytosis efficiency and can also assess for differences in intracellular signaling and cell survival.

Early lab peptide affinity results are mixed. In several experiments, decreasing TCR affinity decreased trogocytosis efficiency (fig. 31B), except in two experiments where all peptides had similar trogocytosis efficiencies (fig. 31C). In fig. 31B, the bar graph (left) shows a ~32% and ~66% decrease in trogocytosed CD80 MFI compared to the strong agonist (MCC, yellow) to the intermediate agonist (MCC-A, blue) and the weak agonist (MCC-K99A, red), respectively. P-values from bar graphs in fig. 31C (left) showed no significant differences in the average MFI of trogocytosed CD80 ($p > 0.05$) between the different peptides. Discrepancies in the data may be due to differences in

experimental setups between the fig. 31B and C experiments. In fig. 31B, AD10 T cells were used and in fig. 31C, AND x B10.BR T cells were used. AD10 T cells have shown 10-fold higher affinity for MCC-K99A compared to AND x B10.BR T cells (211). Both AND x B10.BR and AD10 T cells have shown similar affinities for MCC and MCC-A (212, 213). The results in fig. 31 may be due to variations in affinity by the two mouse strain's TCR for the peptides. Further experiments are necessary to resolve these discrepancies.

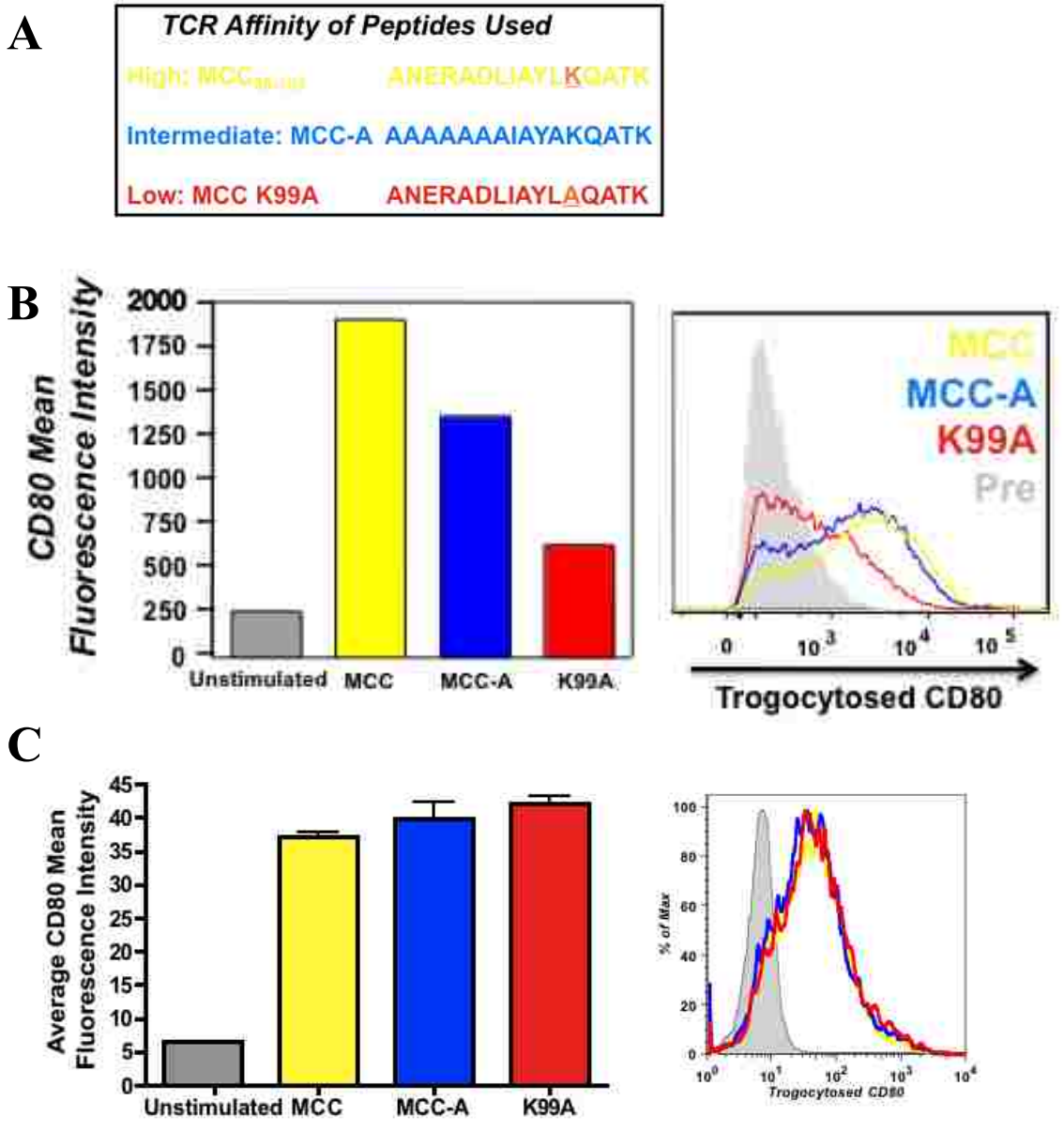

Figure 31: Peptide affinity and trogocytosis. Analysis of trogocytosis efficiency by $CD4^+$ T cells using peptides with differential TCR affinity. Using the standard *in vitro* trogocytosis assay, T cells were co-cultured with the fibroblast cell line P13.9H, loaded with an agonist peptide (MCC) (yellow), intermediate-affinity peptide (MCC-A) (blue) or a very weak agonist altered peptide ligand (MCC-K99A) (red). Peptides shown in A. Trogocytosis was measured using anti-CD80. (B) Using AD10 T cells, bar graphs (left) and histogram overlay (right) showing the MFI and staining of trogocytosed CD80 between T cells cultured with the different peptides. Results in B provided by Sean Wolfe and Timmon Hayes. (C) Using AND T cells, bar graphs (left) show the average MFI over two different experiments for trogocytosed CD80. (right) The histogram overlay shows CD80 staining in one of the two peptide affinity experiments from the bar graph. Bars in B represent mean ± SEM. Unstimulated samples (B and C) represent $CD4^+$ T cells without stimulation from APC. $P > 0.05$ for bar graphs in C.

Gene expression of trog$^+$ T cells

I have shown that sustained signaling occurs in $trog^+$ T cells, but the biological effects that the sustained signaling has on these T cells is unclear. Using qRT-PCR, gene expression can be analyzed to measure differences between $trog^+$ and $trog^-$ T cells. In 2005, Zhou *et al.* showed that autopresentation by APC derived presentasomes led to increases in transcription factors AP-1 and NFκB (161), but they did not look directly at how trogocytosis affects T cell gene expression. I performed a number of early qRT-PCR experiments looking at FACS-sorted $trog^-$ and $trog^+$ T cells following recovery from the standard *in vitro* trogocytosis assay. The data shown in fig. 32 are unclear, showing unexpected decreases in cell cycle promoting molecules, c-Fos and p27, in $trog^+$ T cells. Similarly, there are increases in both IFNγ and IL-4. These results suggest that there was an APC contamination in our samples that could cause these results. Repeating these experiments will help to pinpoint if there are differences in effector cytokine production in $trog^+$ and $trog^-$ cells.

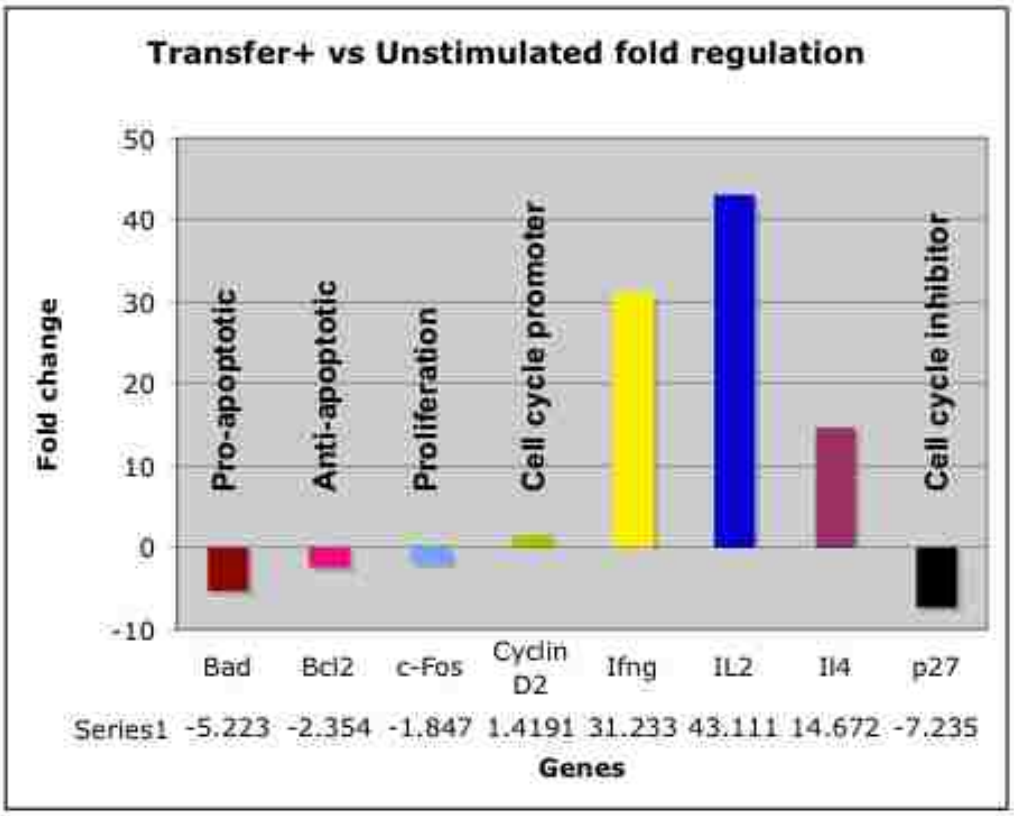

Figure 32. qRT-PCR of trog$^+$ T cells. FACS purified trog$^+$ T cell's gene expression was compared to unstimulated T cells. qRT-PCR was performed using primers to cell cycle molecules: c-Fos, p27, and Cyclin D2, apoptosis molecules: Bcl-2 and Bad, and cytokines: IFNγ, IL-2, and IL-4. qRT-PCR was performed by the Molecular Biology core at the University of Montana on the BioRad iCycler 5 (Hercules, CA). Fold change numbers were generated using $\Delta\Delta C_t$ method using Microsoft Excel.

T cell subsets and trogocytosis

As suggested from the qRT-PCR data (fig. 32), trogocytosis may be influenced by the effector function of the T cell. Analyzing effector function, specifically within T cell subsets, will help to determine the role of trogocytosis in an immune response. FACS-sorted trog$^+$ and trog$^-$ T cells, after recovery from APC, can be analyzed using both qRT-PCR and ELISAs.

Promoting the differentiation of T cells into T_H1 or T_H2 cells can help us determine which subset performs trogocytosis more efficiently. Prior to adding the primed AD10 T cells to the standard *in vitro* trogocytosis assay, we can supplement the primed cultures with cytokines to induce differentiation. By adding IL-4 or IFNγ to the cultures we can induce the cells to become T_H2 cells or T_H1 cells, respectively. Preliminary results by Lindsay Thuesen suggest that T_H2 cells perform trogocytosis more efficiently (data not shown). This experiment, combined with the qRT-PCR and ELISA data, could determine if there is a specific T cell subset that performs trogocytosis more efficiently.

T-T Ag presentation

Further studies on T-T presentation could expand on the role of trogocytosis in T cell function. Zhou *et al.* showed that $CD4^+$ T cells could present trogocytosed Ag to naïve T cells, causing increases in CD25 and proliferation of the naïve T cells (159). In contrast, Helft *et al.* showed that T-T presentation led to inhibition of effector/memory T cells (158). Experiments comparing T-T presentation on different responder T cells could help define the potential role of T-T presentation in modulating immune responses.

Understanding the interactions between responder T cells and $trog^+$ T cells should be characterized. Is an immune synapse formed? What is the efficiency? And what is required for T-T Ag presentation? $Trog^+$ and $trog^-$ FACS-sorted T cells, following recovery from the standard *in vitro* trogocytosis assay, could be placed in culture with naïve T cells for varying durations of time and ratios of sorted versus naïve cells to determine the length of time and cell dilution needed for efficient Ag presentation. We

could measure the expression of activation markers (like CD69 and CD25) to determine T-T presentation.

Understanding the requirements for T-T Ag presentation, as described above, will help us develop a standard assay for T-T presentation. Once an assay is created, imaging could be done to determine if an immune synapse is formed between the T-APC and the naïve responding cell. Imaging the interface between the two cells for prototypical immune synapse markers (like TCR, MHC, costimulatory molecules (CD80), signaling molecules (PKCθ), and adhesion molecules (ICAM-1)) will allow us to determine if there is segregation of molecules into distinct SMACs, like those found in mature immune synapses.

References

1. Romagnani, S. 2000. T-cell subsets (Th1 versus Th2). *Ann Allergy Asthma Immunol* 85:9-18.

2. Jankovic, D., Z. Liu, and W. C. Gause. 2001. Th1- and Th2-cell commitment during infectious disease: asymmetry in divergent pathways. *Trends Immunol* 22:450-457.

3. Street, N. E., and T. R. Mosmann. 1991. Functional diversity of T lymphocytes due to secretion of different cytokine patterns. *FASEB J* 5:171-177.

4. Harrington, L. E., R. D. Hatton, P. R. Mangan, H. Turner, T. L. Murphy, K. M. Murphy, and C. T. Weaver. 2005. Interleukin 17-producing CD4+ effector T cells develop via a lineage distinct from the T helper type 1 and 2 lineages. *Nat Immunol* 6:1123-1132.

5. Schaerli, P., K. Willimann, A. B. Lang, M. Lipp, P. Loetscher, and B. Moser. 2000. CXC chemokine receptor 5 expression defines follicular homing T cells with B cell helper function. *J Exp Med* 192:1553-1562.

6. Gershon, R. K., and K. Kondo. 1970. Cell interactions in the induction of tolerance: the role of thymic lymphocytes. *Immunology* 18:723-737.

7. Matzinger, P. 1994. Tolerance, danger, and the extended family. *Annu Rev Immunol* 12:991-1045.

8. Schwartz, R. H. 1992. Costimulation of T lymphocytes: the role of CD28, CTLA-4, and B7/BB1 in interleukin-2 production and immunotherapy. *Cell* 71:1065-1068.

9. Schwartz, R. H. 1990. A cell culture model for T lymphocyte clonal anergy. *Science* 248:1349-1356.

10. Quezada, S. A., L. Z. Jarvinen, E. F. Lind, and R. J. Noelle. 2004. CD40/CD154 interactions at the interface of tolerance and immunity. *Annu Rev Immunol* 22:307-328.

11. Iezzi, G., K. Karjalainen, and A. Lanzavecchia. 1998. The duration of antigenic stimulation determines the fate of naive and effector T cells. *Immunity* 8:89-95.

12. Richie, L. I., P. J. Ebert, L. C. Wu, M. F. Krummel, J. J. Owen, and M. M. Davis. 2002. Imaging synapse formation during thymocyte selection: inability of

CD3zeta to form a stable central accumulation during negative selection. *Immunity* 16:595-606.

13. Mercep, M., A. M. Weissman, S. J. Frank, R. D. Klausner, and J. D. Ashwell. 1989. Activation-driven programmed cell death and T cell receptor zeta eta expression. *Science* 246:1162-1165.

14. Schwartz, R. H. 2003. T cell anergy. *Annu Rev Immunol* 21:305-334.

15. Schonrich, G., U. Kalinke, F. Momburg, M. Malissen, A. M. Schmitt-Verhulst, B. Malissen, G. J. Hammerling, and B. Arnold. 1991. Down-regulation of T cell receptors on self-reactive T cells as a novel mechanism for extrathymic tolerance induction. *Cell* 65:293-304.

16. Zanders, E. D., J. R. Lamb, M. Feldmann, N. Green, and P. C. Beverley. 1983. Tolerance of T-cell clones is associated with membrane antigen changes. *Nature* 303:625-627.

17. Reinherz, E. L., O. Acuto, M. Fabbi, A. Bensussan, C. Milanese, H. D. Royer, S. C. Meuer, and S. F. Schlossman. 1984. Clonotypic surface structure on human T lymphocytes: functional and biochemical analysis of the antigen receptor complex. *Immunol Rev* 81:95-129.

18. Bankovich, A. J., L. R. Shiow, and J. G. Cyster. 2010. CD69 suppresses sphingosine 1-phosophate receptor-1 (S1P1) function through interaction with membrane helix 4. *J Biol Chem* 285:22328-22337.

19. Yamashita, I., T. Nagata, T. Tada, and T. Nakayama. 1993. CD69 cell surface expression identifies developing thymocytes which audition for T cell antigen receptor-mediated positive selection. *Int Immunol* 5:1139-1150.

20. Martinez-Martin, N., E. Fernandez-Arenas, S. Cemerski, P. Delgado, M. Turner, J. Heuser, D. J. Irvine, B. Huang, X. R. Bustelo, A. Shaw, and B. Alarcon. 2011. T Cell Receptor Internalization from the Immunological Synapse Is Mediated by TC21 and RhoG GTPase-Dependent Phagocytosis. *Immunity* 35:208-222.

21. Dietrich, J., X. Hou, A. M. Wegener, and C. Geisler. 1994. CD3 gamma contains a phosphoserine-dependent di-leucine motif involved in down-regulation of the T cell receptor. *Embo J* 13:2156-2166.

22. Monjas, A., A. Alcover, and B. Alarcon. 2004. Engaged and bystander T cell receptors are down-modulated by different endocytotic pathways. *J Biol Chem* 279:55376-55384.

23. Valitutti, S., S. Muller, M. Cella, E. Padovan, and A. Lanzavecchia. 1995. Serial triggering of many T-cell receptors by a few peptide-MHC complexes. *Nature* 375:148-151.

24. Itoh, Y., B. Hemmer, R. Martin, and R. N. Germain. 1999. Serial TCR engagement and down-modulation by peptide:MHC molecule ligands: relationship to the quality of individual TCR signaling events. *J Immunol* 162:2073-2080.

25. Valitutti, S., S. Muller, M. Dessing, and A. Lanzavecchia. 1996. Signal extinction and T cell repolarization in T helper cell-antigen-presenting cell conjugates. *Eur J Immunol* 26:2012-2016.

26. Schuh, K., T. Twardzik, B. Kneitz, J. Heyer, A. Schimpl, and E. Serfling. 1998. The interleukin 2 receptor alpha chain/CD25 promoter is a target for nuclear factor of activated T cells. *J Exp Med* 188:1369-1373.

27. Cantrell, D. A., and K. A. Smith. 1984. The interleukin-2 T-cell system: a new cell growth model. *Science* 224:1312-1316.

28. Robb, R. J., A. Munck, and K. A. Smith. 1981. T cell growth factor receptors. Quantitation, specificity, and biological relevance. *J Exp Med* 154:1455-1474.

29. Bradley, L. M., G. G. Atkins, and S. L. Swain. 1992. Long-term CD4+ memory T cells from the spleen lack MEL-14, the lymph node homing receptor. *J Immunol* 148:324-331.

30. Hengel, R. L., V. Thaker, M. V. Pavlick, J. A. Metcalf, G. Dennis, Jr., J. Yang, R. A. Lempicki, I. Sereti, and H. C. Lane. 2003. Cutting edge: L-selectin (CD62L) expression distinguishes small resting memory CD4+ T cells that preferentially respond to recall antigen. *J Immunol* 170:28-32.

31. Haynes, B. F., M. J. Telen, L. P. Hale, and S. M. Denning. 1989. CD44--a molecule involved in leukocyte adherence and T-cell activation. *Immunol Today* 10:423-428.

32. Doyle, C., and J. L. Strominger. 1987. Interaction between CD4 and class II MHC molecules mediates cell adhesion. *Nature* 330:256-259.

33. Huet, S., H. Groux, B. Caillou, H. Valentin, A. M. Prieur, and A. Bernard. 1989. CD44 contributes to T cell activation. *J Immunol* 143:798-801.

34. Krogsgaard, M., Q. J. Li, C. Sumen, J. B. Huppa, M. Huse, and M. M. Davis. 2005. Agonist/endogenous peptide-MHC heterodimers drive T cell activation and sensitivity. *Nature* 434:238-243.

35. Williams, A. F., and A. D. Beyers. 1992. T-cell receptors. At grips with interactions. *Nature* 356:746-747.

36. Davis, S. J., and P. A. van der Merwe. 2006. The kinetic-segregation model: TCR triggering and beyond. *Nat Immunol* 7:803-809.

37. Bu, J. Y., A. S. Shaw, and A. C. Chan. 1995. Analysis of the interaction of ZAP-70 and syk protein-tyrosine kinases with the T-cell antigen receptor by plasmon resonance. *Proc Natl Acad Sci U S A* 92:5106-5110.

38. Artyomov, M. N., M. Lis, S. Devadas, M. M. Davis, and A. K. Chakraborty. 2010. CD4 and CD8 binding to MHC molecules primarily acts to enhance Lck delivery. *Proc Natl Acad Sci U S A* 107:16916-16921.

39. Lovatt, M., A. Filby, V. Parravicini, G. Werlen, E. Palmer, and R. Zamoyska. 2006. Lck regulates the threshold of activation in primary T cells, while both Lck and Fyn contribute to the magnitude of the extracellular signal-related kinase response. *Mol Cell Biol* 26:8655-8665.

40. Zhang, W., J. Sloan-Lancaster, J. Kitchen, R. P. Trible, and L. E. Samelson. 1998. LAT: the ZAP-70 tyrosine kinase substrate that links T cell receptor to cellular activation. *Cell* 92:83-92.

41. Bubeck Wardenburg, J., C. Fu, J. K. Jackman, H. Flotow, S. E. Wilkinson, D. H. Williams, R. Johnson, G. Kong, A. C. Chan, and P. R. Findell. 1996. Phosphorylation of SLP-76 by the ZAP-70 protein-tyrosine kinase is required for T-cell receptor function. *J Biol Chem* 271:19641-19644.

42. Yablonski, D., M. R. Kuhne, T. Kadlecek, and A. Weiss. 1998. Uncoupling of nonreceptor tyrosine kinases from PLC-gamma1 in an SLP-76-deficient T cell. *Science* 281:413-416.

43. Sommers, C. L., L. E. Samelson, and P. E. Love. 2004. LAT: a T lymphocyte adapter protein that couples the antigen receptor to downstream signaling pathways. *Bioessays* 26:61-67.

44. Dombroski, D., R. A. Houghtling, C. M. Labno, P. Precht, A. Takesono, N. J. Caplen, D. D. Billadeau, R. L. Wange, J. K. Burkhardt, and P. L. Schwartzberg. 2005. Kinase-independent functions for Itk in TCR-induced regulation of Vav and the actin cytoskeleton. *J Immunol* 174:1385-1392.

45. Samelson, L. E. 2002. Signal transduction mediated by the T cell antigen receptor: the role of adapter proteins. *Annu Rev Immunol* 20:371-394.

46. Wu, J. N., and G. A. Koretzky. 2004. The SLP-76 family of adapter proteins. *Semin Immunol* 16:379-393.

47. Desai, D. M., M. E. Newton, T. Kadlecek, and A. Weiss. 1990. Stimulation of the phosphatidylinositol pathway can induce T-cell activation. *Nature* 348:66-69.

48. Reynolds, L. F., C. de Bettignies, T. Norton, A. Beeser, J. Chernoff, and V. L. Tybulewicz. 2004. Vav1 transduces T cell receptor signals to the activation of the Ras/ERK pathway via LAT, Sos, and RasGRP1. *J Biol Chem* 279:18239-18246.

49. Liu, K. Q., S. C. Bunnell, C. B. Gurniak, and L. J. Berg. 1998. T cell receptor-initiated calcium release is uncoupled from capacitative calcium entry in Itk-deficient T cells. *J Exp Med* 187:1721-1727.

50. Berg, L. J., L. D. Finkelstein, J. A. Lucas, and P. L. Schwartzberg. 2005. Tec family kinases in T lymphocyte development and function. *Annu Rev Immunol* 23:549-600.

51. Majerus, P. W., T. S. Ross, T. W. Cunningham, K. K. Caldwell, A. B. Jefferson, and V. S. Bansal. 1990. Recent insights in phosphatidylinositol signaling. *Cell* 63:459-465.

52. Williams, R. L. 1999. Mammalian phosphoinositide-specific phospholipase C. *Biochim Biophys Acta* 1441:255-267.

53. Feske, S., Y. Gwack, M. Prakriya, S. Srikanth, S. H. Puppel, B. Tanasa, P. G. Hogan, R. S. Lewis, M. Daly, and A. Rao. 2006. A mutation in Orai1 causes immune deficiency by abrogating CRAC channel function. *Nature* 441:179-185.

54. Cahalan, M. D. 2009. STIMulating store-operated Ca(2+) entry. *Nat Cell Biol* 11:669-677.

55. Hogan, P. G., L. Chen, J. Nardone, and A. Rao. 2003. Transcriptional regulation by calcium, calcineurin, and NFAT. *Genes Dev* 17:2205-2232.

56. Rao, A. 1994. NF-ATp: a transcription factor required for the co-ordinate induction of several cytokine genes. *Immunol Today* 15:274-281.

57. Vandenberghe, P. A., and J. L. Ceuppens. 1990. Flow cytometric measurement of cytoplasmic free calcium in human peripheral blood T lymphocytes with fluo-3, a new fluorescent calcium indicator. *J Immunol Methods* 127:197-205.

58. Delon, J., N. Bercovici, R. Liblau, and A. Trautmann. 1998. Imaging antigen recognition by naive $CD4^+$ T cells: compulsory cytoskeletal alterations for the triggering of an intracellular calcium response. *Eur J Immunol* 28:716-729.

59. Isakov, N., and A. Altman. 2002. Protein kinase C(theta) in T cell activation. *Annu Rev Immunol* 20:761-794.

60. Ebinu, J. O., D. A. Bottorff, E. Y. Chan, S. L. Stang, R. J. Dunn, and J. C. Stone. 1998. RasGRP, a Ras guanyl nucleotide- releasing protein with calcium- and diacylglycerol-binding motifs. *Science* 280:1082-1086.

61. Tognon, C. E., H. E. Kirk, L. A. Passmore, I. P. Whitehead, C. J. Der, and R. J. Kay. 1998. Regulation of RasGRP via a phorbol ester-responsive C1 domain. *Mol Cell Biol* 18:6995-7008.

62. Egawa, T., B. Albrecht, B. Favier, M. J. Sunshine, K. Mirchandani, W. O'Brien, M. Thome, and D. R. Littman. 2003. Requirement for CARMA1 in antigen receptor-induced NF-kappa B activation and lymphocyte proliferation. *Curr Biol* 13:1252-1258.

63. Su, B., J. Cheng, J. Yang, and Z. Guo. 2001. MEKK2 is required for T-cell receptor signals in JNK activation and interleukin-2 gene expression. *J Biol Chem* 276:14784-14790.

64. Samelson, L. E. 2011. Immunoreceptor signaling. *Cold Spring Harb Perspect Biol* 3.

65. Mercurio, F., H. Zhu, B. W. Murray, A. Shevchenko, B. L. Bennett, J. Li, D. B. Young, M. Barbosa, M. Mann, A. Manning, and A. Rao. 1997. IKK-1 and IKK-2: cytokine-activated IkappaB kinases essential for NF-kappaB activation. *Science* 278:860-866.

66. Foletta, V. C., D. H. Segal, and D. R. Cohen. 1998. Transcriptional regulation in the immune system: all roads lead to AP-1. *J Leukoc Biol* 63:139-152.

67. Macian, F., F. Garcia-Cozar, S. H. Im, H. F. Horton, M. C. Byrne, and A. Rao. 2002. Transcriptional mechanisms underlying lymphocyte tolerance. *Cell* 109:719-731.

68. Henney, C. S., and J. E. Bubbers. 1973. Antigen-T lymphocyte interactions: inhibition by cytochalasin B. *J Immunol* 111:85-90.

69. Holsinger, L. J., I. A. Graef, W. Swat, T. Chi, D. M. Bautista, L. Davidson, R. S. Lewis, F. W. Alt, and G. R. Crabtree. 1998. Defects in actin-cap formation in Vav-deficient mice implicate an actin requirement for lymphocyte signal transduction. *Curr Biol* 8:563-572.

70. von Andrian, U. H., and T. R. Mempel. 2003. Homing and cellular traffic in lymph nodes. *Nat Rev Immunol* 3:867-878.

71. Linsley, P. S., W. Brady, L. Grosmaire, A. Aruffo, N. K. Damle, and J. A. Ledbetter. 1991. Binding of the B cell activation antigen B7 to CD28 costimulates

T cell proliferation and interleukin 2 mRNA accumulation. *J Exp Med* 173:721-730.

72. Garcon, F., D. T. Patton, J. L. Emery, E. Hirsch, R. Rottapel, T. Sasaki, and K. Okkenhaug. 2008. CD28 provides T-cell costimulation and enhances PI3K activity at the immune synapse independently of its capacity to interact with the p85/p110 heterodimer. *Blood* 111:1464-1471.

73. Okkenhaug, K., A. Bilancio, G. Farjot, H. Priddle, S. Sancho, E. Peskett, W. Pearce, S. E. Meek, A. Salpekar, M. D. Waterfield, A. J. Smith, and B. Vanhaesebroeck. 2002. Impaired B and T cell antigen receptor signaling in p110delta PI 3-kinase mutant mice. *Science* 297:1031-1034.

74. June, C. H., J. A. Ledbetter, M. M. Gillespie, T. Lindsten, and C. B. Thompson. 1987. T-cell proliferation involving the CD28 pathway is associated with cyclosporine-resistant interleukin 2 gene expression. *Mol Cell Biol* 7:4472-4481.

75. Kasakura, S., and L. Lowenstein. 1965. A factor stimulating DNA synthesis derived from the medium of leukocyte cultures. *Nature* 208:794-795.

76. Gordon, J., and L. D. MacLean. 1965. A lymphocyte-stimulating factor produced in vitro. *Nature* 208:795-796.

77. Kupfer, A., S. J. Singer, C. A. Janeway, and S. L. Swain. 1987. Coclustering of CD4 (L3T4) molecule with the T-cell receptor is induced by specific direct interaction of helper T cells and antigen-presenting cells. *Proc Natl Acad Sci U S A* 84:5888-5892.

78. Monks, C. R., B. A. Freiberg, H. Kupfer, N. Sciaky, and A. Kupfer. 1998. Three-dimensional segregation of supramolecular activation clusters in T cells. *Nature* 395:82-86.

79. Grakoui, A., S. K. Bromley, C. Sumen, M. M. Davis, A. S. Shaw, P. M. Allen, and M. L. Dustin. 1999. The immunological synapse: a molecular machine controlling T cell activation. *Science* 285:221-227.

80. Kaizuka, Y., A. D. Douglass, R. Varma, M. L. Dustin, and R. D. Vale. 2007. Mechanisms for segregating T cell receptor and adhesion molecules during immunological synapse formation in Jurkat T cells. *Proc Natl Acad Sci U S A* 104:20296-20301.

81. Varma, R., G. Campi, T. Yokosuka, T. Saito, and M. L. Dustin. 2006. T cell receptor-proximal signals are sustained in peripheral microclusters and terminated in the central supramolecular activation cluster. *Immunity* 25:117-127.

82. Vardhana, S. 2010. Essential role of ubiquitin and TSG101 protein in formation and function of the central supramolecular activation cluster. *Molecular Cellular Biology* 24:531-540.

83. van der Merwe, P. A., S. J. Davis, A. S. Shaw, and M. L. Dustin. 2000. Cytoskeletal polarization and redistribution of cell-surface molecules during T cell antigen recognition. *Semin Immunol* 12:5-21.

84. Dustin, M. L., and J. A. Cooper. 2000. The immunological synapse and the actin cytoskeleton: molecular hardware for T cell signaling. *Nat Immunol* 1:23-29.

85. Freiberg, B. 2000. Spatial-temporal visualization of molecular events during T cell/antigen presenting cell interactions. In *Microbiology & Immunology*. University of Colorado Health Sciences Center, Denver.

86. Thauland, T. J., Y. Koguchi, S. A. Wetzel, M. L. Dustin, and D. C. Parker. 2008. Th1 and Th2 cells form morphologically distinct immunological synapses. *J Immunol* 181:393-399.

87. Appay, V., J. J. Zaunders, L. Papagno, J. Sutton, A. Jaramillo, A. Waters, P. Easterbrook, P. Grey, D. Smith, A. J. McMichael, D. A. Cooper, S. L. Rowland-Jones, and A. D. Kelleher. 2002. Characterization of CD4(+) CTLs ex vivo. *J Immunol* 168:5954-5958.

88. Stinchcombe, J. C., G. Bossi, S. Booth, and G. M. Griffiths. 2001. The Immunological Synapse of CTL Contains a Secretory Domain and Membrane Bridges. *Immunity* 15:751-761.

89. Ju, S. T., H. Cui, D. J. Panka, R. Ettinger, and A. Marshak-Rothstein. 1994. Participation of target Fas protein in apoptosis pathway induced by CD4+ Th1 and CD8+ cytotoxic T cells. *Proc Natl Acad Sci U S A* 91:4185-4189.

90. Roberts, J. 2003. Dissecting the Immunological Synapse. In *The Scientist*. http://www.the-scientist.com/?articles.view/articleNo/14727/title/Dissecting-the-Immunological-Synapse/

91. Dustin, M. L., and A. S. Shaw. 1999. Costimulation: building an immunological synapse. *Science* 283:649-650.

92. Bromley, S. K., W. R. Burack, K. G. Johnson, K. Somersalo, T. N. Sims, C. Sumen, M. M. Davis, A. S. Shaw, P. M. Allen, and M. L. Dustin. 2001. The immunological synapse. *Annu Rev Immunol* 19:375-396.

93. Skokos, D., G. Shakhar, R. Varma, J. C. Waite, T. O. Cameron, R. L. Lindquist, T. Schwickert, M. C. Nussenzweig, and M. L. Dustin. 2007. Peptide-MHC

potency governs dynamic interactions between T cells and dendritic cells in lymph nodes. *Nat Immunol* 8:835-844.

94. Dustin, M. L., and T. A. Sptinger. 1989. T-cell receptor crosslinking transiently stimulates adhesiveness through LFA-1. *Nature* 341:619-624.

95. Dustin, M. L. 2003. Coordination of T cell activation and migration through formation of the immunological synapse. *Ann N Y Acad Sci* 987:51-59.

96. Campi, G., R. Varma, and M. L. Dustin. 2005. Actin and agonist MHC-peptide complex-dependent T cell receptor microclusters as scaffolds for signaling. *J Exp Med* 202:1031-1036.

97. Lee, K. H., A. D. Holdorf, M. L. Dustin, A. C. Chan, P. M. Allen, and A. S. Shaw. 2002. T cell receptor signaling precedes immunological synapse formation. *Science* 295:1539-1542.

98. Cemerski, S., J. Das, E. Giurisato, M. A. Markiewicz, P. M. Allen, A. K. Chakraborty, and A. S. Shaw. 2008. The balance between T cell receptor signaling and degradation at the center of the immunological synapse is determined by antigen quality. *Immunity* 29:414-422.

99. Anikeeva, N., K. Somersalo, T. N. Sims, V. K. Thomas, M. L. Dustin, and Y. Sykulev. 2005. Distinct role of lymphocyte function-associated antigen-1 in mediating effective cytolytic activity by cytotoxic T lymphocytes. *Proc Natl Acad Sci U S A* 102:6437-6442.

100. Beal, A. M., N. Anikeeva, R. Varma, T. O. Cameron, P. J. Norris, M. L. Dustin, and Y. Sykulev. 2008. Protein kinase C theta regulates stability of the peripheral adhesion ring junction and contributes to the sensitivity of target cell lysis by CTL. *J Immunol* 181:4815-4824.

101. Huse, M., B. F. Lillemeier, M. S. Kuhns, D. S. Chen, and M. M. Davis. 2006. T cells use two directionally distinct pathways for cytokine secretion. *Nat Immunol* 7:247-255.

102. Doherty, M., D. G. Osborne, D. L. Browning, D. C. Parker, and S. A. Wetzel. 2010. Anergic CD4+ T cells form mature immunological synapses with enhanced accumulation of c-Cbl and Cbl-b. *J Immunol* 184:3598-3608.

103. Wetzel, S. A., T. W. McKeithan, and D. C. Parker. 2005. Peptide-specific intercellular transfer of MHC class II to CD4+ T cells directly from the immunological synapse upon cellular dissociation. *J Immunol* 174:80-89.

104. Patel, D. M., and M. D. Mannie. 2001. Intercellular exchange of class II major histocompatibility complex/peptide complexes is a conserved process that

requires activation of T cells but is constitutive in other types of antigen presenting cell. *Cell Immunol* 214:165-172.

105. Huang, J. F., Y. Yang, H. Sepulveda, W. Shi, I. Hwang, P. A. Peterson, M. R. Jackson, J. Sprent, and Z. Cai. 1999. TCR-Mediated internalization of peptide-MHC complexes acquired by T cells. *Science* 286:952-954.

106. Hwang, I., J. F. Huang, H. Kishimoto, A. Brunmark, P. A. Peterson, M. R. Jackson, C. D. Surh, Z. Cai, and J. Sprent. 2000. T cells can use either T cell receptor or CD28 receptors to absorb and internalize cell surface molecules derived from antigen-presenting cells. *J Exp Med* 191:1137-1148.

107. Hudrisier, D., J. Riond, H. Mazarguil, J. E. Gairin, and E. Joly. 2001. CTLs rapidly capture membrane fragments from target cells in a TCR signaling-dependent manner. *J Immunol* 166:3645-3649.

108. Joly, E., and D. Hudrisier. 2003. What is trogocytosis and what is its purpose? *Nat Immunol* 4:815.

109. Marciano-Cabral, F., K. L. Zoghby, and S. G. Bradley. 1990. Cytopathic action of Naegleria fowleri amoebae on rat neuroblastoma target cells. *J Protozool* 37:138-144.

110. Brown, T. 1979. Observations by immunofluorescence microscopy and electron microscopy on the cytopathogenicity of Naegleria fowleri in mouse embryo-cell cultures. *J Med Microbiol* 12:363-371.

111. Daubeuf, S., A. Aucher, C. Bordier, A. Salles, L. Serre, G. Gaibelet, J. C. Faye, G. Favre, E. Joly, and D. Hudrisier. 2010. Preferential transfer of certain plasma membrane proteins onto T and B cells by trogocytosis. *PLoS One* 5:e8716.

112. Hudson, L., J. Sprent, J. F. Miller, and J. H. Playfair. 1974. B cell-derived immunoglobulin on activated mouse T lymphocytes. *Nature* 251:60-62.

113. Lorber, M. I., M. R. Loken, A. M. Stall, and F. W. Fitch. 1982. I-A antigens on cloned alloreactive murine T lymphocytes are acquired passively. *J Immunol* 128:2798-2803.

114. Nepom, J. T., B. Benacerraf, and R. N. Germain. 1981. Acquisition of syngeneic I-A determinants by T cells proliferating in response to poly ($Gly^{60}Ala^{30}$, Tyr^{10}). *J Immunol* 127:888-892.

115. Sharrow, S. O., B. J. Mathieson, and A. Singer. 1981. Cell surface appearance of unexpected host MHC determinants on thymocytes from radiation bone marrow chimeras. *J Immunol* 126:1327-1335.

116. Mannie, M. D., S. K. Rendall, P. Y. Arnold, J. P. Nardella, and G. A. White. 1996. Anergy-associated T cell antigen presentation. A mechanism of infectious tolerance in experimental autoimmune encephalomyelitis. *J Immunol* 157:1062-1070.

117. Arnold, P. Y., D. K. Davidian, and M. D. Mannie. 1997. Antigen Presentation by T cells: T cell receptor ligation promotes antigen acquisition from professional antigen-presenting cells. *European Journal of Immunology* 27:3198-3205.

118. Arnold, P. Y., and M. D. Mannie. 1999. Vesicles bearing MHC class II molecules mediate transfer of antigen from antigen-presenting cells to CD4+ T cells. *Eur J Immunol* 29:1363-1373.

119. Patel, D. M., P. Y. Arnold, G. A. White, J. P. Nardella, and M. D. Mannie. 1999. Class II MHC/peptide complexes are released from APC and are acquired by T cell responders during specific antigen recognition. *J Immunol* 163:5201-5210.

120. Patel, D. M., R. W. Dudek, and M. D. Mannie. 2001. Intercellular exchange of class II MHC complexes: ultrastructural localization and functional presentation of adsorbed I-A/peptide complexes. *Cell Immunol* 214:21-34.

121. Walker, M. R., and M. D. Mannie. 2002. Acquisition of functional MHC class II/peptide complexes by T cells during thymic development and CNS-directed pathogenesis. *Cell Immunol* 218:13-25.

122. Hwang, I., and J. Sprent. 2001. Role of actin cytoskeleton in T cell absorption and internalization of ligands from APC. *J Immunol* 166:5099-5107.

123. Espinosa, E., J. Tabiasco, D. Hudrisier, and J. J. Fournie. 2002. Synaptic transfer by human gamma delta T cells stimulated with soluble or cellular antigens. *J Immunol* 168:6336-6343.

124. Hudrisier, D., and P. Bongrand. 2002. Intercellular transfer of antigen-presenting cell determinants onto T cells: molecular mechanisms and biological significance. *Faseb J* 16:477-486.

125. Hudrisier, D., J. Riond, L. Garidou, C. Duthoit, and E. Joly. 2005. T cell activation correlates with an increased proportion of antigen among the materials acquired from target cells. *Eur J Immunol* 35:2284-2294.

126. Hudrisier, D., A. Aucher, A. L. Puaux, C. Bordier, and E. Joly. 2007. Capture of target cell membrane components via trogocytosis is triggered by a selected set of surface molecules on T or B cells. *J Immunol* 178:3637-3647.

127. Riond, J., J. Elhmouzi, D. Hudrisier, and J. E. Gairin. 2007. Capture of membrane components via trogocytosis occurs in vivo during both dendritic cells and target cells encounter by CD8(+) T cells. *Scand J Immunol* 66:441-450.

128. Daubeuf, S., M. A. Lindorfer, R. P. Taylor, E. Joly, and D. Hudrisier. 2010. The direction of plasma membrane exchange between lymphocytes and accessory cells by trogocytosis is influenced by the nature of the accessory cell. *J Immunol* 184:1897-1908.

129. Aucher, A., E. Magdeleine, E. Joly, and D. Hudrisier. 2008. Capture of plasma membrane fragments from target cells by trogocytosis requires signaling in T cells but not in B cells. *Blood*.

130. Sabzevari, H., J. Kantor, A. Jaigirdar, Y. Tagaya, M. Naramura, J. Hodge, J. Bernon, and J. Schlom. 2001. Acquisition of CD80 (B7-1) by T cells. *J Immunol* 166:2505-2513.

131. Batista, F. D., and M. S. Neuberger. 2000. B cells extract and present immobilized antigen: implications for affinity discrimination. *Embo J* 19:513-520.

132. Batista, F. D., D. Iber, and M. S. Neuberger. 2001. B cells acquire antigen from target cells after synapse formation. *Nature* 411:489 - 494.

133. Herrera, O. B., D. Golshayan, R. Tibbott, F. Salcido Ochoa, M. J. James, F. M. Marelli-Berg, and R. I. Lechler. 2004. A novel pathway of alloantigen presentation by dendritic cells. *J Immunol* 173:4828-4837.

134. Russo, V., D. Zhou, C. Sartirana, P. Rovere, A. Villa, S. Rossini, C. Traversari, and C. Bordignon. 2000. Acquisition of intact allogeneic human leukocyte antigen molecules by human dendritic cells. *Blood* 95:3473-3477.

135. Carlin, L. M., K. Eleme, F. E. McCann, and D. M. Davis. 2001. Intercellular transfer and supramolecular organization of human leukocyte antigen C at inhibitory natural killer cell immune synapses. *J Exp Med* 194:1507-1517.

136. Sjöström, A., M. Eriksson, C. Cerboni, M. H. Johansson, C. L. Sentman, K. Karre, and P. Hoglund. 2001. Acquisition of external major histocompatibility complex class I molecules by natural killer cells expressing inhibitory Ly49 receptors. *J Exp Med* 194:1519-1530.

137. Tabiasco, J., E. Espinosa, D. Hudrisier, E. Joly, J. J. Fournie, and A. Vercellone. 2002. Active trans-synaptic capture of membrane fragments by natural killer cells. *Eur J Immunol* 32:1502-1508.

138. Zimmer, J., V. Ioannidis, and W. Held. 2001. H-2D Ligand Expression by Ly49A^{+} Natural Killer (NK) Cells Precludes Ligand Uptake from Environmental Cells: Implications for NK Cell Function. *J Exp Med* 194:1531-1539.

139. Harshyne, L. A., S. C. Watkins, A. Gambotto, and S. M. Barratt-Boyes. 2001. Dendritic cells acquire antigens from live cells for cross-presentation to CTL. *J Immunol* 166:3717-3723.

140. Zhang, Q. J., X. L. Li, D. Wang, X. C. Huang, J. M. Mathis, W. M. Duan, D. Knight, R. Shi, J. Glass, D. Q. Zhang, L. Eisenbach, and W. A. Jefferies. 2008. Trogocytosis of MHC-I/peptide complexes derived from tumors and infected cells enhances dendritic cell cross-priming and promotes adaptive T cell responses. *PLoS One* 3:e3097.

141. Roda-Navarro, P., and H. T. Reyburn. 2007. Intercellular protein transfer at the NK cell immune synapse: mechanisms and physiological significance. *FASEB J* 21:1636-1646.

142. Tatari-Calderone, Z., R. T. Semnani, T. B. Nutman, J. Schlom, and H. Sabzevari. 2002. Acquisition of CD80 by human T cells at early stages of activation: functional involvement of CD80 acquisition in T cell to T cell interaction. *J Immunol* 169:6162-6169.

143. Baba, E., Y. Takahashi, J. Lichtenfeld, R. Tanaka, A. Yoshida, K. Sugamura, N. Yamamoto, and Y. Tanaka. 2001. Functional CD4 T cells after intercellular molecular transfer of 0X40 ligand. *J Immunol* 167:875-883.

144. Gary, R., S. Voelkl, R. Palmisano, E. Ullrich, J. J. Bosch, and A. Mackensen. 2012. Antigen-specific transfer of functional programmed death ligand 1 from human APCs onto CD8+ T cells via trogocytosis. *J Immunol* 188:744-752.

145. Game, D. S., N. J. Rogers, and R. I. Lechler. 2005. Acquisition of HLA-DR and costimulatory molecules by T cells from allogeneic antigen presenting cells. *Am J Transplant* 5:1614-1625.

146. Tsang, J. Y. S., J. C. Chai, and R. Lechler. 2003. Antigen Presentation by mouse CD4^{+} T cells involving acquired MHC class II:peptide complexes: another mechanism to limit clonal expansion. *Blood* 101:2704-2710.

147. Xiang, J., H. Huang, and Y. Liu. 2005. A new dynamic model of CD8+ T effector cell responses via CD4+ T helper-antigen-presenting cells. *J Immunol* 174:7497-7505.

148. Daubeuf, S., M. A. Lindorfer, R. P. Taylor, E. Joly, and D. Hudrisier. 2010. The Direction of Plasma Membrane Exchange between Lymphocytes and Accessory

Cells by Trogocytosis Is Influenced by the Nature of the Accessory Cell. *J Immunol* 184:1897-1908.

149. Kedl, R. M., B. C. Schaefer, J. W. Kappler, and P. Marrack. 2002. T cells down-modulate peptide-MHC complexes on APCs in vivo. *Nat Immunol* 3:27-32.

150. Wülfing, C., C. Sumen, M. D. Sjaastad, L. C. Wu, M. L. Dustin, and M. M. Davis. 2002. Costimulation and endogenous MHC ligands contribute to T cell recognition. *Nat Immunol* 3:42-47.

151. Krummel, M. F., M. D. Sjaastad, C. Wülfing, and M. M. Davis. 2000. Differential clustering of CD4 and CD3ζ during T cell recognition. *Science* 289:1349-1352.

152. Nagy, Z., B. E. Elliott, M. Nabholtz, P. H. Krammer, and B. Pernis. 1976. Specific binding of alloantigens to T cells activated in the mixed lymphocyte reaction. *Journal of Experimental Medicine* 143:648-658.

153. Hayball, J. D., B. W. Robinson, and R. A. Lake. 2004. CD4+ T cells cross-compete for MHC class II-restricted peptide antigen complexes on the surface of antigen presenting cells. *Immunol Cell Biol* 82:103-111.

154. Lee, K. H., A. R. Dinner, C. Tu, G. Campi, S. Raychaudhuri, R. Varma, T. N. Sims, W. R. Burack, H. Wu, J. Wang, O. Kanagawa, M. Markiewicz, P. M. Allen, M. L. Dustin, A. K. Chakraborty, and A. S. Shaw. 2003. The immunological synapse balances T cell receptor signaling and degradation. *Science* 302:1218-1222.

155. Dopfer, E. P., S. Minguet, and W. W. Schamel. 2011. A new vampire saga: the molecular mechanism of T cell trogocytosis. *Immunity* 35:151-153.

156. Shi, M., S. Hao, T. Chan, and J. Xiang. 2006. CD4(+) T cells stimulate memory CD8(+) T cell expansion via acquired pMHC I complexes and costimulatory molecules, and IL-2 secretion. *J Leukoc Biol* 80:1354-1363.

157. Umeshappa, C. S., H. Huang, Y. Xie, Y. Wei, S. J. Mulligan, Y. Deng, and J. Xiang. 2009. CD4+ Th-APC with acquired peptide/MHC class I and II complexes stimulate type 1 helper CD4+ and central memory CD8+ T cell responses. *J Immunol* 182:193-206.

158. Helft, J., A. Jacquet, N. T. Joncker, I. Grandjean, G. Dorothee, A. Kissenpfennig, B. Malissen, P. Matzinger, and O. Lantz. 2008. Antigen-specific T-T interactions regulate CD4 T-cell expansion. *Blood* 112:1249-1258.

159. Zhou, G., Z. C. Ding, J. Fu, and H. I. Levitsky. 2011. Presentation of acquired peptide-MHC class II ligands by CD4+ regulatory T cells or helper cells

differentially regulates antigen-specific CD4+ T cell response. *J Immunol* 186:2148-2155.

160. Choi, E. Y., K. C. Jung, H. J. Park, D. H. Chung, J. S. Song, S. D. Yang, E. Simpson, and S. H. Park. 2005. Thymocyte-thymocyte interaction for efficient positive selection and maturation of CD4 T cells. *Immunity* 23:387-396.

161. Zhou, J., Y. Tagaya, R. Tolouei-Semnani, J. Schlom, and H. Sabzevari. 2005. Physiological relevance of antigen presentasome (APS), an acquired MHC/costimulatory complex, in the sustained activation of CD4+ T cells in the absence of APCs. *Blood* 105:3238-3246.

162. Su, M. W., P. R. Walden, D. B. Golan, and H. N. Eisen. 1993. Cognate peptide-induced destruction of CD8+ cytotoxic T lymphocytes is due to fratricide. *J Immunol* 151:658-667.

163. Mannie, M. D., and M. S. Norris. 2001. MHC class-II-restricted antigen presentation by myelin basic protein-specific CD4+ T cells causes prolonged desensitization and outgrowth of CD4- responders. *Cell Immunol* 212:51-62.

164. Chai, J. G., I. Bartok, D. Scott, J. Dyson, and R. Lechler. 1998. T:T antigen presentation by activated murine CD8+ T cells induces anergy and apoptosis. *J Immunol* 160:3655-3665.

165. Pichler, W. J., and T. Wyss-Coray. 1994. T cells as antigen-presenting cells. *Immunol Today* 15:312-315.

166. Lanzavecchia, A., E. Roosnek, T. Gregory, P. Berman, and S. Abrignani. 1988. T cells can present antigens such as HIV gp120 targeted to their own surface molecules. *Nature* 334:530-532.

167. Hewitt, C. R., and M. Feldmann. 1989. Human T cell clones present antigen. *J Immunol* 143:762-769.

168. Siliciano, R. F., T. Lawton, C. Knall, R. W. Karr, P. Berman, T. Gregory, and E. L. Reinherz. 1988. Analysis of host-virus interactions in AIDS with anti-gp120 T cell clones: effect of HIV sequence variation and a mechanism for CD4+ cell depletion. *Cell* 54:561-575.

169. Wyss-Coray, T., C. Brander, K. Frutig, and W. J. Pichler. 1992. Discrimination of human CD4 T cell clones based on their reactivity with antigen-presenting T cells. *Eur J Immunol* 22:2295-2302.

170. Wyss-Coray, T., C. Brander, F. Bettens, D. Mijic, and W. J. Pichler. 1992. Use of antibody/peptide constructs of direct antigenic peptides to T cells: evidence for T cell processing and presentation. *Cell Immunol* 139:268-273.

171. LaSalle, J. M., P. J. Tolentino, G. J. Freeman, L. M. Nadler, and D. A. Hafler. 1992. Early signaling defects in human T cells anergized by T cell presentation of autoantigen. *J Exp Med* 176:177-186.

172. Barnaba, V., C. Watts, M. de Boer, P. Lane, and A. Lanzavecchia. 1994. Professional presentation of antigen by activated human T cells. *Eur J Immunol* 24:71-75.

173. Nakada, M., K. Nishizaki, T. Yoshino, M. Okano, T. Yamamoto, Y. Masuda, N. Ohta, and T. Akagi. 1999. CD80 (B7-1) and CD86 (B7-2) antigens on house dust mite-specific T cells in atopic disease function through T-T cell interactions. *J Allergy Clin Immunol* 104:222-227.

174. Sidhu, S., S. Deacock, V. Bal, J. R. Batchelor, G. Lombardi, and R. I. Lechler. 1992. Human T cells cannot act as autonomous antigen-presenting cells, but induce tolerance in antigen-specific and alloreactive responder cells. *J Exp Med* 176:875-880.

175. Benoist, C., and D. Mathis. 1990. Regulation of major histocompatibility complex class-II genes: X, Y and other letters of the alphabet. *Annu Rev Immunol* 8:681-715.

176. Mostbock, S., M. Catalfamo, Y. Tagaya, J. Schlom, and H. Sabzevari. 2007. Acquisition of antigen presentasome (APS), an MHC/costimulatory complex, is a checkpoint of memory T-cell homeostasis. *Blood* 109:2488-2495.

177. Kennedy, R., A. H. Undale, W. C. Kieper, M. S. Block, L. R. Pease, and E. Celis. 2005. Direct Cross-Priming by Th Lymphocytes Generates Memory Cytotoxic Responses. *Journal of Immunology* 174:3967-3977.

178. Cox, J. H., A. J. McMichael, G. R. Screaton, and X. N. Xu. 2007. CTLs target Th cells that acquire bystander MHC class I-peptide complex from APCs. *J Immunol* 179:830-836.

179. Lombardi, G., R. Hargreaves, S. Sidhu, N. Imami, L. Lightstone, S. Fuller-Espie, M. Ritter, P. Robinson, A. Tarnok, and R. Lechler. 1996. Antigen presentation by T cells inhibits IL-2 production and induces IL-4 release due to altered cognate signals. *J Immunol* 156:2769-2775.

180. Rachmilewitz, J., and A. Lanzavecchia. 2002. A temporal and spatial summation model for T-cell activation: signal integration and antigen decoding. *Trends Immunol* 23:592-595.

181. Gunzer, M., A. Schafer, S. Borgmann, S. Grabbe, K. S. Zanker, E. B. Brocker, E. Kampgen, and P. Friedl. 2000. Antigen presentation in extracellular matrix:

interactions of T cells with dendritic cells are dynamic, short lived, and sequential. *Immunity* 13:323-332.

182. Underhill, D. M., M. Bassetti, A. Rudensky, and A. Aderem. 1999. Dynamic interactions of macrophages with T cells during antigen presentation. *J Exp Med* 190:1909-1914.

183. Kaye, J., N. J. Vasquez, and S. M. Hedrick. 1992. Involvement of the same region of the T cell antigen receptor in thymic selection and foreign peptide recognition. *J Immunol* 148:3342-3353.

184. Wetzel, S. A., T. W. McKeithan, and D. C. Parker. 2002. Live-cell dynamics and the role of costimulation in immunological synapse formation. *J Immunol* 169:6092-6101.

185. Chow, S., D. Hedley, P. Grom, R. Magari, J. W. Jacobberger, and T. V. Shankey. 2005. Whole blood fixation and permeabilization protocol with red blood cell lysis for flow cytometry of intracellular phosphorylated epitopes in leukocyte subpopulations. *Cytometry A* 67:4-17.

186. Bolte, S., and F. P. Cordeliéres. 2006. A guided tour into subcellular colocalization analysis in light microscopy. *J Microsc* 224:213-224.

187. Rasband, W. S. 1997-2009. ImageJ. National Institues of Health:http://rsb.info.nih.gov/ij/.

188. Faroudi, M., R. Zaru, P. Paulet, S. Muller, and S. Valitutti. 2003. Cutting edge: T lymphocyte activation by repeated immunological synapse formation and intermittent signaling. *J Immunol* 171:1128-1132.

189. Hanke, J. H., J. P. Gardner, R. L. Dow, P. S. Changelian, W. H. Brissette, E. J. Weringer, B. A. Pollok, and P. A. Connelly. 1996. Discovery of a novel, potent, and Src family-selective tyrosine kinase inhibitor. Study of Lck- and FynT-dependent T cell activation. *J Biol Chem* 271:695-701.

190. Umeshappa, C. S., and J. Xiang. 2010. Tumor-derived HLA-G1 acquisition by monocytes through trogocytosis: possible functional consequences. *Cell Mol Life Sci* 67:4107-4108.

191. Lo, W. L., N. J. Felix, J. J. Walters, H. Rohrs, M. L. Gross, and P. M. Allen. 2009. An endogenous peptide positively selects and augments the activation and survival of peripheral CD4+ T cells. *Nat Immunol* 10:1155-1161.

192. Osborne, D. G., and S. A. Wetzel. 2012. Trogocytosis Results in Sustained Intracellular Signaling in CD4+ T Cells. *J Immunol* 189:4728-4739.

193. van Oers, N. S., N. Killeen, and A. Weiss. 1996. Lck regulates the tyrosine phosphorylation of the T cell receptor subunits and ZAP-70 in murine thymocytes. *J Exp Med* 183:1053-1062.

194. Perez, O. D., and G. P. Nolan. 2006. Phospho-proteomic immune analysis by flow cytrometry: from mechanism to translational medicine at the single-cell level. *Immunological Reviews* 210:208-228.

195. Huppa, J. B., and M. M. Davis. 2003. T-cell-antigen recognition and the immunological synapse. *Nat Rev Immunol* 3:973-983.

196. Huppa, J. B., M. Gleimer, C. Sumen, and M. M. Davis. 2003. Continuous T cell receptor signaling required for synapse maintenance and full effector potential. *Nat Immunol* 4:749-755.

197. Kupfer, A., and S. J. Singer. 1989. Cell biology of cytotoxic and helper T cell functions: immunofluorescence microscopic studies of single cells and cell couples. *Annu Rev Immunol* 7:309-337.

198. Hwang, I., X. Shen, and J. Sprent. 2003. Direct stimulation of naive T cells by membrane vesicles from antigen-presenting cells: distinct roles for CD54 and B7 molecules. *Proc Natl Acad Sci U S A* 100:6670-6675.

199. Sprent, J., and C. D. Surh. 2003. Cytokines and T cell homeostasis. *Immunol Lett* 85:145-149.

200. Sprent, J. 2005. Direct stimulation of naive T cells by antigen-presenting cell vesicles. *Blood Cells Mol Dis* 35:17-20.

201. Kovar, M., O. Boyman, X. Shen, I. Hwang, R. Kohler, and J. Sprent. 2006. Direct stimulation of T cells by membrane vesicles from antigen-presenting cells. *Proc Natl Acad Sci U S A* 103:11671-11676.

202. Rechavi, O., I. Goldstein, H. Vernitsky, B. Rotblat, and Y. Kloog. 2007. Intercellular transfer of oncogenic H-Ras at the immunological synapse. *PLoS One* 2:e1204.

203. HoWangYin, K. Y., J. Caumartin, B. Favier, M. Daouya, L. Yaghi, E. D. Carosella, and J. LeMaoult. 2011. Proper regrafting of Ig-like transcript 2 after trogocytosis allows a functional cell-cell transfer of sensitivity. *J Immunol* 186:2210-2218.

204. Adams, C. L., A. M. Grierson, A. M. Mowat, M. M. Harnett, and P. Garside. 2004. Differences in the kinetics, amplitude, and localization of ERK activation in anergy and priming revealed at the level of individual primary T cells by laser scanning cytometry. *J Immunol* 173:1579-1586.

205. Cullinan, P., A. I. Sperling, and J. K. Burkhardt. 2002. The distal pole complex: a novel membrane domain distal to the immunological synapse. *Immunol Rev* 189:111-122.

206. Allenspach, E. J., P. Cullinan, J. Tong, Q. Tang, A. G. Tesciuba, J. L. Cannon, S. M. Takahashi, R. Morgan, J. K. Burkhardt, and A. I. Sperling. 2001. ERM-dependent movement of CD43 defines a novel protein complex distal to the immunological synapse. *Immunity* 15:739-750.

207. Chang, J. T., V. R. Palanivel, I. Kinjyo, F. Schambach, A. M. Intlekofer, A. Banerjee, S. A. Longworth, K. E. Vinup, P. Mrass, J. Oliaro, N. Killeen, J. S. Orange, S. M. Russell, W. Weninger, and S. L. Reiner. 2007. Asymmetric T lymphocyte division in the initiation of adaptive immune responses. *Science* 315:1687-1691.

208. Mempel, T. R., S. E. Henrickson, and U. H. von Adrian. 2004. T-cell priming by dendritic cells in lymph nodes occurs in three distinct phases. *Nature* 427:154-159.

209. Madrenas, J., R. L. Wange, J. L. Wang, N. Isakov, L. E. Samelson, and R. N. Germain. 1995. Zeta phosphorylation without ZAP-70 activation induced by TCR antagonists or partial agonists. *Science* 267:515-518.

210. Kersh, B. E., G. J. Kersh, and P. M. Allen. 1999. Partially phosphorylated T cell receptor zeta molecules can inhibit T cell activation. *J Exp Med* 190:1627-1636.

211. Page, D. M., J. Alexander, K. Snoke, E. Appella, A. Sette, S. M. Hedrick, and H. M. Grey. 1994. Negative selection of $CD4^+$ $CD8^+$ thymocytes by T-cell receptor peptide antagonists. *Proceedings of the National Academy of Sciences of the United States of America* 91:4057-4061.

212. Sorger, S. B., Y. Paterson, P. J. Fink, and S. M. Hedrick. 1990. T cell receptor junctional regions and the MHC molecule affect the recognition of antigenic peptides by T cell clones. *J Immunol* 144:1127-1135.

213. Wang, R., Y. Wang-Zhu, C. R. Gabaglia, K. Kimachi, and H. M. Grey. 1999. The stimulation of low-affinity, nontolerized clones by heteroclitic antigen analogues causes the breaking of tolerance established to an immunodominant T cell epitope. *J Exp Med* 190:983-994.